Volcanic impacts on modern glaciers: A global synthesis

Barr, I., Lynch, C., Mullan, D., De Siena, L., & Spagnolo, M. (2018). Volcanic impacts on modern glaciers: A global synthesis. *Earth-Science Reviews*. Advance online publication. https://doi.org/10.1016/j.earscirev.2018.04.008

Published in:
Earth-Science Reviews

Document Version:
Peer reviewed version

Volcanic impacts on modern glaciers: a global synthesis

Iestyn D. Barr[1]*, Colleen M. Lynch[2], Donal Mullan[2], Luca De Siena[3], Matteo Spagnolo[3]

School of Science and the Environment, Manchester Metropolitan University, Manchester, UK

School of Natural and Built Environment, Queen's University Belfast, Belfast, UK

School of Geosciences, University of Aberdeen, Aberdeen, UK

***Corresponding author**

Dr Iestyn Barr

Email: i.barr@mmu.ac.uk

School of Science and Environment, Manchester Metropolitan University, Manchester, M1 5GD, UK

Tel: +44 (0)161 247 1202

Keywords

Glaciers; volcanoes; volcanic impacts; glacier dimensions; glacier dynamics, hazards.

Abstract

Volcanic activity can have a notable impact on glacier behaviour (dimensions and dynamics). This is evident from the palaeo-record, but is often difficult to observe for modern glaciers. However, documenting and, if possible, quantifying volcanic impacts on modern glaciers is important if we are to predict their future behaviour (including crucial ice masses such as the West Antarctic Ice Sheet) and to monitor and mitigate glacio-volcanic hazards such as floods (including jökulhlaups) and lahars. This review provides an assessment of volcanic impacts on the behaviour of modern glaciers (since AD 1800) by presenting and summarising a global dataset of documented examples. The study reveals that shorter-term (days-to-months) impacts are typically destructive, while longer-term (years-to-decades) are more likely protective (e.g., limiting climatically driven ice loss). However, because these events are difficult to observe, particularly before the widespread availability of global satellite data, their

frequency and importance are likely underestimated. The study also highlights that because the frequency and nature of volcano-glacier interactions may change with time (e.g., glacier retreat may lead to an increase in explosive volcanic activity), predicting their future importance is difficult. Fortunately, over coming years, continued improvements in remotely sensed data will increase the frequency, and enhance the quality, of observations of volcanic impacts on glaciers, allowing an improved understanding of their past and future operation.

1. Introduction

Climate exerts a first-order control on the behaviour (i.e., dimensions and dynamics) of modern glaciers. For example, glaciers typically grow in response to reduced atmospheric temperatures and/or increased solid precipitation (Cook et al., 2005; Bolch, 2007). Despite this, other non-climatic factors also play a role. One notable example is volcanic activity, which can directly affect glacier behaviour, and/or modulate glacier response to climate forcing (Major and Newhall, 1989; Chapman et al., 2000; Kirkbride and Dugmore, 2003).

Volcanic activity is known to impact climate, which in turn regulates glacier behaviour (e.g., Hammer et al., 1980; Rampino and Self, 1993; McConnell et al., 2017; Cooper et al., 2018); however, the focus here is on the more direct volcanic impacts on glaciers. These include instances where glacier behaviour has been directly affected by subglacial heating, subglacial dome growth, subglacial eruptions, lava flows (supraglacial and subglacial), supraglacial pyroclastic density currents, supraglacial tephra deposition, floods and lahars, and the supraglacial deposition of other glacio-volcanic products. These types of interactions have received considerable interest since the 2010 subglacial eruption of Eyjafjallajökull, Iceland (Gudmundsson et al., 2012; Sigmundsson et al., 2010). This has included a focus on glacio-volcanic activity on Mars (Scanlon et al., 2014), , and consideration of the role of subglacial volcanic and geothermal activity in governing the future stability of ice sheets (de Vries et al., 2017; Iverson et al., 2017; Seroussi et al., 2017) (Section 3.3.). This latter aspect has received considerable attention over recent years due to the possibility that future subglacial volcanic activity might change the bed conditions of the West Antarctic Ice Sheet, potentially triggering, or contributing to, its rapid collapse and global sea level rise (Blankenship et al. 1993; Vogel et al. 2006;

Corr and Vaughan 2008; de Vries et al., 2017). Interactions between volcanoes and glaciers have also developed as an area of interest because of their potential to result in hazards, including floods, lahars, and other debris flows, which have had devastating impacts on mountain communities globally during recent centuries (Blong, 1984; Pierson et al., 1990; Chernomorets et al., 2007; Tuffen, 2010). Finally, observed changes in glacier behaviour can serve as useful indicators of, and precursors to, periods of volcanic activity (e.g., observed ice loss was an early precursor to the 2009 eruption of Mount Redoubt, Bleick et al., 2013). Thus, monitoring, documenting, and, if possible, predicting volcanic impacts on glaciers is of global scientific and socio-economic importance (Pierson et al., 1990; Mazzocchi et al., 2010).

Instances where volcanic activity directly affects glacier behaviour (i.e., the focus of this paper) typically occur either because glaciers are located on active volcanoes, or because volcanic products (e.g., ash/tephra) interact with glaciers in adjacent (sometimes non-volcanic) regions. Though evidence for past volcanic impacts on glaciers is seen in the palaeo-record (Smellie and Edwards, 2016), establishing their importance for modern glaciers is challenging because glacio-volcanic regions are often remote and inaccessible. Thus, until recently, volcanic impacts on modern glaciers were rarely directly observed and were poorly understood. Fortunately, increased attention on glacio-volcanic regions, facilitated by rapid developments in remote sensing, has led to repeat observations and monitoring programs that are now elucidating some key aspects of volcano-glacier interactions (Curtis and Kyle, 2017). Major and Newhall (1989) made an early, and important, contribution to recognising the global impact of volcanic activity on snow and ice, with a particular focus on floods and lahars. Delgado Granados et al. (2015) provided a review of recent volcano-glacier interactions in South and Central America, and Smellie and Edwards (2016) provided a global review of volcano-glacier interactions, mainly (though not exclusively) focused on the palaeo (Quaternary) record. The present paper builds on these overviews by focusing specifically on the glaciological consequences of volcanic activity globally since AD 1800. Here, the term ‘volcanic activity’ is used to encompass explosive and effusive volcanic eruptions, as well as released geothermal energy and landscape changes (e.g., dome growth) induced by deep volcanic sources at active or dormant volcanoes.

2. Observed volcanic impacts on modern glaciers

Here, we outline how volcanic activity can directly influence the behaviour of modern glaciers. As alluded to in section 1., the volcanic processes considered are subglacial heat flow; subglacial dome growth, subglacial eruptions, lava flows (supraglacial and subglacial), supraglacial pyroclastic density currents, supraglacial tephra deposition, floods and lahars, and the supraglacial deposition of other glacio-volcanic products. Below we outline how each mechanism can affect glaciers, with reference to a global dataset of examples. This structure means that we focus on different mechanisms (and their glaciological impacts) discretely, while in reality (e.g., during a single eruption) many of the mechanisms likely act in conjunction (sometimes triggering one another). This can make it difficult to isolate or quantify the specific glaciological impact of a particular mechanism, and the fact that mechanisms may be operating in conjunction (with a combined glaciological impact) should be kept in mind throughout.

The locations of volcanoes mentioned in the text are illustrated in Fig. 1, and outlined in Table 1. Detailed information about each period of volcanic activity and associated glaciological consequences is presented in Supplementary Table 1 (alongside relevant citations), in a kmz. file for viewing and editing in Goole Earth™ (Supplementary data 1), and interactions are schematically illustrated in Fig. 2. We do not consider indirect impacts, such as glacier growth in response to volcanically triggered climatic cooling (e.g., Hammer et al., 1980; Rampino and Self, 1993; McConnell et al., 2017; Cooper et al., 2018), and do not directly consider seismic impacts on glaciers, though in many cases, seismic and volcanic activity may be linked.

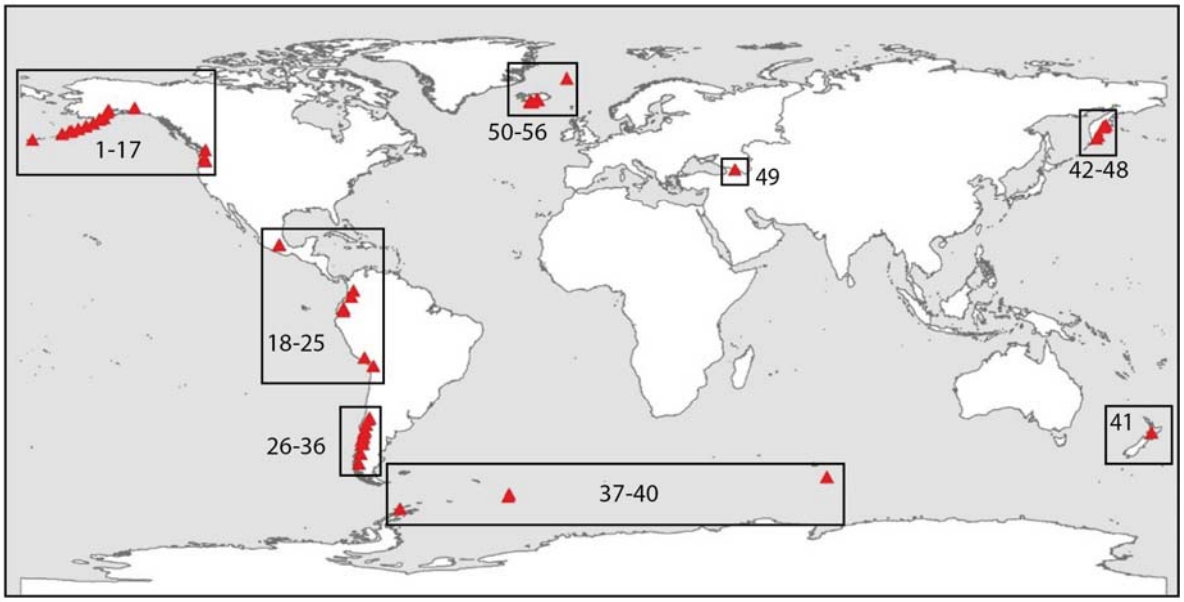

Fig. 1. Red triangles showing locations where the behaviour of modern (post AD 1800) glaciers has been affected by volcanic activity. Numbers refer to specific volcanoes, detailed in Table 1 and Supplementary Table 1 (where volcanic events and associated glaciological consequences are also described).

Table 1. Volcanoes and periods of volcanic activity discussed in this review. Detailed information is provided in Supplementary Table 1.

Volcano number	Volcano name	Location	Lat, Lon	Periods of activity
1	Great Sitkin	USA (Alaska)	52.08°N, 176.13°W	1945
2	Makushin	USA (Alaska)	53.89°N, 166.92°W	1983
3	Mount Westdahl	USA (Alaska)	54.52°N, 164.65°W	1978, 1991–92
4	Mount Shishaldin	USA (Alaska)	54.76°N, 163.97°W	1999
5	Mount Pavlof	USA (Alaska)	55.42°N, 161.89°W	2013
6	Mount Veniaminof	USA (Alaska)	56.17°N, 159.38°W	1983–84, 1993–95, 2013
7	Mount Chiginagak	USA (Alaska)	57.14°N, 156.99°W	2004–05
8	Novarupta	USA (Alaska)	58.27°N, 155.16°W	1912
9	Trident Volcanic group	USA (Alaska)	58.24°N, 155.10°W	1953–60
10	Mount Katmai	USA (Alaska)	58.26°N, 154.98°W	1912
11	Fourpeaked Mountain	USA (Alaska)	58.77°N, 153.67°W	2006
12	Mount Redoubt	USA (Alaska)	60.49°N, 152.74°W	1966–68, 1989–90, 2008–09
13	Mount Spurr (Crater Peak)	USA (Alaska)	61.30°N, 152.25°W	1953, 1992, 2004–06

14	Mount Wrangell	USA (Alaska)	62.00°N, 144.02°W	1899, 1964–ongoing, 1999
15	Mount Baker	USA (Cascade Arc)	48.78°N, 121.81°W	1958–76
16	Mount St Helens	USA (Cascade Arc)	46.20°N, 122.18°W	1980, 2004–06
17	Mount Hood	USA (Cascade Arc)	45.37°N, 121.70°W	1853–1869, 1907
18	Iztaccíhuatl	Mexico	19.18°N, 98.64°W	Late 20th century
19	Popocatépetl	Mexico	19.02°N, 98.63°W	1994–2001
20	Nevado del Ruiz	Columbia	4.90°N, 75.32°W	1985
21	Nevado del Huila	Columbia	2.93°N, 76.03°W	2007–12
22	Cotopaxi	Ecuador	0.68°S, 78.44°W	1877
23	Tungurahua	Ecuador	1.47°S, 78.44°W	1999–2001
24	Nevado Sabancaya	Peru	17.78°S, 71.85°W	1986–88, 1990–98
25	Volcán Guallatiri	Chile	18.42°S, 69.09°W	Late 20th Century
26	Tinguiririca	Chile	34.81°S, 70.35°W	1994, 2006/07
27	Volcán Peteroa (Planchón-Peteroa)	Chile	35.27°S, 70.58°W	1963–91, 1991, 2004–07, 2010–11
28	Nevados de Chillán	Chile	36.86°S, 71.38°W	1973–86
29	Volcán Llaima	Chile	38.69°S, 71.73°W	1979, 1994, 2008
30	Volcán Villarrica	Chile	39.42°S, 71.93°W	1971, 1984–85, various
31	Puyehue-Cordón Caulle	Chile	40.59°S, 72.12°W	2011
32	Volcán Calbuco	Chile	41.33°S, 72.61°W	1961
33	Volcán Michinmahuida	Chile	42.79°S, 72.44°W	2007–08
34	Volcán Chaitén	Chile	42.84°S, 72.65°W	2008
35	Volcán Hudson	Chile	45.90°S, 72.97°W	1971, 1991, 2011
36	Volcán Lautaro	Chile	49.02°S, 73.55°W	Various 20th Century
37	Deception Island	Sub-Antarctic	62.97°S, 60.65°W	1969
38	Bristol Island	Sub-Antarctic	59.04°S, 26.53°W	1935–1962
39	Mt Belinda	Sub-Antarctic (Montagu Island)	58.42°S, 26.33°W	2001–07
40	Mawson Peak	Sub-Antarctic (Heard Island)	53.11°S, 73.51°E	2006-08
41	Mount Ruapehu	New Zealand	39.28°S, 175.57°E	1995–96, 2007
42	Mutnovsky	Russia (Kamchatka)	52.45°N, 158.20°E	2000, ongoing
43	Avachinsky	Russia (Kamchatka)	53.26°N, 158.83°E	1945, 1991
44	Tolbachik	Russia (Kamchatka)	55.82°N, 160.38°E	1975–76, 2012–13
45	Bezymianny	Russia (Kamchatka)	55.98°N, 160.59°E	1955–57
46	Klyuchevskoy	Russia (Kamchatka)	56.06°N, 160.64°E	1944–45, 1953, 1966–68, 1977–80, 1982–83, 1984–85, 1985–86, 1986–90, 2005–10

47	Ushkovsky	Russia (Kamchatka)	56.07°N, 160.47°E	1959–60, 1982–84
48	Shiveluch	Russia (Kamchatka)	56.65°N, 161.36°E	1964
49	Mount Kazbek	Russia/Georgia (Caucasus)	42.70°N, 44.52°E	Various 20th and 21st Century (possible)
50	Beerenberg	Norway (Jan Mayen Island)	71.08°N, 8.16°W	1970–72
51	Grímsvötn	Iceland	64.42°N, 17.33°W	1934, 2004, 2011
52	Gjálp fissure	Iceland	64.52°N, 17.39°W	1996
53	Bárðarbunga	Iceland	64.64°N, 17.53°W	2014
54	Katla	Iceland	63.63°N, 19.05°W	1918
55	Eyjafjallajökull/ Fimmvörðuháls;	Iceland	63.63°N, 19.62°W	2010
56	Hekla	Iceland	63.98°N, 19.70°W	1947

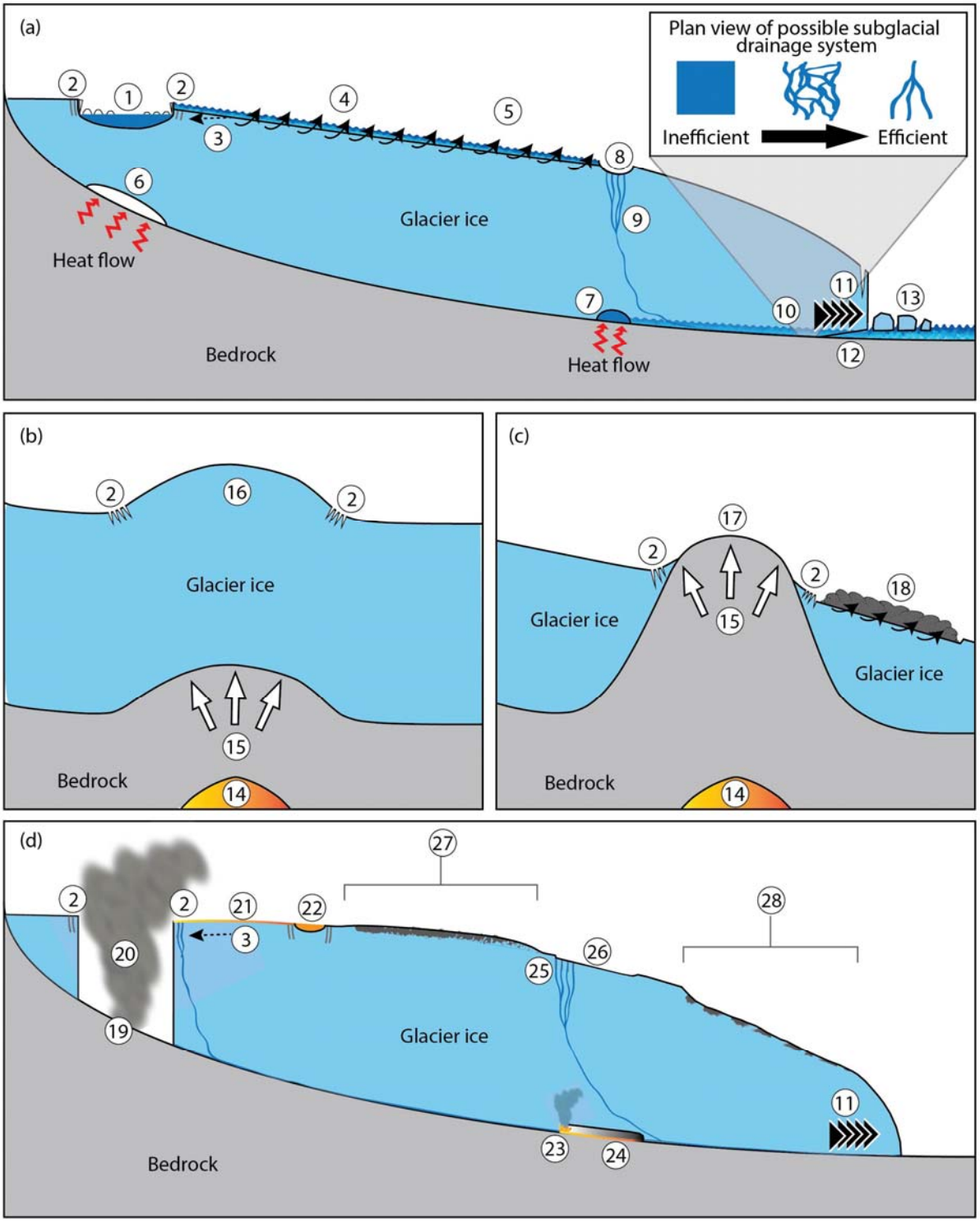

Fig. 2. Schematic illustrations of the impacts that different forms of volcanic activity can have on glacier behaviour. Different forms of activity include (a) enhanced subglacial heat flow and flood/lahars, (b) Subglacial volcanic dome growth, (c) volcanic dome extrusion and a pyroclastic density current, and (d) a subglacial volcanic eruption, lava flows, and supraglacial tephra deposition. Numbers in this figure refer to different processes or features. (1) Lake filled supraglacial cauldron, with ice breaking from

vertical cauldron walls. (2) Zones of crevassing and fracturing. (3) Local reversal in ice flow direction. (4) Supraglacial flood (formed by lake drainage) transitioning to a lahar. (5) Supraglacial channel/canyon formed by ice melt, erosion and entrainment (by a flood/lahar). (6) Subglacial cavity caused by enhanced heat flow. (7) Subglacial lake formed by enhanced heat flow. (8) Supraglacial depression formed above a subglacial lake. (9) Crevasses (above a subglacial lake) acting as a route for supraglacial meltwater drainage to the bed. (10) Subglacial meltwater drainage with inset plan view of different possible drainage styles. (11) Glacier advance/acceleration due to subglacial meltwater drainage (more widespread if drainage is inefficient). (12) Glacier front uplifted by subglacial flooding. (13) Ice blocks torn from a glacier front by subglacial flooding. (14) Magma upwelling. (15) Subglacial dome growth. (16) Glacier doming. (17) Dome extrusion through a glacier. (18) Pyroclastic density current (due to dome collapse) and associated supraglacial channel (formed by ice melt, erosion and entrainment). (19) Subglacial eruption. (20) Ice crater. (21) Supraglacial lava flow and associated melt channel. (22) Supraglacial lava ponding and associated crevasse bounded melt pit. (23) Site of small and/or phreatic eruption (with lava fountain). (24) Subglacial lava flow and associated melt cavity. (25) Crevasses (above the site of a small subglacial eruption) acting as a route for supraglacial meltwater drainage to the bed. (26) Supraglacial depression formed above a subglacial lava flow melt cavity. (27) Reduced melt under thick and/or continuous supraglacial tephra. (28) Increased melt under thin and/or discontinuous supraglacial tephra. These illustrations are not to scale, with some aspects exaggerated to highlight specific phenomena. For reasons of simplicity/clarity, the illustrations also depict glaciers with shallow surface gradients, whereas many volcano-occupying glaciers are steeper (though the processes shown here are likely to operate for both steep and shallow glaciers).

2.1. Enhanced subglacial heat flow

Enhanced subglacial heat flow (geothermal heating) (Fig. 2a) can occur without associated volcanic activity, or prior-to, during, or after periods of activity. The main glaciological consequence is subglacial melt. This can lead to the formation of subglacial cavities or lakes (Fig. 2a, points 6 & 7), which can, in turn, cause subsidence and fracturing of the ice surface (Gudmundsson et al., 1997) (Fig. 2a, points 1 & 8). Increased subglacial melt can also cause glacier retreat (Salamatin et al., 2000) or

advance/acceleration (Sturm et al., 1991; Rivera et al., 2012) (Fig. 2a, point 11). Here (below), we consider documented examples of these different outcomes.

2.1.1. Surface subsidence and fracturing

Instances where enhanced subglacial heat flow has caused the subsidence and fracturing of glacier surfaces are documented from many glacio-volcanic regions globally, including the USA, Chile, sub-Antarctic Islands, Kamchatka, and Mexico (Supplementary Table 1). In many cases, subglacial heating initially results in the formation of supraglacial melt pits/holes (Fig. 3a), which become enlarged to form cauldrons (Fig. 3b) as subglacial heating continues (e.g., Mount Wrangell 1964–ongoing; Mount Baker 1975–76; Mount Makushin 1983; Mount Redoubt 1989–1990, 2009; Mount Chiginagak 2004–05; Mount Spurr 2004–06). These cauldrons can be filled by lakes (Fig. 3c) (e.g., Mount Wrangell 1964–ongoing; Mount Baker 1975–76; Mount Veniaminof 1983–84; Mount Chiginagak 2004–05; Mount Spurr 2004–06), which often act to increase the cavity size as ice falls/calves from the vertical or overhanging ice walls (e.g., Mount Baker 1975–76; Mount Spurr 2004–06) (Fig. 2a, point 1). Lakes can entirely or partially drain, forming large englacial and/or subglacial channels, which result in further surface depressions and/or melt holes (e.g., Mount Spurr 2004–06). Lakes can also overflow, and generate supraglacial channels (Smellie, 2006). Sometimes, drainage events are large enough to trigger floods and lahars (Section 2.7.) (e.g., Mount Chiginagak 2004–05), though not always (e.g., Mount Baker 1975–76; Mount Veniaminof 1983–84).

Ice surrounding supraglacial ice cauldrons is often fractured, forming encircling arcuate/concentric crevasses (e.g., Mount Veniaminof 1983–84; Mount Spurr 2004–06) (Fig. 3d; Fig. 2a, point 2). These crevasses are partly a reflection of localised reversals in ice flow direction, as ice begins to flow back towards the cauldrons, perpetuating melt (Fig. 2a, point 3). In some cases, enhanced subglacial heat flow can result in the formation of ice surface fissures (e.g., Deception Island 1969; Volcán Iztaccíhuatl during the late 20th century). These can be an important route for supraglacial water to drain to the glacier bed (Fig. 2a, point 9), where it accumulates along with subglacially-derived meltwater and potentially promotes ice advance and/or acceleration (Section 2.1.3.).

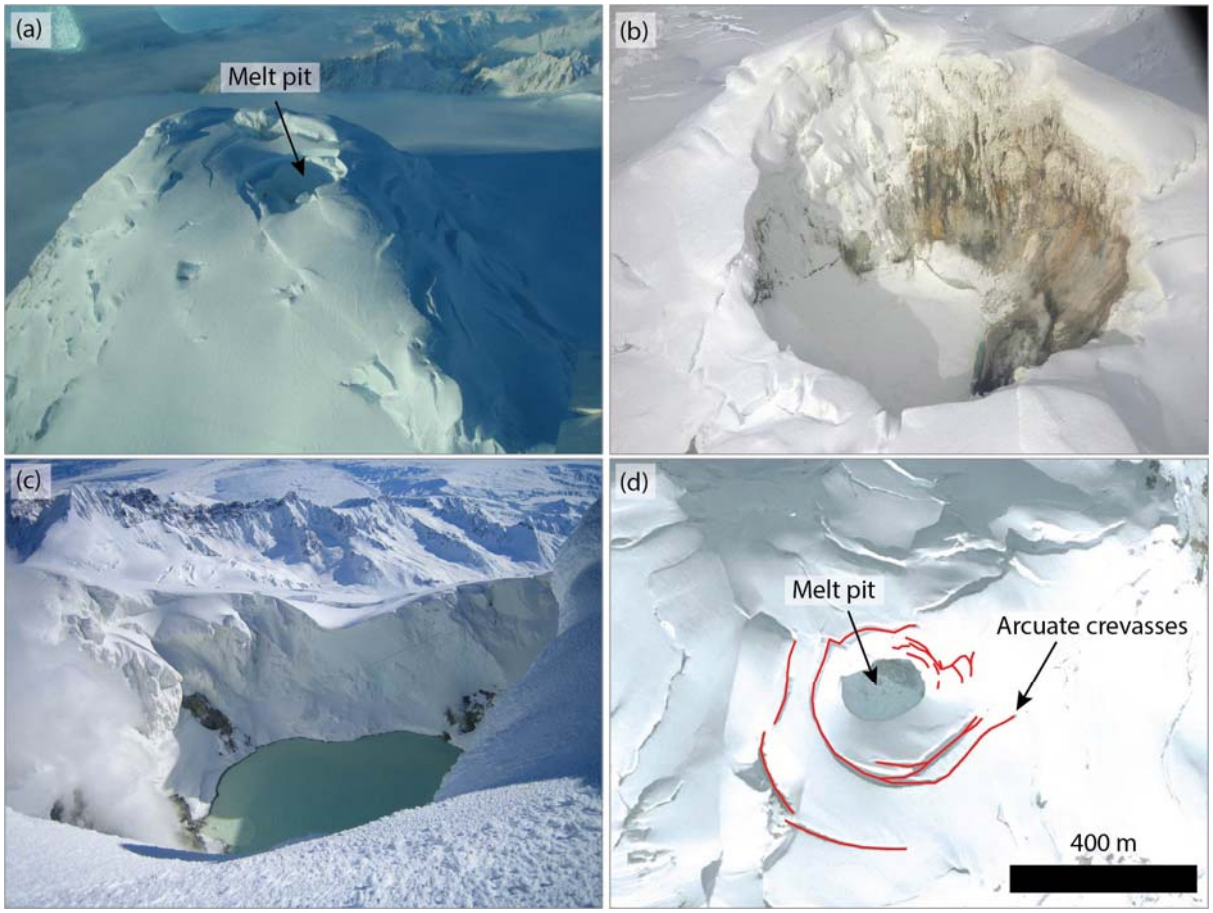

Fig. 3. Evidence of ice surface subsidence and fracturing during the 2004–06 period of enhanced subglacial heat flow at Mount Spurr. In this example, a summit melt pit (a), enlarged to form a summit ice cauldron (b), occupied by a lake (c). During formation of the melt pit, adjacent ice became fractured, with encircling arcuate crevasses (marked as red in 'd'). (a) Photograph taken by M.L. Coombs (AVO/USGS) on October 30, 2004. Image obtained from the AVO/USGS database (http://www.avo.alaska.edu/images/image.php?id=5). (b) Photograph taken by R.G. McGimsey (AVO/USGS) on June 28, 2007. Image obtained from the AVO/USGS database (http://www.avo.alaska.edu/images/image.php?id=13305). (c) Photograph taken by N. Bluett (AVO/USGS) on March 22, 2006. Image obtained from the AVO/USGS database (http://www.avo.alaska.edu/images/image.php?id=9657). (d) DigitalGlobe™ image, taken on August 11, 2004, viewed in GoogleEarth™.

2.1.2. Glacier retreat

Instances where enhanced subglacial heat flow has caused observable glacier retreat are comparatively rare (Supplementary Table 1). One example comes from Volcán Villarrica, where, over recent years, Pichillancahue-Turbio Glacier retreated at a faster rate than others in the region, partly due to enhanced geothermal heating (Rivera et al., 2012). A second example comes from Volcán Iztaccíhuatl, where geo- and hydro-thermal heat flow caused accelerated melt and glacier retreat during the late 20th century (Delgado Granados et al., 2005). For example, Ayoloco Glacier experienced a rapid increase in the rate of area loss (i.e., between 1958 and1982 the glacier lost 12% of its area, but between 1982 and 1998 lost 43%), and Centro Oriental Glacier almost entirely disappeared due to geothermally-driven increased melt over this period (Delgado Granados et al., 2005).

2.1.3. Glacier advance and/or acceleration

Instances where enhanced subglacial heat flow has caused (or appears to have caused) glacier advance and/or acceleration are documented in Alaska, Chile, Kamchatka, and the Caucasus (Supplementary Table 1). For example, at Mount Wrangell, there was increased heat flux following a major regional earthquake in 1964. As a result, the three glaciers which emanate from the volcano's North Crater (Ahtna Glacier, and South and Centre MacKeith Glaciers) have advanced since 1965 (at a rate of 5–18 m a^{-1}), unlike others on the volcano or elsewhere in the Wrangell Mountains (Sturm et al., 1991). It is assumed that this advance resulted from meltwater, which drained down the northeast flank of the volcano and lubricated the glacier bed (Sturm et al., 1991). These glaciers have also come to show little seasonal variation in their surface velocity, unlike most glaciers not subject to volcanic impacts (Iken and Bindschadler, 1986; Bartholomew, 2011), thus supporting the idea that volcanically-produced meltwater is driving changes in flow conditions (Sturm et al., 1991). At Volcán Peteroa, subglacial geothermal heating before phreatomagmatic explosions in 1991 and 2010 caused subglacial melt, increased basal sliding, and glacier advance during the 1963–1990 and 2004–2007 periods (Liaudat et al., 2014). At Volcán Michinmahuida, subglacial geothermal heating a few months prior to the 2008 eruption of Volcán Chaitén (~ 15 km to the west) is thought to have caused glacier advance and acceleration (Rivera et al., 2012). For example, Glaciar Amarillo retreated ~ 76 m yr^{-1} between 1961 and 2007, but advanced 243 ± 49 m between November 2007 and September 2009 (coinciding with the

220 period of subglacial geothermal heating), after which, glacier retreat resumed (Rivera et al., 2012). At
221 Ushkovsky**,** strengthening of seismic (and perhaps volcanic) activity is thought to have caused
222 Bilchenok Glacier (which emanates from the NW corner of the ice-filled caldera) to advance by 1050–
223 1150 m and 700–800 m in 1959–1960 and 1982–84, respectively (Muraviev et al., 2011, 2012;
224 Muraviev and Muraviev, 2016). Finally, at Mount Kazbek, periods of increased subglacial volcanic
225 and/or geothermal activity may have caused the acceleration, advance, and destabilisation of local
226 glaciers at various periods during the 20th and 21st centuries (Chernomorets et al., 2007).
227 While the periods of glacier advance/acceleration outlined above likely occurred due to
228 enhanced meltwater accumulation at the ice-bed interface, which reduced basal drag and promoted basal
229 sliding and advance, the exact cause of these events is often unclear. In many cases, multiple causes
230 may have acted together. For example, the advance of Glaciar Amarillo at Volcán Michinmahuida
231 between November 2007 and September 2009 may have been caused by combination of increased
232 subglacial heating and supraglacial tephra deposition (Rivera et al., 2012).
233
234 **2.1.4. Overall glaciological impacts of enhanced subglacial heat flow**
235 The most common and conspicuous glaciological impact of enhanced subglacial heat flow is the
236 subsidence and fracturing of glacier surfaces (Fig. 2a, points 1, 2 & 8). This occurs in response to the
237 formation of subglacial melt-cavities and lakes (Fig. 2a, points 6 & 7). Subsidence and fracturing not
238 only reflect changes in glacier geometry, but potentially have additional, indirect, impacts on glacier
239 behaviour. In particular, sites of supraglacial subsidence can cause local reversals in ice flow direction
240 (Fig. 2a, point 3), and fracture zones are a potential route for meltwater drainage to the glacier bed (Fig.
241 2a, point 9). The accumulation of meltwater at the glacier bed (from subglacial or supraglacial sources)
242 is potentially the most important glaciological consequence of enhanced subglacial heat flow, since
243 basal lubrication can facilitate glacier advance and/or acceleration (Fig. 2a, points 10 & 11).
244 Documented examples of advance/acceleration in response to enhanced subglacial heating are certainly
245 more common than examples of glacier retreat. However, making clear (unequivocal) links between
246 subglacial heating and changes in glacier behaviour is difficult, since geothermal heating is often poorly
247 monitored and subglacial environments are notoriously difficult to observe.

248

249 **2.2. Subglacial dome growth**

250 Magma upwelling can result in ground deformation, and the growth of (often hot) lava domes (Melnik
251 and Sparks, 1999) (Fig. 2b & c, points 14 & 15). Periods of dome growth can occur without associated
252 volcanic activity, or before, during, or after periods of activity. Subglacial dome growth can cause
253 deformation and fracturing of the ice surface (Fig. 2b & c, points 2 & 16). In some cases, lava domes
254 can extrude through the overlying ice (i.e., they become subaerial), where they cause further glacier
255 displacement and fracturing (Fig. 2c, points 2, 15 & 17). Some extruded domes are also susceptible to
256 gravitational collapse and/or destruction by explosions (dome growth and destruction can occur
257 repeatedly), resulting in (hot) supraglacial pyroclastic density currents (Fig. 2c, point 18) (Section 2.5.).
258 Here (below), we consider documented examples of subglacial dome growth (both with and without
259 subsequent extrusion) and associated glaciological impacts.

260

261 **2.2.1. Subglacial dome growth, ice deformation and fracturing**

262 There are two notable examples of glacier deformation due to subglacial dome growth, without
263 extrusion through the overlying ice (Supplementary Table 1). The first is from Mount St Helens, when,
264 prior to the major 1980 eruption, minor eruptions and bulging resulted in crevassing and ice avalanches
265 on overlying glaciers (Brugman and Post, 1981). More recently, at Nevado del Huila in 2007–12,
266 subglacial domes formed between the South and Central peaks, and caused deformation of the overlying
267 glacier surface (Delgado Granados et al., 2005).

268

269 **2.2.2. Dome extrusion and glacier displacement**

270 There are only two documented examples of volcanic domes extruding through overlying glaciers
271 (Supplementary Table 1). The earliest observation, based on a single photograph, comes from Great
272 Sitkin, where, in 1945, a dome formed beneath, and then emerged through, the caldera glacier, resulting
273 in a melt hole surrounded by bulged and crevassed ice (Simons and Mathewson, 1955). A better-
274 documented example comes from Mount St Helens, where, following the major 1980 eruption, the ice-
275 free summit crater became occupied by a ~ 1 km^2, up to 200 m thick glacier (Schilling et al., 2004;

Walder et al., 2008). An eruption beneath this glacier in 2004–06 resulted in the formation of solid lava spines (parts of a subglacial dome), which extruded through the ice in the southern part of the Crater Glacier (Walder et al., 2007, 2008, 2010). As a result, the glacier was split into two parts, East Crater Glacier and West Crater Glacier, which were then squeezed between the growing lava dome and the crater walls (Walder et al., 2007, 2008). Because of this squeeze, the surfaces of the two glaciers buckled, forming multiple crevasses, and both glaciers locally doubled in thickness (at a rate of 0.6 m d^{-1}) (Walder et al., 2008). During this period, associated ice melt was limited, though both glaciers lost some volume. Since dome growth has stopped (in 2006), the glaciers have thinned in their upper reaches, and thickened in their lower (as 'normal' flow has resumed and ice has been redistributed downslope), and the terminus of East Crater Glacier has advanced (Walder et al., 2008).

2.2.3. Overall glaciological impacts of subglacial dome growth

The glaciological implications of subglacial dome growth are likely more important, and more conspicuous, for small/thin glaciers (e.g., mountain glaciers) than for large ice masses (e.g., continental ice sheets). Documented examples of domes deforming glaciers remain comparatively rare, and this is particularly true of dome extrusion. Despite this, in cases of subglacial dome growth and extrusion, the glaciological consequences can be extreme. This is most clearly documented at Mount St Helens, where the behaviour of a developing crater glacier(s) was severely disrupted by dome extrusion in 2004–06 (Section 2.2.2). The fracturing of ice surfaces in response to subglacial dome growth might also have indirect implications for glacier behaviour, since meltwater pathways to the glacier bed are potentially opened. Despite this, we are not aware of documented examples of glacier advance or acceleration in response to dome growth.

2.3. Subglacial eruptions

Subglacial volcanic eruptions (explosive or effusive) can have both thermal and mechanical impacts on overlying glaciers (Fig. 2d), leading to (i) the formation of ice craters, and associated fractures (Fig. 2d, points 20 & 2); (ii) partial glacier destruction; (iii) complete glacier destruction; and (iv) glacier

advance/acceleration (Fig. 2d, point 11). Documented examples of these different impacts are considered below.

2.3.1. Ice craters and fractures

The formation of ice craters (Fig. 4a & Fig 2d, point 20) is perhaps the most common glaciological consequence of subglacial volcanic eruptions. Examples have been documented in many glacio-volcanic regions globally, including Alaska, Chile, Columbia, Iceland, Kamchatka and in the Sub-Antarctic Islands (Supplementary Table 1). These craters are typically hundreds of metres deep and wide, and reflect notable ice loss. For example, between the 14th and 20th of April 2010, ~10% (~0.08 km^3) of the pre-eruption caldera ice at Eyjafjallajökull was destroyed by crater formation (Magnússon et al., 2012). As with ice cauldrons (Section 2.1.1.), craters are often surrounded by concentric crevasses, reflecting local reversals in ice flow direction (e.g., Nevado del Ruiz 1985; Volcán Hudson 1991, 2011; Gjálp 1996) (Fig. 4a; Fig. 2d, point 3), but not where the ice is comparatively thin (e.g., Eyjafjallajökull 2010).

Above less explosive vents and bedrock fissures (particularly those experiencing phreatic eruptions) (Fig 2d, point 23), smaller melt-pits and ice-fissures can form, often surrounded by heavily crevassed and deformed ice (e.g., Mount Westdahl 1991–92; Fourpeaked Mountain 2006) (Fig. 4b). Ice fissures can be kilometers long and hundreds of metres wide. They are a potential route for supraglacial water to drain subglacially (Section 2.1.1.) (Fig. 2d, point 25), but are also a means by which subglacial or englacial meltwater (which is often heated) can emerge at the surface and contribute to further supraglacial melt (potentially triggering lahars and/or floods) (e.g., Nevado del Huila 2007–12). The heavy fracturing of glaciers during subglacial eruptions can also leave them susceptible to subsequent erosion if, for example, they are later swept by pyroclastic density currents (Section 2.5.). Notable examples of heavily crevassed ice surfaces due to subglacial eruptions include the upper section of Chestnina Glacier following suspected volcanic activity at Mount Wrangell in 1999 (McGimsey et al., 2004); the southern part of the continuous ice rim at Mount Spurr, where ice was eroded into pinnacles following an eruption in 1953 (Juhle and Coulter, 1955); and the glacier on the west flank of Nevado del Huila as a result of eruptions in 2007–12 (Worni et al., 2012). In some cases, it has been suggested

that heavy crevassing reflects volcanically induced glacier advance, even though the behaviour itself may not have been observed (e.g., on the upper section of Chestnina Glacier at Mount Wrangell in 1999).

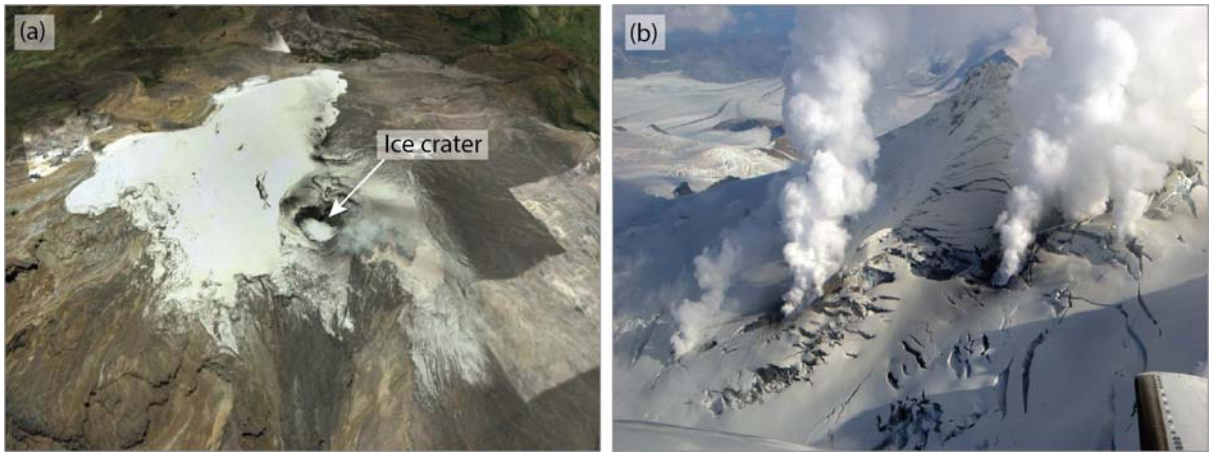

Fig. 4. Consequences of subglacial volcanic eruptions. (a) An ice crater (Arenas Crater) at Nevado del Ruiz, which opened repeatedly during multiple late 20th century eruptions. DigitalGlobe™ image, taken on November 10, 2015, viewed in GoogleEarth™. (b) Supraglacial crevasses, ice fissures and melt pits formed in 2006 above active subglacial vents at Fourpeaked Mountain. Photograph taken by C. Read (AVO/USGS) on September 24, 2006. Image obtained from the AVO/USGS database (http://www.avo.alaska.edu/image.php?id=11205). Description based on Neal et al. (2009).

2.3.2. Partial glacier destruction

The partial destruction of glaciers during subglacial volcanic eruptions is relatively common (Supplementary Table 1), and typically involves glacier beheading (i.e., the destruction of part of a glacier's accumulation zone). For example, White River Glacier, now Coalman Glacier, was partially beheaded during an eruption of Mount Hood between 1894 and 1912 (Lillquist and Walker, 2006). Shoestring, Forsyth, Ape, and Nelson Glaciers were beheaded during the 1980 eruption of Mount St Helens (Brugman and Post, 1981) (Fig. 5). The glacier draining the NW flank of Volcán Hudson was partially beheaded during an eruption in 1971, as 50–80% (60 km^2) of the volcano's intra-caldera ice was destroyed (Fuenzalida, 1976; Rivera and Bown, 2013). Tolbachinsky Glacier was partially

beheaded (i.e., the surface area of intra-caldera ice reduced from 1.54 to 0.5 km^2) during the 1975–76 eruption of Tolbachik (Vinogradov and Muraviev, 1982), and the 1982–83 eruption of Klyuchevskoy partially beheaded Kellya Glacier (Vinogradov and Muraviev, 1985). Beheading of this type is often a direct result of volcanic blasts, but can also occur during summit collapse. A notable example comes from Alaska, where the eruption of Novarupta in 1912 led to the collapse of the glacier-clad summit of Mount Katmai (~ 9 km to the east) (Hildreth and Fierstein, 2000, 2003, 2012). This collapse formed a ~ 5.5 km^3 summit caldera (Fig. 6) and partially beheaded Metrokin Glacier and Knife Creek Glaciers 3 and 4 (Hildreth and Fierstein, 2012). This glacier beheading left ice cliffs surrounding the crater rim (these cliffs were effectively the upper-ends of each glacier), with ice avalanches frequently falling into the crater, where the ice soon melted (Hildreth and Fierstein, 2012). Over a period of decades, these ice cliffs slowly thinned and retreated from the caldera rim (due to ice flow and melting). Part of the icefield outside the caldera experienced a reversal in flow direction as an ice tongue advanced into the caldera, ultimately terminating at (and calving into) the caldera-occupying lake (Fig. 6b).

It is notable that despite dramatic changes to glacier accumulation areas during glacier beheading (particularly at Mount Katmai in 1912 and Mount St Helens in 1980), these events rarely result in quick observable glacier retreat, likely because associated deposits (including tephra) act to insulate glacier surfaces, leading to stagnation (Sections 2.6.2. and 2.8.1.). However, over the longer-term (i.e., over decades), some beheaded glaciers have retreated or disappeared entirely (e.g., Shoestring, Nelson, Forsyth, and Dryer Glaciers at Mount St Helens).

In addition to cases of beheading, subglacial eruptions have directly destroyed parts of glacier ablation zones (tongues). For example, the 1977–80 eruption of Klyuchevskoy destroyed part of Shmidta Glacier's tongue (Muraviev et al., 2010, 2011; Muraviev and Muraviev, 2016). However, such cases are very rare, likely because glacier tongues rarely overlie volcanic vents (since eruptions tend to occur near the summits of volcanic edifices).

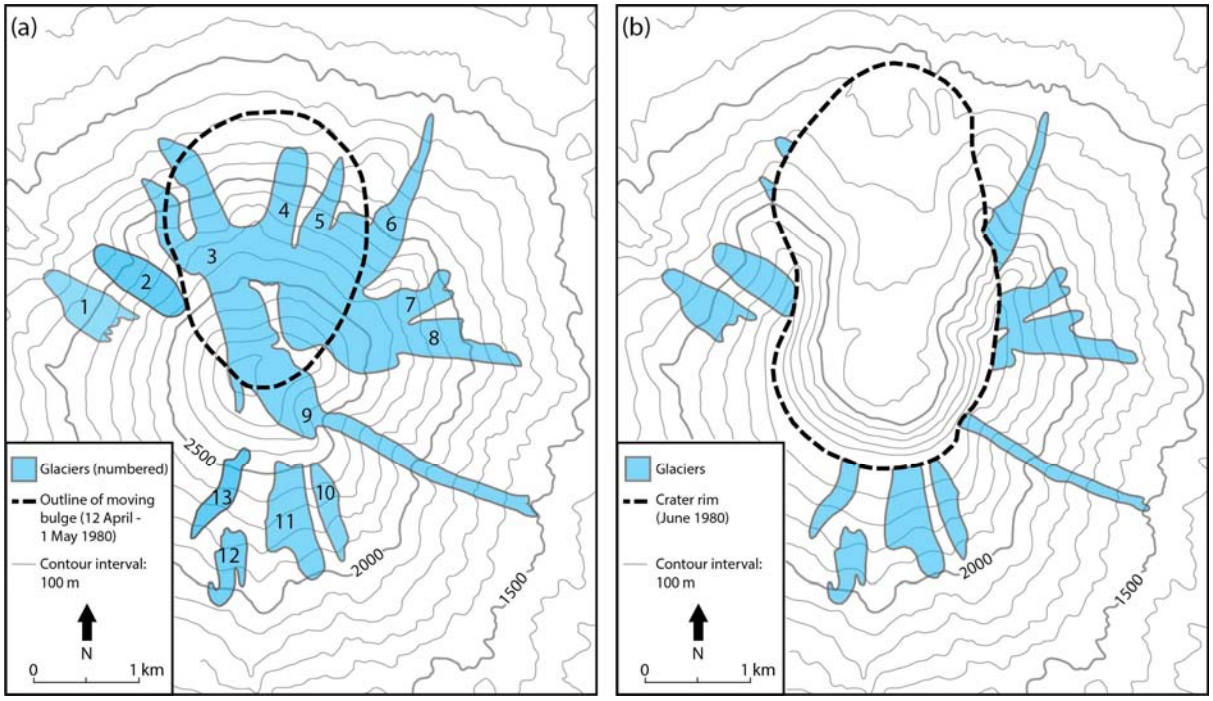

Fig. 5. Glaciers occupying Mount St. Helens (a) before, and (b) after the 1980 eruption. Numbered glaciers are: (1) Talus, (2), Toutle, (3) Wishbone, (4) Loowit, (5) Leschi, (6) Forsyth, (7) Nelson, (8) Ape, (9) Shoestring, (10) unnamed, (11) Swift, (12) unnamed, and (13) Dryer. The eruption beheaded some glaciers, and completely destroyed others. Figure based on Brugman and Post (1981).

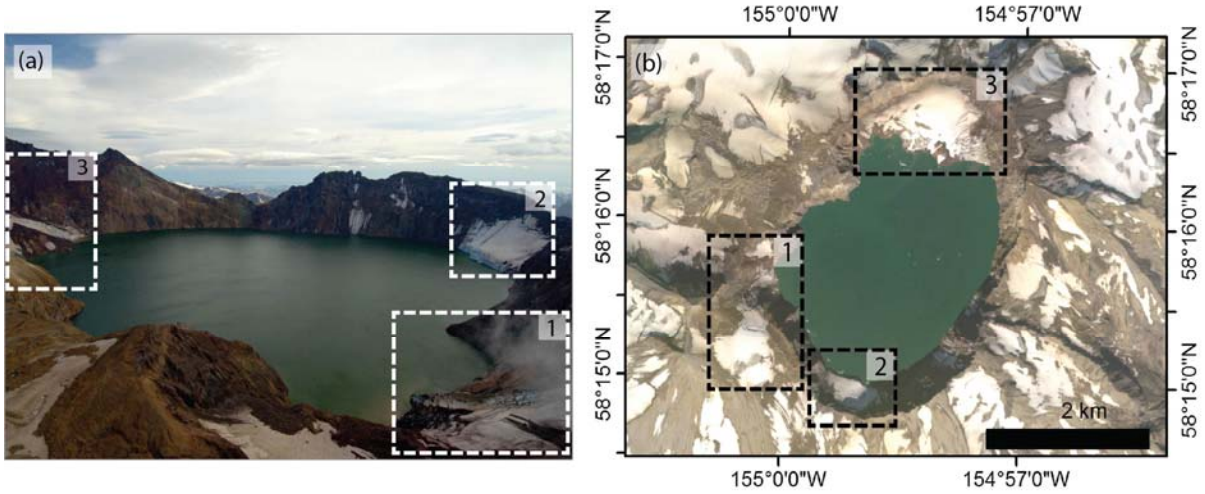

Fig. 6. Lake-filled caldera at Mount Katmai, formed due to summit collapse during the 1912 eruption of Novarupta (~ 9 km to the west). This figure shows an ice tongue extending from outside the SW margin of the caldera (dashed box 1), and two 'new' intra-caldera glaciers, one at the crater's southern margin (dashed box 2), and one at its northern margin (dashed box 3). (a) Photograph taken by C. Read

388 (AVO/USGS) on September 8, 2009, and obtained from the AVO/USGS database
389 (http://www.avo.alaska.edu/images/image.php?id=19191). (b) RapidEye™ image (September 1,
390 2016).
391
392 **2.3.3. Complete glacier destruction**
393 Cases of complete glacier destruction due to subglacial eruptions are rare (Supplementary Table 1). In
394 fact, the only conclusive, documented examples relate to the 1980 eruption of Mount St Helens, which
395 destroyed Loowit and Leschi Glaciers (Fig. 5). Though rare, these instances are interesting because they
396 potentially allow the initiation, style, and timing of glacier (re)growth to be directly observed (Section
397 3.1.3.).
398
399 **2.3.4. Glacier advance/acceleration**
400 As with enhanced subglacial heating (Section 2.1.), subglacial volcanic eruptions can result in
401 meltwater accumulation at the ice-bed interface, with the potential to promote subglacial sliding, glacier
402 advance and/or acceleration. For example, following the 1953 eruption of Klyuchevskoy Volcano,
403 Sopochny Glacier advanced 1–2 km; following the 1966–68 eruption, Vlodavtsa Glacier advanced 2.2
404 km; and following the 1977–80 eruption, Shmidta Glacier advanced until 1987, when part of the glacier
405 tongue was destroyed by a second eruption, before advancing again following the 2005–10 eruption
406 (Muraviev and Muraviev, 2016). Similarly, a fissure eruption at Tolbachik in 1975–76 caused the
407 advance of Cheremoshny Glacier (Muraviev et al., 2011), and several effusive events and low-intensity
408 explosive activity at Mt Belinda in 2001–07 (from a pyroclastic cone within an ice-filled caldera)
409 apparently caused an adjacent valley glacier to advance ('surge') a few hundred metres into the sea
410 (Smellie and Edwards, 2016).
411
412 **2.3.5. Overall glaciological impacts of subglacial eruptions**
413 The overall glaciological impact of subglacial eruptions is typically destructive, often involving
414 considerable ice loss. The most common outcome is the formation of ice craters, melt pits and fractures
415 (crevasses/ice-fissures). Despite their prevalence, smaller surface fractures and/or melt pits likely have

little notable or long-term impact on glacier behaviour. By contrast, large ice surface cauldrons likely persist for a considerable time and re-open during repeated periods of activity. Larger surface cauldrons and fractures might also have an indirect impact on glacier behaviour, since they are a potential route for meltwater drainage to the bed, and can cause local reversals in ice flow direction (Fig. 2a, point 3). Examples of glacier beheading due to subglacial eruptions are comparatively common, but since beheading tends to coincide with supraglacial tephra/debris deposition, glaciers that might otherwise retreat (due to the loss of their accumulation areas) tend to stagnate (Section 2.6.2.). Complete glacier destruction is rare, as is the destruction of parts of glacier ablation zones (tongues).

2.4. Lava flows

Lava is produced during both effusive and explosive volcanic eruptions (Fig. 2d, points 19 and 23), and can flow supraglacially and/or subglacially (Fig. 2d, points 21 and 24). Supraglacial lava flows (and their glaciological consequences) are often conspicuous (i.e., they stand-out against the ice/snow over which they flow), whereas subglacial flows are extremely difficult to observe. The latter are often inferred from either lava flows disappearing into (or emerging from) glaciers, or from their impact at the ice surface (e.g., where they form supraglacial channels or depressions) (Fig. 2d, points 21 & 22). The primary glaciological impact of lava flows is to cause ice melt, and documented examples of both supraglacial and subglacial flows with glaciological consequences are discussed below.

2.4.1. Supraglacial lava flows

Documented supraglacial lava flows are comparatively common and often result from lava fountaining (e.g., at Beerenberg 1970–72; Volcán Villarrica 1971; Mount Westdahl 1991–92; Volcán Llaima 2008; Mount Pavlof 2013) or emanate from summit lava lakes (e.g., Volcán Llaima 2008) (Supplementary Table 1). They can extend for hundreds or thousands of meters, and produce notable supraglacial melt (e.g., Beerenberg 1970–72; Volcán Llaima 1979, 2008; Klyuchevskoy 1984–85, 1985–86, 1986–90; Volcán Hudson 1991; Mount Westdahl 1991–92; Mount Shishaldin 1999; Mt Belinda 2001–07; Mount Pavlof 2013). However, where lava effusion rates are low and/or surface debris is thick/extensive this melt is not always rapid (Section 3.2.1.). One common consequence of supraglacial lava flows is the

formation of ice surface channels (sometimes tens of metres deep) (e.g., Volcán Villarrica 1971, 1984–85; Klyuchevskoy 1985–86; Mount Belinda 2001–07; Mawson Peak 2006–08; Volcán Llaima 2008) (Fig. 2d, point 21). These channels form as a direct consequence of melting, but can also develop through resulting hydrological erosion (e.g., Mount Shishaldin 1999). Where supraglacial lava flows begin to pond (Fig. 2d, point 22), crevasse-bounded depressions (melt pits) can form (e.g., Mount Veniaminof 1983–84, 1993–95, 2013; Mawson Peak 2006–08), into which supraglacial channels may extend. One example comes from Mawson Peak, where, in 2007, supraglacial lava flows (Fig 7a) and associated ponding appear to have melted supraglacial channels and a crevasse-bounded depression (Fig. 7b) (Patrick and Smellie, 2013).

Direct observations of the glaciological impacts of supraglacial lava flows are hindered by the snow often covering the higher altitude sectors of glaciers, i.e., where lava typically flows. Interactions between lava and snow are thus better observed and understood than interactions between lava and glaciers (e.g., Edwards et al., 2012, 2013, 2014, 2015). Much of this research indicates that lava's impact on snow varies according to differences in the velocity and style of lava flows, and the thickness and distribution of supra-snowpack debris (including tephra) (Edwards et al., 2014, 2015). In many cases, lava can flow across snow without causing substantial melt (Edwards et al., 2014, 2015), and snow typically protects underlying glacial ice (e.g., Hekla 1947; Eyjafjallajökull/Fimmvörðuháls 2010; Tolbachik 2012–13) (Edwards at al., 2012, 2014). However, since snowmelt is partly inhibited by trapped air (which limits heat transfer), the rate of melting can notably increase when lava comes into direct contact with ice (e.g., Villarrica 1984–85) due to the reduced pore space relative to snow (Naranjo et al., 1993; Edwards et al., 2013, 2015).

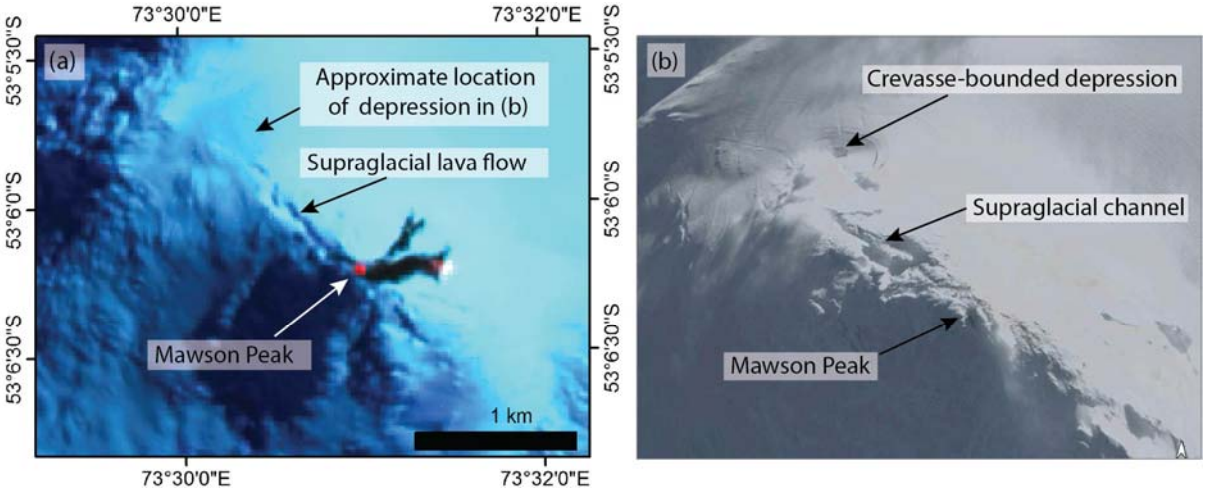

Fig. 7. (a) Supraglacial lava flows emanating from the summit of Mawson Peak on 17 February, 2007 (Landsat 7 ETM+ image). (b) Image from 13 May 2007 (DigitalGlobe™ image viewed obliquely in GoogleEarth™), showing a supraglacial channel and crevasse-bounded depression (melt pit), presumed to have been formed by the earlier supraglacial lava flow (shown in 'a') and subsequent ponding (not shown in 'a').

2.4.2. Subglacial lava flows

Subglacial lava flows are very difficult to observe, and, as a result, documented instances of their glaciological impact are far rarer than for supraglacial flows. Despite this, their impacts on glaciers have been observed in Chile and Iceland (Supplementary Table 1). As with supraglacial examples, subglacial lava flows can be kilometres long (e.g., Volcán Llaima in 1994; Eyjafjallajökull 2010) and usually result in ice melt (e.g., beneath Huemules Glacier during the 1971 eruption of Volcán Hudson) (Fig. 2d, point 24). Melting typically occurs above an advancing lava front (e.g., beneath Gígjökull during the 2010 eruption of Eyjafjallajökull). In some cases, subglacial melt can be violent, as ice and water rapidly vaporise when they interact with lava. One example comes from the western summit glacier at Volcán Llaima in 1994, when lava flow resulted in violent subglacial melt through the overlying glacier, and formed a subaerial ice channel up to ~ 150 m wide and ~ 2 km long (Moreno and Fuentealba, 1994). In some cases, subglacial lava flows have also resulted in doming, fracturing and subsidence of overlying

ice (e.g., Volcán Calbuco in 1961; Volcán Llaima 1994) (Fig. 2d, point 26), though the exact mechanisms involved remain unclear (Klohn, 1963).

2.4.3. Overall glaciological impacts of lava flows

The overall glaciological impact of lava flows is to cause ice melt, leading to the formation of supraglacial and/or subglacial channels and melt pits (Fig 2d, points 21, 22, 24 & 26). However, this melting is often localised, and likely has limited impact on overall glacier behaviour. In addition, the extent of melt is partly determined by lava effusion rates (Section 3.2.1.1.), and melt does not always occur, particularly if the glacier is protected by considerable surface snow or debris (Section 2.8.2.).

2.5. Supraglacial pyroclastic density currents

Pyroclastic density currents are hot, gravity-driven mixtures of volcanic debris and gas that emanate from volcanoes (Druitt, 1998). They are direct products of eruptions, or occur following dome growth and subsequent collapse (Section 2., Fig. 2c, point 18). Dilute pyroclastic density currents are often referred to as surges, and more concentrated examples as flows (Burgisser and Bergantz, 2002). The primary glaciological impact of pyroclastic density currents is to cause ice loss through melting and abrasion/erosion (Julio-Miranda et al., 2005; Waythomas et al., 2013), and documented examples are discussed below.

2.5.1. Melt, erosion/abrasion

Pyroclastic density currents have resulted in observed glacier mass loss in the USA, Chile, Columbia, Ecuador, and Mexico (Supplementary Table 1). They often melt and entrain snow and ice (with ice blocks up to metres in diameter), and can transition from hot-dry surges to cold-wet flows (i.e., forming lahars—Section 2.7.) as they progress down-glacier (e.g., Mount Redoubt 1989–90). Because of melt and entrainment, supraglacial pyroclastic density currents often cut ice channels/gullies (Fig. 2c, point 18), up to tens of metres deep, sometimes with associated snow and ice levees (e.g., Cotopaxi 1877; Nevado del Ruiz 1985; Popocatépetl 1994–01; Mount Redoubt 2009). An example comes from Nevado

514 del Ruiz during the 1985 eruption, when pyroclastic density currents cut surface channels 2–4 m deep
515 and up to 100 m wide into Nereidas, Azufrado and Lagunillas Glaciers (Pierson et al., 1990).
516 Pyroclastic density currents are particularly destructive if funneled through topographically
517 confined sections of ice, or cross steep and fractured icefalls (e.g., Drift Glacier during the 1966–68,
518 1989–90 and 2009 eruptions of Mount Redoubt; Kidazgeni Glacier during the 1992 eruption of Mount
519 Spurr; and Nereidas, Azufrado and Lagunillas Glaciers during the 1985 eruption of Nevado del Ruiz),
520 when crevasses can be mechanically abraded and seracs planed smooth (e.g., Nevado del Ruiz 1985).
521 In extreme cases, sections of ice can be scoured to bedrock, effectively beheading glaciers by separating
522 their accumulation and ablation zones. A notable example comes from the eruptions of Mount Redoubt
523 in 1966–68 and 1989–90, when a ~100 m thick gorge section of Drift Glacier was scoured to bedrock
524 by supraglacial pyroclastic density currents (Trabant et al., 1994) (Fig. 8). This separated the glacier's
525 accumulation and ablation zones, and reduced ice flux on the lower, piedmont section of Drift Glacier
526 by more than 50% (Sturm et al., 1986).
527 Where pyroclastic density currents emerge from steeper, confined sections of glaciers onto
528 shallower piedmont lobes (or other parts of the ablation area), they can still incise channels into the
529 glacier surface (sometimes exploiting pre-existing longitudinal crevasses). For example, at Mount
530 Redoubt in 1989–90 and 2009, channels in Drift Glacier's piedmont lobe were 10–100 m deep and
531 wide, and formed a deeply incised ice-canyon system, which extended to the glacier bed (Trabant and
532 Meyer, 1992) (Fig. 9). However, the extent of scouring tends to diminish down-slope and is minimal at
533 glacier termini (e.g., Nevado del Ruiz in 1985). In fact, the lower sections of glaciers are often more
534 likely to be covered by debris derived from pyroclastic density currents (e.g., Mount Spurr 1992)
535 (Section 2.8.), protecting the surface from further incision (Section 2.8.2).
536 In general, dilute, fast-moving pyroclastic surges have limited glaciological impact since they
537 are unable to produce much melting (i.e., they do not have enough thermal mass), but higher-density
538 pyroclastic flows efficiently melt and entrain glacial ice. This was exemplified during the 1985 eruption
539 of Nevado del Ruiz, when both dilute pyroclastic surges and concentrated pyroclastic flows were
540 produced. The former caused no significant melting, while the latter eroded and melted into the
541 underlying glaciers (Pierson et al., 1990). During the 1985 eruption, pyroclastic density currents also

promoted ice and rock avalanches that led to major ice losses from glaciers in the Azufrado, Lagunillas and Farallon-Guali basins—destroying the 10–15 m thick crevassed terminus of Lagunillas Glacier and the hanging glaciers on the headwall of the Azufrado valley (Pierson et al., 1990).

2.5.2. Overall glaciological impacts of pyroclastic density currents

Pyroclastic density currents are some of the most glaciologically destructive volcanic events, as they rapidly melt and entrain ice, particularly on steep and crevassed sections of glaciers (e.g., at icefalls). In extreme cases, they can scour glacier ice to bedrock (effectively causing glacier beheading), and are known to produce voluminous lahars (McNutt et al., 1991) (Section 2.7). However, the glaciological impact of pyroclastic density currents is partly determined by the concentration of clasts present, with concentrated flows more destructive than dilute surges, and is limited where pre-existing surface debris is extensive/thick (Section 2.8.2.).

Fig. 8. The upper 'gorge' section of Drift Glacier (a) following the 1989–90 eruption of Mount Redoubt, and (b) immediately prior to the 2009 eruption. In (a), this section of the glacier has recently been scoured to bedrock (by pyroclastic density currents), effectively beheading the glacier. In (b) the glacier has recovered from beheading during the the 1989–90 eruption, but due to a period of unrest prior to the 2009 eruption, a prominent melt hole/pit is evident above a water fall shown in the 1990 image. Photographs taken by G. McGimsey (AVO/USGS), and obtained from the AVO/USGS database (http://www.avo.alaska.edu/images/image.php?id=16578).

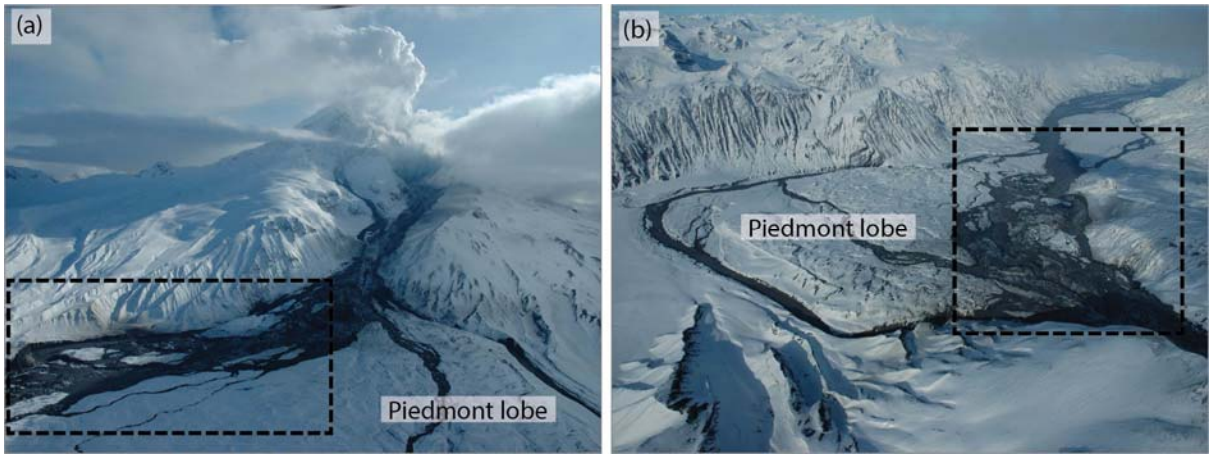

Fig. 9. Channels (in dashed boxes) and debris on the piedmont lobe section of Drift Glacier, formed by pyroclastic density currents and associated lahars following the 2009 eruption of Mount Redoubt. (a) View towards the south. (b) View towards the north. Photographs taken by G. McGimsey (AVO/USGS) on March 26, 2009. Images obtained from the AVO/USGS database (http://www.avo.alaska.edu/images/image.php?id=47241; http://www.avo.alaska.edu/images/image.php?id=47251). Descriptions based on McGimsey et al. (2014).

2.6. Supraglacial deposition of tephra

The deposition of tephra (ash, rock fragments and particles ejected by volcanic eruptions) can occur on glaciers occupying volcanoes or on glaciers down-wind of source eruptions. The glaciological impact depends on many factors including tephra temperature, thickness, spatial coverage, pre-existing surface

577 debris, and weather conditions during and after deposition (Brook et al., 2011; Nield et al., 2013). For
578 example, the impact of tephra cover is likely to be less important for glaciers that are debris- or snow-
579 covered prior to tephra deposition (Rivera et al., 2012). In many cases, directly following deposition,
580 supraglacial tephra causes increased melt due to its elevated temperature (though, except in a narrow
581 zone close to the vent, many fall deposits are probably cold when they land), relative to the ice on which
582 it lands. Once cooled, the impact might still be to promote melt, particularly if the tephra deposit is thin
583 and/or discontinuous (Fig. 2d, point 28), as the albedo of the ice surface is reduced (Richardson and
584 Brook, 2010). However, when tephra is more continuous, and particularly once it exceeds a threshold
585 thickness, surface melt is likely to reduce (Fig. 2d, point 27). This effect is due, in large part, to the low
586 thermal conductivity of the tephra, and (to a lesser degree) to its ability to shield ice from solar radiation
587 (Brook et al., 2011; Rivera et al., 2012; Wilson et al., 2013). Thus, the glaciological impact of tephra
588 cover is largely governed by its thickness, and whether or not the threshold thickness, which varies from
589 glacier to glacier, is exceeded (Kirkbride and Dugmore, 2003). Documented examples of supraglacial
590 tephra causing increased or decreased melt, and associated changes in glacier dimensions, are discussed
591 below.
592
593 **2.6.1. Increased melt**
594 Examples of supraglacial tephra deposition resulting in increased melt and/or glacier recession come
595 from Chile, the Sub-Antarctic Islands, Ecuador, Iceland, Mexico, and New Zealand (Supplementary
596 Table 1). For example, on Deception Island, a short-lived eruption in 1969 deposited supraglacial tephra
597 which lowered the ice surface albedo, and resulted in particularly negative mass balance for three
598 subsequent years (up to 1973) (Orheim and Govorukha, 1982). In some cases, increased melt is caused
599 by tephra deposition on glaciers that are kilometres away from source eruptions. For example, during
600 the 2008 eruption of Volcán Chaitén, tephra deposition increased melt at glaciers occupying Volcán
601 Michinmahuida, ~ 15 km to the east (Alfano et al., 2011; Rivera et al., 2012). Similarly, following the
602 1999–2001 eruption of Tungurahua Volcano, tephra deposition on glaciers occupying Chimborazo
603 Volcano, ~ 40 km to the west, led to increased melt and small-scale glacier retreat (Morueta-Holme et
604 al., 2015; La Frenierre and Mark, 2017).

Where glaciers are present on tephra-producing volcanoes, their upper reaches (i.e., in close proximity to vents) can become covered by thick tephra, promoting ice preservation, while lower sections are covered by comparatively thin tephra, promoting ice loss and glacier disintegration (Wilson et al., 2013). For example, during the 1994–2001 eruptive period at Popocatépetl, the upper part of the glacier occupying its summit was covered with thick tephra, whilst its lower reaches were covered with a thinner, discontinuous tephra layer. As a result, ice melt was suppressed in the upper part of the glacier, where a flat area began to form, and ice began to thicken. This region was separated from the lower section of the glacier, where rapid ice loss resulted in 'stair-like' morphology (Julio-Miranda et al., 2008). Because of this differential ablation, the glacier surface steepened, and ice was transmitted towards the terminus as a kinematic wave of ice thickening (Julio-Miranda et al., 2008). This did not cause glacier advance, but led to increased melt as ice was transferred into the ablation zone. As a result, the glacier front retreated dramatically in 2000, and much of the remainder began to fragment (by a combination of differential ablation and tephra remobilisation) (Julio-Miranda et al., 2008). By 2001, the glacier had fragmented into a set of ice blocks. Though these ice blocks were insulated on their upper surfaces, their tephra-free flanks were exposed to ablation. Ultimately, tephra deposition notably enhanced climate-related glacier recession, with ~ 53% of the glacier's surface area lost between 1996 and 2001 (Julio-Miranda et al., 2008). In 2004, the glacier disappeared completely (or at least the remaining ice was no longer flowing) (Julio-Miranda et al., 2008).

Despite such instances, making clear links between tephra deposition and glacier retreat can sometimes be difficult. For example, at Volcán Lautaro, eruptions during the 20th century deposited tephra on some adjacent glaciers (many of these were outlets of the South Patagonian Ice Field). O'Higgins Glacier experienced rapid retreat (~ 14.6 km between 1945 and 1986). However, whether this was the result of increased calving or supraglacial tephra deposition (and perhaps geothermal heating) is unclear (Lopez et al., 2010).

In addition to tephra, other volcanic materials (including 'bombs') can be ejected from volcanoes, land supraglacially, and cause ice-melt. For example, during the 1994–2001 eruptive period at Popocatépetl, incandescent material landed supraglacially, and formed melt holes and impact craters (via physical impact and subsequent melting) (Julio-Miranda et al., 2008). The parts of glaciers where

633 ejected material typically lands (i.e., in a glacier's upper reaches, in proximity to vents) are often snow
634 covered, hence melt pits have been observed in supraglacial snow (e.g., Nevado del Ruiz, 1985; Belinda
635 2001–07) (Pierson et al., 1990; Smellie and Edwards, 2016), but impacts on underlying ice often remain
636 unclear. In addition, melt due to the supraglacial deposition of ejecta is often very localised, and is likely
637 to have little (if any) impact on overall glacier behaviour.
638
639 **2.6.2. Decreased melt**
640 There are numerous documented instances where supraglacial tephra deposition has resulted in
641 decreased melt and/or glacier stagnation (preservation). This includes examples from the USA, Chile,
642 Iceland, Jan Mayen Island, and Kamchatka (Supplementary Table 1). For example, tephra deposited on
643 the surface of Svínafellsjökull during the 2011 eruption of Grímsvötn is estimated to have reduced
644 ablation rates by up to 59% (Nield et al., 2013). Kozelsky Glacier stagnated over much of the 20th
645 century in response to supraglacial tephra deposited during the 1945 eruption of Avachinsky
646 (Vinogradov and Muraviev, 1982; Muraviev et al., 2011). The same happened to Knife Creek Glacier
647 and two of the Mount Griggs Glaciers following the 1912 eruption of Novarupta (Hildreth and Fierstein,
648 2012).
649 A small number of glaciers are thought to have advanced in response to tephra-related decreases
650 in melt. For example, Gígjökull advanced following the deposition of Hekla tephra in 1947 (Kirkbride
651 and Dugmore, 2003), and Knife Creek Glaciers 1, 2, 4, 5 and one of the Mount Griggs Glaciers
652 advanced following the 1912 eruption of Novarupta (Hildreth and Fierstein, 2012). However, given
653 overall climatically driven glacier mass loss during the late 20th century, in many cases ice insulation
654 beneath supraglacial tephra has simply slowed the rate of recession. For example, following the 1970–
655 72 eruption of Beerenberg, supraglacial tephra reduced surface ablation and thus slowed the rate of
656 retreat at Sørbreen (this continued up to 1978) (Anda et al., 1985). Similarly, due to a mantle of
657 supraglacial tephra, the late 20th century retreat of Pichillancahue-Turbio Glacier at Volcán Villarrica
658 has been slower than for other glaciers in the region (Masiokas et al., 2009).
659
660 **2.6.3. Overall glaciological impacts of supraglacial tephra deposition**

661 The overall glaciological impacts of supraglacial tephra deposition are complex, with documented
662 examples of both increased and decreased melt. The former are often instances where tephra cover is
663 thin and/or discontinuous (Fig 2d. point 28), while the latter reflect thick and/or continuous coverage
664 (Fig 2d, point 27). There are also documented examples of glacier advance or retreat in response to
665 supraglacial tephra deposition, but making conclusive causal links between changes in glacier
666 dimensions and periods of deposition is difficult. In many cases, tephra distributes heterogeneously
667 across a glacier's surface and therefore enhances melt on some portions, and restricts it on others. This
668 differential melting can result in an undulating ice surface, and in some cases has a notable impact on
669 glacier dynamics and mass balance.
670
671 **2.7. Floods and lahars**
672 Floods (including jökulhlaups—glacier outburst floods) and lahars (mixed meltwater and debris) are a
673 common consequence of glacio-volcanic activity, extensively studied in the wider geo-hazards
674 framework (Major and Newhall, 1989). Floods are distinguishable from lahars by their debris content
675 (i.e., floods are dilute, while lahars are concentrated with debris). However, they are grouped together
676 here, since initially dilute floods can transition into lahars as they accumulate debris (e.g., Mount
677 Shishaldin 1999) (Fig. 2a, point 4), and their triggers and glaciological impacts are often similar. Floods
678 and lahars are caused by sudden ice melt linked to many of the processes described in previous sections
679 of this paper, including: melt caused by enhanced subglacial heat flow (e.g., Mount Kazbek various 20th
680 and 21st century); melt during subglacial eruptions (e.g., Hekla 1947); hot subglacial water migrated to
681 the glacier surface through ice fissures (e.g., Deception Island 1969; Mount Westdahl 1991–92; Nevado
682 del Huila 2007–12); melt caused by supra- and sub-glacial lava flows (e.g., Beerenberg 1970–72;
683 Volcán Llaima 1979, 1994, 2008; Klyuchevskoy 1984–85, 1985–86, 1986–90; Volcán Hudson 1991;
684 Mount Westdahl 1991–92; Mount Pavlof 2013); melt caused by pyroclastic density currents (e.g.,
685 Cotopaxi 1877; Volcán Calbuco 1961; Mount St Helens 1980; Mount Spurr 1992; Popocatépetl 1994–
686 01; Mount Redoubt 2009; Mount Pavlof 2013); and melt generated by the supraglacial deposition of
687 tephra (e.g., Volcán Hudson 1991). The glaciological consequences of floods and lahars (i.e., the focus
688 of interest here) include supraglacial and subglacial melt/erosion (including ice break-off) (Fig. 2a,

689 point 13) and glacier advance/acceleration. Documented examples of these different outcomes are
690 discussed below.
691
692 **2.7.1. Supraglacial melt/erosion**
693 Examples of floods and/or lahars causing supraglacial melt/erosion are common and are reported in
694 Alaska, Chile, Columbia, the Sub-Antarctic Islands, Ecuador, Iceland, Kamchatka, and New Zealand
695 (Supplementary Table 1). These (often warm) floods and lahars can cut supraglacial channels/canyons
696 (with vertical ice walls) as they melt and entrain ice (e.g., Mount Westdahl 1978 and 1991–92; Mount
697 Shishaldin 1999; Fourpeaked Mountain 2006) (Fig. 10; Fig. 2a, point 5). Supraglacial channels can be
698 kilometres long (e.g., channels cut into the surface of Vatnajökull during the 1996 eruption of Gjálp;
699 and on the surface of the glacier occupying the NE flank of Mount Pavlof following its 2013 eruption)
700 and terminate in newly developed, or pre-existing, moulins or cauldron-shaped collapse features (e.g.,
701 on Drift Glacier during the 1966–68 eruption of Mount Redoubt; and on Vatnajökull during the 1996
702 eruption of Gjálp) (Fig. 2a, point 8).
703

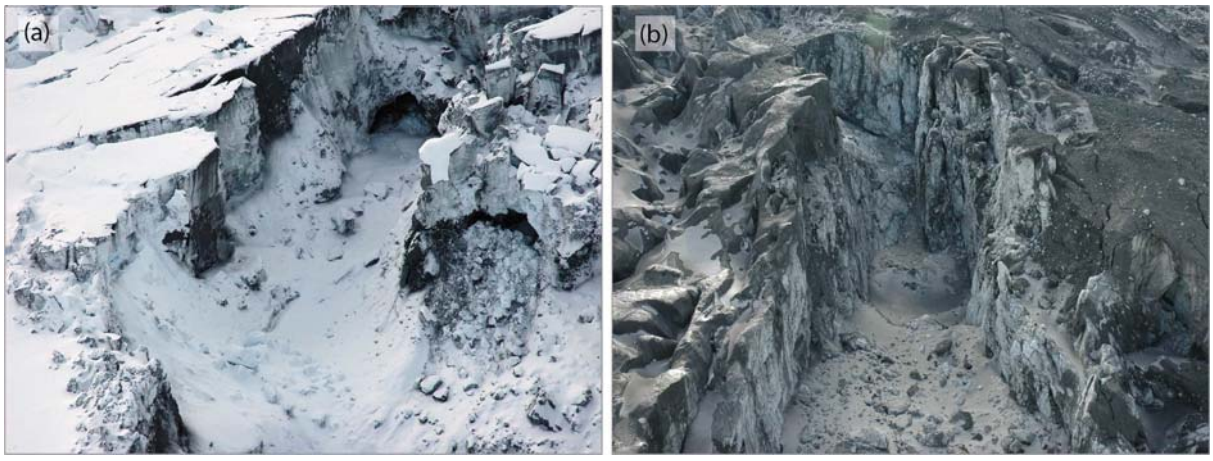

704
705 Fig. 10. Supraglacial channels cut by an outflow event (lahar/flood) during the 2006 eruption of
706 Fourpeaked Mountain (channels are cut into a glacier on the mountain's NW flank). (a) The point of
707 origin of the outflow event. (b) A deeply incised canyon (~ 100 m deep and wide). Both photographs
708 taken by K.L. Wallace (AVO/USGS) on September 25, 2006. Images obtained from the AVO/USGS

709 database (http://www.avo.alaska.edu/image.php?id=11837;
710 http://www.avo.alaska.edu/image.php?id=11848). Descriptions based on Neal et al (2009).
711
712 **2.7.2. Subglacial melt/erosion**
713 Documented instances of floods or lahars causing subglacial melt/erosion are comparatively rare, likely
714 reflecting difficulties with observing subglacial environments (Section 3.2.2.). Despite this, there are
715 two notable examples from Iceland (Supplementary Table 1). The first occurred following the 1996
716 eruption of Gjálp, when warm (15–20°C) meltwater travelled 15 km along a narrow channel beneath
717 Vatnajökull and into Grímsvötn subglacial lake, exiting it later as a jökulhlaup (Gudmundsson et al.,
718 1997). Subglacial melting occurred along the meltwater flow path into Grímsvötn, inside the lake, and
719 on the jökulhlaup path out of the lake, and resulted in supraglacial subsidence and the formation of a
720 shallow linear depression in the ice surface (Gudmundsson et al., 1997). The second example occurred
721 during the first days following the main explosive eruption at Eyjafjallajökull, in 2010, when meltwater
722 drained beneath Gígjökull in several jökulhlaups (Magnússon et al., 2012). Ice-melt and mechanical
723 erosion occurred along the subglacial flood path due to the thermal and frictional energy of floodwaters,
724 forming a subglacial channel. However, because of the high water pressures, floodwaters destroyed the
725 roof of the channel, and emerged supraglacially as a slurry flow (Magnússon et al., 2012). Thus,
726 drainage was subglacial for the first 1–1.5 km, but then water emerged, and drained supraglacially down
727 both sides of the glacier.
728 Documented examples of subglacial floods breaking blocks of ice from glacier termini (Fig.
729 2a, point 13) are rare and only reported in Iceland. For example, at Katla, in 1918, an eruption beneath
730 a ~ 400 m thick section of the Mýrdalsjökull ice cap caused a major jökulhlaup, with water flowing
731 both supraglacially and subglacially. The force of the subglacial meltwater is considered to have torn
732 icebergs (50–60 m diameter) from the glacier terminus, where it also blasted a 1,460–1,830 m long,
733 366–550 m wide, and 145 m deep gorge (Russell et al., 2010). Similarly, at Grímsvötn in 1934,
734 subglacial melt led to a large jökulhlaup that removed ice blocks from the terminus of Skeidarárjökull,
735 resulting in 40-m-high fracture faces (Nielsen, 1937).
736

737 **2.7.3. Glacier advance/acceleration**

738 Documented examples of floods and/or lahars causing glacier advance/acceleration are uncommon, and
739 the evidence connecting these events is rarely clear. Despite this, there are examples from Alaska, the
740 Sub-Antarctic Islands, and Iceland (Supplementary Table 1). For example, at Deception Island, in 1969,
741 a large jökulhlaup flowed across the summit ice cap. Downslope from the ice fissures from which this
742 flood emanated, the ice experienced a short-lived surge-like advance (Smellie and Edwards, 2016). At
743 Katla during the 1918 jökulhlaup, while icebergs were torn from the glacier front (Section 2.7.2.), the
744 whole glacier terminus floated (Fig. 2a, point 12) and may have moved forward (Smellie and Edwards,
745 2016). On Montagu Island in 2001–07, subglacial melt, triggered by the eruption of Mt Belinda caused
746 an adjacent valley glacier to advance a few hundred metres into the sea (Smellie and Edwards, 2016).
747 Finally, during the 2004 Grímsvötn eruption, a jökulhlaup (the onset of which preceded the eruption by
748 four days) apparently caused the short-term (monthly) flow velocity of Skeidarárjökull (an outlet of
749 Vatnajökull) to increase by up to 0.4 m d^{-1}, compared to annual values (Martinis et al., 2007; Sigurðsson
750 et al., 2014) (Fig. 11). This acceleration occurred over the entire width of the glacier, and was potentially
751 caused by increased subglacial sliding due to widespread basal lubrication (Martinis et al., 2007;
752 Sigurðsson et al., 2014).
753
754 **2.7.4. Overall glaciological impacts of floods and lahars**

755 The overall glaciological impact of floods and lahars is typically destructive, casing ice melt, erosion,
756 entrainment, and, in a small number of cases, ice-block break-off from glacier termini. There are
757 examples where floods are presumed to have caused glacier advance/acceleration. However, this only
758 relates to a small number of cases, and the evidence is rarely clear. Many of the better-documented
759 examples of interactions between floods/lahars and glaciers come from Iceland, where glaciers are
760 comparatively accessible, close to settlements, and easily observed.
761

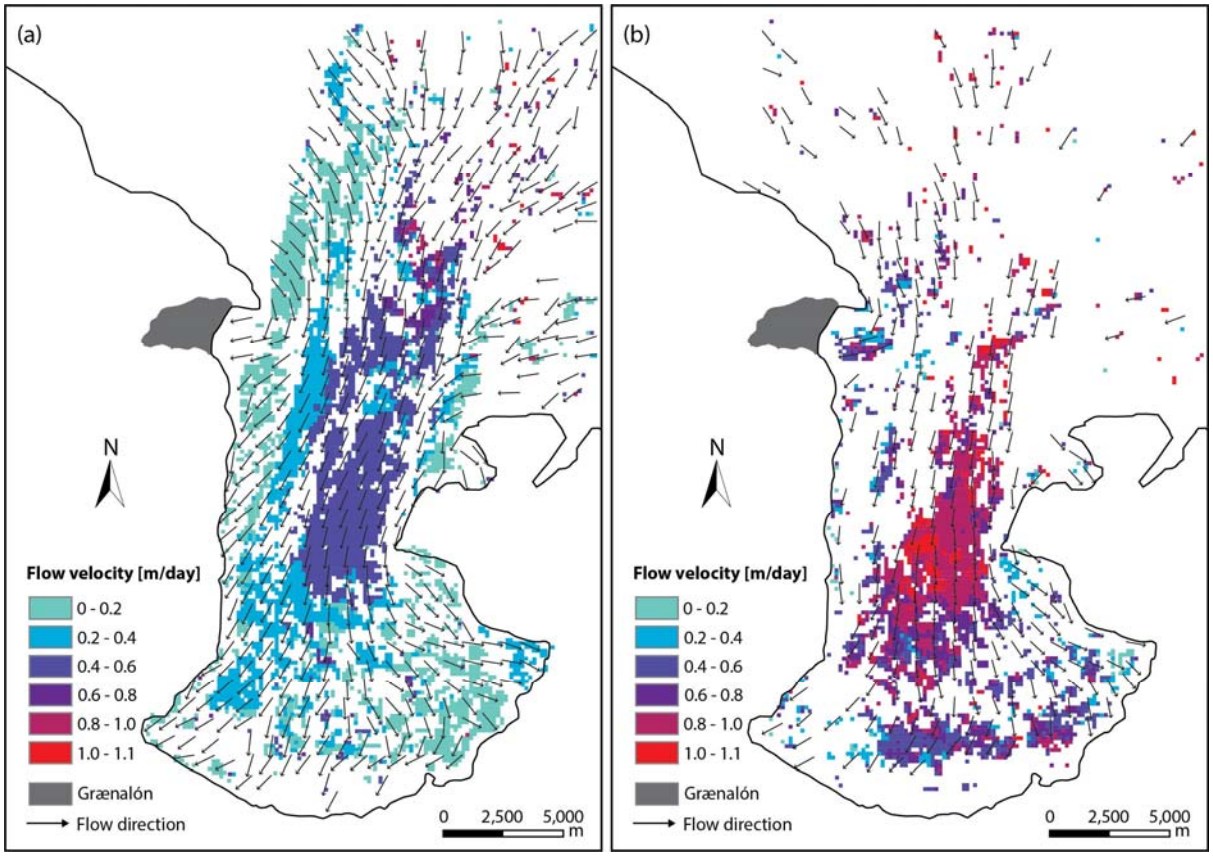

Fig. 11. Surface velocity fields at Skeidarárjökull (an outlet of Vatnajökull), derived from ASTER satellite images (Martinis et al., 2007). (a) Velocity between September 27, 2004 and July 28, 2005 (i.e., approximately annual velocity). (b) Velocities during a period (i.e., from September 27, 2004 to November 30, 2004) which coincides with the 2004 eruption of Grímsvötn (November 1–6). The accelerated flow in (b) is thought to result from increased glacier sliding, related to widespread basal lubrication caused by a subglacial jökulhlaup. Figure modified from Sigurðsson et al. (2014).

2.8. Supraglacial deposition of other glacio-volcanic products

Many of the glacio-volcanic processes outlined in this paper not only have direct glaciological impacts, but also result in debris which, when deposited supraglacially, can impact glacier response to other forcing mechanisms (e.g., climate). In almost all cases, the glaciological consequence is that the debris acts to reduce ice ablation, and/or protects ice from further thermal and/or mechanical erosion. Documented examples of these scenarios are discussed below.

2.8.1. Reduced ablation

Debris derived from pyroclastic density currents (e.g., Novarupta 1912; Bezymianny 1955–57), avalanches/landslides (Klyuchevskoy 1944–45; Mount Redoubt 1989–90), and floods/lahars (Mount Redoubt 1966–68, 1989–90, 2009) has acted to insulate glacier ice (Supplementary Table 1). The main result is typically a slowing in the rate of climatically driven glacier retreat/mass-loss. However, in some cases, the insulating impact of surface debris is thought to have caused glacier advance. The most notable example is Erman Glacier, which has advanced by ~ 4 km since the 1944–45 eruption of nearby Klyuchevskoy volcano (from which the glacier partly emanates). This glacial advance is ongoing (Fig. 12), despite regional atmospheric warming, and is thought to reflect the impact of landslide debris which was deposited on the glacier's accumulation area during the 1944–45 eruption, and subsequently spread to cover the ablation area where it likely acted to insulate the underlying ice (Muraviev and Muraviev, 2016; Dokukin et al., 2017).

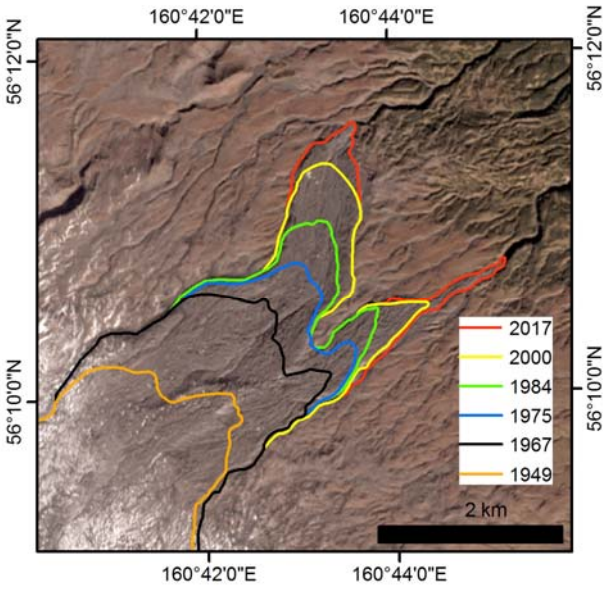

Fig. 12. Post-1949 advance of Erman Glacier (Kamchatka) following the supraglacial deposition of landslide debris during the 1944–45 eruption of Klyuchevskoy volcano (from which the glacier partly emanates). Image based on Muraviev and Muraviev (2016).

2.8.2. Glacier protection from erosion

796 Instances where supraglacial deposits derived from the glacio-volcanic processes outlined in this review
797 have acted to protect ice from subsequent erosion/incision are best documented at Mount Redoubt
798 (Supplementary Table 1). For example, floods and lahars during the 1989–90 and 2009 eruptions led to
799 the formation of a supraglacial 'ice diamict', composed of gravel-sized clasts of glacier ice, rock, and
800 pumice in a matrix of sand, ash, and ice (frozen pore water) (Waitt et al., 1994). On the piedmont section
801 of Drift Glacier (Fig. 9), these deposits were 1–10 m thick, and protected the underlying ice from
802 thermal and mechanical erosion by later supraglacial pyroclastic density currents and lahars (Gardner
803 et al., 1994).
804
805 **2.8.3. Overall glaciological impacts of the supraglacial deposition of other glacio-volcanic**
806 **products**
807 The primary glaciological consequence of supraglacial pyroclastic, avalanche, lahar and flood deposits
808 is to insulate the underlying ice, and protect it from further thermal and/or mechanical erosion. This
809 typically promotes glacier preservation/stagnation, and partly acts to counter the otherwise largely
810 glaciologically destructive impacts of volcanic activity.
811
812 **3. Present and future volcanic impacts on glaciers**
813 Here, we use the information outlined in section 2 to address three general questions about volcanic
814 impacts on glaciers. 1. What are the overall glaciological consequences of volcanic activity? 2. How
815 many of Earth's glaciers are impacted by such activity? 3. What is the future importance of volcanic
816 impacts on glaciers?
817
818 **3.1. What are the overall glaciological consequences of volcanic activity?**
819 The glaciological consequences of volcanic activity typically relate to local increases in meltwater and
820 debris. However, the importance of different processes and interactions varies according to the
821 timescale under consideration.
822
823 **3.1.1. Short-term**

824 Over the period of days-to-months, the glaciological impacts of volcanic activity are typically
825 destructive, involving ice-melt, erosion and entrainment (e.g., Sections 2.3.2. and 2.3.3). For example,
826 during the 1996 eruption at Gjálp, 3 km^3 of ice melted in just 13 days (when the eruption ended), with
827 a further 1.2 km^3 melting over the following three months (Gudmundsson et al., 1997). One of the key
828 reasons mass loss dominates over the short-term is that it can be caused by a number of processes that
829 typically occur during the early stages of volcanic activity, including enhanced subglacial heat flow,
830 subglacial volcanic eruptions, supra- and sub-glacial lava flows, pyroclastic density currents,
831 floods/lahars, and the supraglacial deposition of hot tephra. In some cases, ice loss due to these
832 processes results in supraglacial subsidence, deformation, and fracturing; in other cases, glaciers are
833 partially or entirely destroyed.
834
835 **3.1.2. Medium-term**
836 Over the period of months-to-years, volcanic activity can act to either destroy or preserve glacial ice.
837 For example, pyroclastic density currents, which are destructive over the short-term, may lead to ice
838 preservation over the medium-term (and perhaps longer; Carey et al., 2010), as their deposits insulate
839 and protect underlying ice (Section 2.8.). These medium-term impacts may also act to counter some of
840 the short-term destruction. For example, following beheading, glaciers that might otherwise rapidly
841 retreat (in response to partial or complete removal of their accumulation areas) often stagnate due to ice
842 protection beneath supraglacial tephra/debris (Section 2.3.2.). Despite such instances, documented
843 cases of volcanic activity causing glacier stagnation and/or advance/acceleration are certainly less
844 common than instances of mass loss and/or glacier retreat. Clear evidence linking volcanic activity to
845 periods of glacier advance or acceleration is particularly scarce. The medium-term impacts of volcanic
846 activity also partly depend on factors such as the weather conditions following eruptions (which control
847 how supraglacial material is re-distributed) (Nield et al., 2013), and glaciological characteristics such
848 as the efficiency of subglacial drainage (Section 3.2.1.2.), and therefore vary from glacier to glacier.
849
850 **3.1.3. Long-term**

Glaciological impacts of volcanism can be observed years-to-decades after periods of activity (e.g., Carey et al., 2010). For example, the advance of Erman Glacier continues to this day, apparently in response to the supraglacial deposition of landslide debris during the 1944–45 eruption of Klyuchevskoy (Fig. 12). In some cases, glaciers that were destroyed or beheaded by volcanic activity fail to recover, and disappear entirely (e.g., Shoestring, Nelson, Forsyth, and Dryer Glaciers at Mount St Helens). In other cases, beheaded glaciers recover and new glaciers form in areas where they were previously destroyed. A notable example of recovery from beheading is Drift Glacier, which was beheaded by pyroclastic density currents during the 1966–68 and 1989–90 eruptions of Mount Redoubt (Section 2.5.1.), but in less than a decade had re-formed (e.g., Fig. 8). Following the 1966–68 beheading, the reconnection of the regenerated part of the glacier and the piedmont section below resulted in a kinematic wave of thickening (of > 70 m) and surface acceleration (by an order of magnitude) in the lower section of the glacier, whilst thinning (by ~ 70 m) occurred in the upper section. These processes were accompanied by surface crevassing, likely reflecting the glacier's return to its pre-eruption equilibrium condition (Sturm et al., 1986).

Notable examples of new glacier formation following destruction by volcanic activity come from Mount St Helens and Mount Katmai. At Mount St Helens, some glaciers were beheaded and some destroyed during the 1980 eruption (Fig. 5), but, by 1999, a ~ 1 km^2 and ~ 200 m thick glacier had reformed in the initially ice-free summit crater (Schilling et al., 2004; Walder et al., 2007). This glacier was later displaced and deformed by subglacial dome extrusion (Section 2.2.). At Mount Katmai, summit collapse and glacier beheading during the 1912 eruption of Novarupta (Section 2.3.2.) generated a glacier-free caldera. Snow and ice then began to accumulate on inward sloping intra-caldera benches (300–400 m above the caldera floor). Snow patches had accumulated by 1917, modest snowfields by 1923, while the earliest confirmed reports of active glacial ice came in 1951. According to Muller and Coulter (1957), intra-caldera glaciers had effectively formed within 20 years of the summit collapse. These 'new' glaciers formed at the crater's northern and southern margins, with an ice tongue at the crater's SW margin extending from outside the caldera (Fig. 6). By 1953/54, the South glacier terminated in cliffs 50–80 m above the caldera lake, and the northern glacier reached halfway down to the lake. By 1987, both terminated just above lake level, but upon reaching the heated lake, melted

879 rapidly. Thus, the volcanic lake (which has increased in depth since its inception) has acted to deter
880 glacier growth/advance (Hildreth and Fierstein, 2012).
881 Overall, despite initial destruction or damage from which some glaciers fail to recover, the
882 long-term glaciological impacts of volcanic activity often appear to be constructive, involving glacier
883 re-growth or the formation on new ice masses.
884
885 **3.2. How many of Earth's glaciers are impacted by volcanic activity?**
886 The dataset presented here (Supplementary Table 1) suggests that observed volcanic impacts on the
887 behaviour of modern glaciers are comparatively rare, and are only documented for ~ 150 glaciers (~
888 0.08% of the global glacier population), during ~ 90 separate volcanic events or periods of activity.
889 However, in considering the importance of these numbers, it is worth focusing on two questions. 1.
890 What determines whether volcanic activity has a glaciological impact? 2. What determines whether
891 volcanic impacts on glaciers are observed?
892
893 **3.2.1. What determines whether volcanic activity has a glaciological impact?**
894 There are numerous documented examples where, despite proven volcano-glacier interactions, volcanic
895 activity has failed to produce an observable glaciological impact. In fact, the nature of volcanic impacts
896 on glaciers, and whether or not volcanic activity has an observable glaciological impact, seems to partly
897 depend on event size and duration, and glacier properties (including glacier size, thermal regime, and
898 the nature of subglacial drainage).
899
900 **3.2.1.1. Event size and duration**
901 Large and/or long-lasting volcanic events are likely to have a greater glaciological impact than
902 smaller/shorter equivalents. In addition, event size and duration may play a role in governing the nature
903 of volcanic impacts (when they occur). For example, during the 1984–85 eruption of Volcán Villarrica,
904 lava flows on the northern and northeastern slopes of the volcanic edifice melted the ice surface into
905 numerous supraglacial channels and generated small floods (Section 2.4.1.), but lava effusion rates (20
906 $m^3 s^{-1}$) were too low to generate large floods/lahars (Moreno, 1993; Delgado Granados et al., 2015).

907 Similar conditions were observed during the early stages of the 1971 eruption, but effusion rates and
908 lava volumes increased as a bedrock fissure opened across the summit crater (with lava fountains up to
909 400 m high and effusion rates up to 500 m^3 s^{-1}). This resulted in sufficient melting of the summit glaciers
910 to generate lahars in five different drainage basins (Marangunic, 1974; Moreno, 1993), thus indicating
911 that the effusion rates of lava flows have a strong control on glaciers, though factors such as the velocity
912 and style of lava flows also play a role (Section 2.4.1.). Similarly, the size and duration of a volcanic
913 eruption might determine its glaciological impact by controlling the thickness and extent of supraglacial
914 tephra deposits—hence determining whether threshold thicknesses are exceeded, whether melt is
915 enhanced or reduced, and whether underlying ice is protected (Section 2.6.). A further consideration
916 here is where and when such materials are deposited. For example, material deposited in a glacier's
917 accumulation area and/or during winter may become quickly snow covered, limiting its impact on
918 surface albedo.
919
920 **3.2.1.2. Glacier properties**
921 Glacier size (horizontal extent and thickness) has some control over the nature of volcanic impacts. For
922 example, dome extrusion has only been observed through small/thin glaciers (Section 2.2.2.), whilst
923 surface craters surrounded by concentric crevasses are more likely to form on thick glaciers (Section
924 2.3.1.). It is also likely that ice sheets are less susceptible to many of the volcanic impacts described in
925 this review because of their substantial thickness (km thick). In particular, subaerial processes (such as
926 supraglacial tephra deposition and pyroclastic density currents) likely have limited overall glaciological
927 impact. By contrast, widespread subglacial melt might have profound implications for ice-sheet stability
928 (Blankenship et al. 1993; Vogel et al. 2006; Corr and Vaughan 2008; de Vries et al., 2017), though our
929 understanding of volcanic impacts on ice sheet behaviour is limited by a dearth of observational
930 information.
931 Another important property that might affect a glacier's response to volcanic activity is the
932 basal thermal regime (i.e., whether cold-based, warm-based, or polythermal). For example, it is assumed
933 that for temperate (warm-based) or polythermal glaciers, increases in subglacial meltwater might not
934 necessarily result in advance/acceleration (as described in Sections 2.1.3. and 2.3.4.) since the bed is

already wet. By contrast, cold-based glaciers are often frozen to their beds with minimal subglacial meltwater drainage, and increased subglacial melt is therefore likely to have a greater impact on glacier behaviour (i.e., resulting in acceleration and/or advance) (Rivera et al., 2012). In the case of cold-based ice sheets, the impact of subglacial melt is difficult to predict, as any meltwater generated might be confined by surrounding frozen-based ice, and therefore spatially limited. Similar difficulties exist in predicting the impact on polythermal glaciers, with their patchwork of cold- and wet-based ice (see Smellie et al., 2014). However, and regardless of the dominant thermal regime, the impact of increased subglacial melt varies from one ice mass to another, and may partly depend on the nature of subglacial meltwater routing. For example, during the 2004 eruption of Grímsvötn, a jökulhlaup apparently caused an increase in the flow velocity of Skeidarárjökull (Fig. 11) (Martinis et al., 2007; Sigurðsson et al., 2014). This acceleration occurred over the entire width of the glacier, and suggests that basal lubrication had a glacier-wide impact on ice dynamics (Sigurðsson et al., 2014). By contrast, following the 1996 Gjálp eruption (Section 2.7.2.), subglacial meltwater drainage and storage (in Grímsvötn subglacial lake) led to localised supraglacial subsidence, but elsewhere the glacier surface remained intact, suggesting that widespread basal sliding was not triggered (Gudmundsson et al., 1997). A possible explanation is that during the 2004 eruption of Grímsvötn, meltwater spread across the glacier bed via distributed, inefficient subglacial drainage, while following the 1996 Gjálp eruption water quickly formed, and drained through, a much more efficient (perhaps pre-existing) subglacial network (Fig. 2a, point 10). Gudmundsson et al., (1997) suggest that the formation of ice surface cauldrons over the eruptive bedrock fissure during the second event may have resulted in steep gradients in basal water pressure, towards the cauldrons (where overburden pressure was reduced), thus limiting the amount of meltwater able to reach the ablation area of the glacier. However, whether such gradients are sufficient to substantially reduce subglacial water drainage is open to question (see Smellie, 2009).

3.2.2. What determines whether volcanic impacts on glaciers are observed?

Observations of volcano-glacier interaction are partly limited by event size and duration (Section 3.2.1.), as well as the weather conditions during periods of activity; the availability of aerial and satellite imagery; the accessibility of the sites; whether events occur supraglacially or subglacially; and luck

(e.g., whether aeroplanes pass close to volcanoes during periods of activity). Thus, in this review, by emphasising 'observed'/'documented' interactions we undoubtedly underestimate the real importance and frequency of volcanic impacts on glaciers, and this is likely to be particularly true for certain types of impacts (e.g., those occurring subglacially). Direct observation was also more difficult before the widespread availability of satellite data, and probably means that events that occurred before the 1970s (when the Landsat satellites were first launched) are dramatically underrepresented. Also, events in comparatively accessible and populated regions (e.g., Iceland) are better represented, and documented in more detail, than in isolated areas (e.g., Kamchatka or the sub-Antarctic Islands). In fact, even with the widespread availability and use of remotely sensed data, some regions are still difficult to robustly and repeatedly observe, often because of limitations with obtaining repeated, cloud-free imagery (e.g., the sub-Antarctic Islands, Patrick and Smellie, 2013). It is also likely that during volcanic events, ash and steam further limit visibility. In all these instances, most of our understanding of the events and their impacts on glaciers is inferred from conditions following the event. The spatial resolution of available remotely sensed imagery also regulates whether events (and which events in particular) are observed. For example, ice surface channels cut by supraglacial lava flows might be too narrow (a few metres wide) to be observed from many satellite sources (e.g., Landsat).

In all, volcanic impacts on glaciers are likely dramatically underrepresented in the observed record, and, in some cases, volcanic impacts on glaciers, though observed, may not have been recognised as such. This is likely to be particularly true at the ice sheet scale, where recognising links between ice dynamics and subglacial volcanic activity is difficult (Section 3.3.). Despite these limitations, over coming years, the number and quality of observations will likely quickly increase, as further high-resolution remote sensing datasets become available (Section 4.).

3.3. What is the future importance of volcanic impacts on glaciers?

In the long-term, as ice masses globally continue to retreat in response to climate warming (Bliss et al., 2014; Radić et al., 2014), their interactions with volcanoes are likely to become less frequent. However, in the short-term, glacier retreat and associated unloading may trigger explosive volcanic activity

990 (Huybers and Langmuir 2009; Watt et al., 2013; Praetorius et al. 2016), with considerable impacts on
991 existing ice masses. In addition, while deglaciation may be widespread, hundreds of volcanoes will
992 remain ice covered over the next decades to centuries (Curtis and Kyle, 2017). Thus, and despite
993 intrinsic difficulties, understanding, predicting and quantifying future volcanic impacts on glaciers is
994 extremely important.

995 For example, it has been suggested that future subglacial volcanic activity could lead to
996 enhanced basal melt, increased ice flow, and overall instability of the West Antarctic Ice Sheet
997 (Blankenship et al. 1993; Vogel et al. 2006; Corr and Vaughan 2008; de Vries et al., 2017), with global
998 implications, including sea level rise. In addition, many settlements, particularly in places such as the
999 Andes, are located at the foot of ice-covered volcanoes (Pierson et al., 1990; Thouret, 1990). Future
1000 eruptions, perhaps exacerbated by climatically driven glacier unloading, could trigger floods/lahars of
1001 extreme magnitude, with devastating impacts on these communities (e.g., during the 1985 eruption of
1002 Nevado del Ruiz, when a lahar killed > 23000 people, Pierson et al., 1990). Indeed, investigating future
1003 volcanic impacts on glaciers is vital if we are to better mitigate associated hazards (Blong, 1984; Tuffen,
1004 2010; Iribarren Anacona et al, 2015; Carrivick and Tweed, 2016). In the longer-term, if interactions
1005 with volcanic activity facilitate complete glacier loss, freshwater availability to communities in and
1006 around ice-covered volcanoes is likely to be considerably reduced (particularly outside rainy seasons),
1007 with notable impacts on human health and wellbeing (Beniston, 2003).
1008
1009 **4. Future research directions**
1010 Predicting future volcanic impacts on glaciers (Section 3.3.) requires an improved understanding of
1011 their interactions. One clear way of achieving this is simply to make more, and more detailed,
1012 observations. Part of this process will involve continued investigation of volcano-glacier interactions
1013 during the Quaternary (Smellie and Edwards, 2016). For events that occurred within recent decades
1014 (i.e., since the 1970s), there is further scope for systematically searching archival satellite and airborne
1015 imagery for undocumented instances of volcano-glacier interaction. In monitoring future events, though
1016 ground-based studies (including the use of ground penetrating radar) will be important for observing
1017 volcanic-glacier interactions, including subglacial environments, developments in satellite and airborne

(including drones) remote sensing are likely to drive the greatest advances in our understanding (see Harris et al., 2016, and papers therein).

4.1. Satellite remote sensing

Recent improvements in the quality and availability of satellite data have opened up opportunities for remotely observing volcano-glacier interactions at unprecedented spatial and temporal scales. Improvements in spatial resolution allow smaller events and features to be observed, while better temporal resolution (i.e., shortening the time interval between image capture at a given location) potentially allows events to be documented as they occur (e.g., over hours to months), and increases the likelihood of obtaining cloud-free images (see Patrick et al., 2016). Recent improvements in satellite data are already allowing global databases of glaciers (e.g., Pfeffer et al., 2014) and volcanoes (e.g., Global Volcanism Program, 2013) to be compiled, and automated (or semi-automated) techniques for near-real-time volcano monitoring to be developed. For example, the MODIS Volcano Thermal Alert System (MODVOLC) is an algorithm that allows near-real-time detection of global lava flows (Wright et al., 2004, 2015). Similar systems for the automated detection, mapping and monitoring of volcanic impacts on glaciers are in their infancy (e.g., Curtis and Kyle, 2017), but will undoubtedly see notable developments over coming years. Despite this progress, observations based on satellite data will continue to be biased towards larger events and particularly those that occur (or are expressed) supraglacially. Smaller events will continue to necessitate the use of other means of observation (particularly airborne remote sensing—Section 4.2), and detailed regional/local observations will continue to represent an ideal source of information and a way to validate near-global analyses.

4.2. Airborne remote sensing

Airborne remote sensing has been a particularly useful means of documenting volcano-glacier interactions over the 20th and early 21st centuries. Historically many of these observations were fortuitous (e.g., pilots observing volcanic activity as they pass by) rather than occurring during flights targeted specifically at observing volcanoes/glaciers. For example, passing airline pilots reported the onset of eruptive activity on the glacier-occupied Mount Westdahl in 1991 (Doukas et al., 1995), and a

local pilot reported heavily crevassed ice on the upper section of Chestnina Glacier following suspected volcanic activity at Mount Wrangell in 1999 (McGimsey et al., 2004). Similarly fortuitous observations are likely to continue in the future, but detailed descriptions of eruptions and their glaciological impacts will rely on targeted flights, flown for the express purpose of documenting events (e.g., Gudmundsson et al., 2007; Stewart et al., 2008; Magnússon et al., 2012). One notable direction for future progress is the use of unmanned aerial vehicles (UAVs), which allow centimetre-scale images to be captured in a quick and cost-effective way (Westoby et al., 2012). Such high-resolution data will allow some of the smaller (less conspicuous) events and features arising from volcano-glacier interactions to be better documented. UAVs are particularly useful in that they can be used to safely monitor otherwise dangerous/inaccessible sites (Corrales et al., 2012; Diaz et al., 2015), and potentially allow for near-continuous and repeat observations. This approach will flourish over coming years, but the use of UAVs requires an operator on the ground, and is therefore only likely during targeted periods of observation. In addition, difficulties with observing subglacial environments are likely to persist.

5. Conclusions

In this paper, we review volcanic impacts on modern glaciers (since AD 1800), supported by a global dataset of examples (Supplementary Table 1). The main findings can be summarised as follows:

1. Instances where volcanic activity has a documented impact on the behaviour of modern glaciers are comparatively rare. However, because of difficulties with observing these events, it is likely that their frequency and importance are underestimated.
2. Shorter-term (days-to-months) impacts are typically destructive, whilst longer-term (years-to-decades) impacts are likely to include reduced ablation, glacier stagnation and/or advance.
3. Predicting the future importance of volcanic impacts on glaciers is difficult because our understanding of their interactions is limited, and because the frequency and nature of volcano-glacier interactions is likely to change with time (e.g., future glacier retreat may lead to an increase in explosive volcanic activity). However, there is considerable interest in this area because volcanic activity may play a role in regulating the future stability of ice sheets (such as

the West Antarctic Ice Sheet), and because there is a need to better mitigate future glacio-volcanic hazards (e.g., floods and lahars).

4. Fortunately, due to improvements in the availability and quality of remotely sensed data, future observations of volcanic impacts on glaciers are likely to be more frequent, and descriptions of these interactions more detailed. However, observations will continue to be biased towards larger events, and monitoring subglacial processes (in particular) is likely to remain challenging.

Acknowledgements

We thank John Smellie and two anonymous reviewers for their corrections, comments and suggestions. We are also grateful to the editor Gillian Foulger. This work was supported by funding from the Engineering and Physical Sciences Research Council (EPSRC) (1492911).

References

Alfano, F., Bonadonna, C., Volentik, A.C., Connor, C.B., Watt, S.F., Pyle, D.M., Connor, L.J., 2011. Tephra stratigraphy and eruptive volume of the May, 2008, Chaitén eruption, Chile. Bulletin of Volcanology 73 (5), 613–630.

Anda, E., Orheim, O., Mangerud, J., 1985. Late Holocene glacier variations and climate at Jan Mayen. Polar Research 3 (2), 129–140.

Bartholomew, I., Nienow, P., Sole, A., Mair, D., Cowton, T., Palmer, S., Wadham, J., 2011. Supraglacial forcing of subglacial drainage in the ablation zone of the Greenland ice sheet. Geophysical Research Letters 38 (8), L08502.

1099 Beniston, M., 2003. Climatic change in mountain regions: a review of possible impacts. Climatic
1100 change 59 (1), 5–31.
1101
1102 Blankenship, D.D., Bell, R.E., Hodge, S.M., Brozena, J.M., Behrendt, J.C., Finn, C.A., 1993. Active
1103 volcanism beneath the West Antarctic ice sheet and implications for ice-sheet stability. Nature, 361
1104 (6412) 526–529.
1105
1106 Bleick, H.A., Coombs, M.L., Cervelli, P.F., Bull, K.F., Wessels, R.L., 2013. Volcano–ice interactions
1107 precursory to the 2009 eruption of Redoubt Volcano, Alaska. Journal of Volcanology and Geothermal
1108 Research 259, 373–388.
1109
1110 Bliss, A., Hock, R., Radić, V., 2014. Global response of glacier runoff to twenty-first century climate
1111 change. Journal of Geophysical Research: Earth Surface 119 (4), 717–730.
1112
1113 Blong, R.J., 1984. Volcanic hazards: a sourcebook on the effects of eruptions. Academic Press, Sydney.
1114
1115 Bolch, T., 2007. Climate change and glacier retreat in northern Tien Shan (Kazakhstan/Kyrgyzstan)
1116 using remote sensing data. Global and Planetary Change 56 (1), 1–12.
1117
1118 Brook, M., Dean, J., Keys, J., 2011. Response of a mid-latitude cirque glacier to climate over the last
1119 two decades: Mangaehuehu glacier, Mt Ruapehu Earth Surface Processes and Landforms 36, 1973–
1120 1980.
1121
1122 Brugman, M.M., Post, A., 1981. Effects of volcanism on the glaciers of Mount St. Helens. Geological
1123 Survey Circular 850-D, 1–11.
1124
1125 Burgisser, A., Bergantz, G.W., 2002. Reconciling pyroclastic flow and surge: the multiphase physics
1126 of pyroclastic density currents. Earth and Planetary Science Letters 202 (2), 405–418.

1127

1128 Carey, R.J., Houghton, B.F. and Thordarson, T., 2010. Tephra dispersal and eruption dynamics of wet
1129 and dry phases of the 1875 eruption of Askja Volcano, Iceland. Bulletin of Volcanology 72 (3), 259–
1130 278.

1131

1132 Carrivick, J.L., Tweed, F.S., 2016. A global assessment of the societal impacts of glacier outburst
1133 floods. Global and Planetary Change 144, 1–16.

1134

1135 Chapman, M.G., Allen, C.C., Gudmundsson, M.T., Gulick, V.C., Jakobsson, S.P., Lucchitta, B.K.,
1136 Skilling, I.P., Waitt, R.B., 2000. Volcanism and ice interactions on Earth and Mars. In: Zimbelman,
1137 J.R. and Gregg, T.K.P., Eds. Environmental effects on volcanic eruptions: From Deep Oceans to Deep
1138 Space. Kluwer Academic/Plenum Publishers, New York, pp. 39–73.

1139

1140 Cook, A.J., Fox, A.J., Vaughan, D.G., Ferrigno, J.G., 2005. Retreating glacier fronts on the Antarctic
1141 Peninsula over the past half-century. Science 308 (5721), 541–544.

1142

1143 Cooper, C.L., Swindles, G.T., Savov, I.P., Schmidt, A., Bacon, K.L., 2018. Evaluating the relationship
1144 between climate change and volcanism. Earth-Science Reviews 177, 238–247.

1145

1146 Corr, H.F., Vaughan, D.G., 2008. A recent volcanic eruption beneath the West Antarctic ice
1147 sheet. Nature Geoscience 1 (2), 122–125.

1148

1149 Corrales, J.A.D.E., Madrigal, Y., Pieri, D., Bland, G., Miles, T., Fladeland, M., 2012. Volcano
1150 monitoring with small unmanned aerial systems. In American Institute of Aeronautics and Astronautics
1151 Infotech Aerospace Conference, pp. 2522.

1152

1153 Curtis, A., Kyle, P., 2017. Methods for mapping and monitoring global glaciovolcanism. Journal of
1154 Volcanology and Geothermal Research 333, 134–144.

Delgado Granados, H., Miranda, P.J., Álvarez, R., Cabral-Cano, E., González, L.C., Mora, F.C., Alonso, M.L., Huggel, C., 2005. Study of Ayoloco Glacier at Iztaccíhuatl volcano (Mexico): hazards related to volcanic activity — ice cover interactions. Zeitschrift für Geomorphologie, Special Issue on Volcanic Geomorphology and Hazards 140, 181–193.

Delgado Granados, H., Miranda, P.J., Núñez, G.C., Alzate, P., Mothes, P., Roa, H.M., Correa, B.E.C. and Ramos, J.C., 2015.Hazards at Ice-Clad Volcanoes: Phenomena, Processes, and Examples From Mexico, Colombia, Ecuador, and Chile. In: Haeberli, W., Whiteman, C. (Eds.) Hazards at Ice-clad volcanoes. Snow and Ice-Related Hazards, Risks, and Disasters. Elsevier, Amsterdam, pp.607–636.

de Vries, M.V.W., Bingham, R.G., Hein, A.S., 2017. A new volcanic province: an inventory of subglacial volcanoes in West Antarctica. Geological Society, London, Special Publications 461, 461–467.

Diaz, J.A., Pieri, D., Wright, K., Sorensen, P., Kline-Shoder, R., Arkin, C.R., Fladeland, M., Bland, G., Buongiorno, M.F., Ramirez, C., Corrales, E., 2015. Unmanned aerial mass spectrometer systems for in-situ volcanic plume analysis. Journal of the American Society for Mass Spectrometry 26 (2), 292–304.

Dokukin, M.D., Seynova, I.B., Savernyuk, E.A., Chernomorets, S.S., 2017. On advancing of glaciers due to activity of the Klyuchevskaya Sopka volcano (Kamchatka). Ice and Snow 57 (1), 10–24.

Doukas, M.P., McGimsey, R.G., Dorava, J.M., 1995. 10 Years of Volcanic Activity in Alaska 1983-1992: A Video. US Geological Survey.

Druitt, T.H., 1998. Pyroclastic density currents. Geological Society, London, Special Publications 145(1), 145–182.

1183 Fuenzalida, R., 1976. The Hudson Volcano. In: González, O. (Ed.), Proceedings of the Symposium on
1184 Andean and Antarctic Volcanology Problems. Napoli, Italy, pp.78–87.
1185
1186 Gardner, C.A., Neal, C.A., Waitt, R.B., Janda, R.J., 1994. Proximal pyroclastic deposits from the 1989–
1187 1990 eruption of Redoubt Volcano, Alaska—stratigraphy, distribution, and physical
1188 characteristics. Journal of Volcanology and Geothermal Research, 62 (1–4), 213–250.
1189
1190 Global Volcanism Program, 2013. Volcanoes of the World, v. 4.5.0 http://dx.doi.org/10.
1191 5479/si.GVP.VOTW4-2013.
1192
1193 Gudmundsson, M.T., Höganadóttir, P., Kristinsson, A.B., Guđbjörnsson, S., 2007. Geothermal activity
1194 in the subglacial Katla caldera, Iceland, 1999–2005, studied with radar altimetry. Annals of
1195 Glaciology 45 (1), 66–72.
1196
1197 Gudmundsson, M.T., Sigmundsson, F. and Bjornsson, H., 1997. Ice-volcano interaction of the 1996
1198 Gjalp subglacial eruption, Vatnajokull, Iceland. Nature, 389 (6654), pp.954–957.
1199
1200 Gudmundsson, M.T., Thordarson, T., Höskuldsson, Á., Larsen, G., Björnsson, H., Prata, F.J., Oddsson,
1201 B., Magnússon, E., Högnadóttir, T., Petersen, G.N., Hayward, C.L., Stevenson, J.A., Jónsdóttir., 2012.
1202 Ash generation and distribution from the April-May 2010 eruption of Eyjafjallajökull, Iceland.
1203 Scientific reports 2 (572), 1–12.
1204
1205 Hammer, C.U., Clausen, H.B., Dansgaard, W., 1980. Greenland ice sheet evidence of post-glacial
1206 volcanism and its climatic impact. Nature 288 (5788), 230–235.
1207 Harris, A.J.L., De Groeve, T., Garel, F., Carn, S.A., 2016. (Eds.) Detecting, modelling and responding
1208 to effusive eruptions. Geological Society of London, Special Publications, 426, Geological Society of
1209 London, UK, pp. 683.
1210

1211 Hildreth, W., Fierstein, J., 2000. Katmai volcanic cluster and the great eruption of 1912. Geological
1212 Society of America Bulletin 112 (10), 1594–1620.
1213
1214 Hildreth, W., Fierstein, J., 2003, Geologic map of the Katmai Volcanic Cluster, Katmai National Park,
1215 Alaska: U.S. Geological Survey Map I-2778, scale 1:63,360.
1216
1217 Hildreth, W., Fierstein, J., 2012. The Novarupta-Katmai Eruption of 1912—Largest Eruption of the
1218 Twentieth Century: Centennial Perspectives. U.S. Geological Survey Professional Paper, 1791.
1219
1220 Huybers, P., Langmuir, C., 2009. Feedback between deglaciation, volcanism, and atmospheric
1221 CO_2. Earth and Planetary Science Letters 286 (3), 479–491.
1222
1223 Iken, A., Bindschadler, R.A., 1986. Combined measurements of subglacial water pressure and surface
1224 velocity of Findelengletscher, Switzerland: conclusions about drainage system and sliding
1225 mechanism. Journal of Glaciology 32 (110), 101–119.
1226
1227 Iribarren Anacona, P., Mackintosh, A., Norton, K.P., 2015. Hazardous processes and events from
1228 glacier and permafrost areas: lessons from the Chilean and Argentinean Andes. Earth Surface Processes
1229 and Landforms 40 (1), 2–21.
1230
1231 Iverson, N.A., Lieb-Lappen, R., Dunbar, N.W., Obbard, R., Kim, E., Golden, E., 2017. The first
1232 physical evidence of subglacial volcanism under the West Antarctic Ice Sheet. Scientific Reports 7, 1–
1233 8.
1234
1235 Julio-Miranda, P., Delgado-Granados, H., Huggel, C., Kääb, A., 2008. Impact of the eruptive activity
1236 on glacier evolution at Popocatépetl Volcano (México) during 1994–2004. Journal of Volcanology and
1237 Geothermal Research, 170 (1), 86–98.
1238

1239 Julio-Miranda, P., González Huesca, A.E., Delgado-Granados, H., Kääb, A., 2005. Glacier melting and
1240 lahar formation during January 22, 2001 eruption, Popocatépetl Volcano (Mexico). Z. Geomorphol. 140,
1241 93–102.
1242
1243 Juhle, W., Coulter, H., 1955. The Mt. Spurr eruption, July 9, 1953. Eos, Transactions American
1244 Geophysical Union 36 (2), 199–202.
1245
1246 Kirkbride, M.P., Dugmore, A.J., 2003. Glaciological response to distal tephra fallout from the 1947
1247 eruption of Hekla, south Iceland. Journal of Glaciology 49 (166), 420–428.
1248
1249 Klohn, E., 1963. The February 1961 eruption of Calbuco volcano. Bulletin of the Seismological Society
1250 of America 53(6), 1435–1436.
1251
1252 La Frenierre, J., Mark, B.G., 2017. Detecting patterns of climate change at Volcán Chimborazo,
1253 Ecuador, by integrating instrumental data, public observations, and glacier change analysis. Annals of
1254 the American Association of Geographers 107 (4), 979–997.
1255
1256 Liaudat, D.T., Penas, P., Aloy, G., 2014. Impact of volcanic processes on the cryospheric system of the
1257 Peteroa Volcano, Andes of southern Mendoza, Argentina. Geomorphology 208, 74–87.
1258
1259 Lillquist, K., Walker, K., 2006. Historical glacier and climate fluctuations at Mount Hood,
1260 Oregon. Arctic, Antarctic, and Alpine Research 38 (3), 399–412.
1261
1262 Lopez, P., Chevallier, P., Favier, V., Pouyaud, B., Ordenes, F., Oerlemans, J., 2010. A regional view of
1263 fluctuations in glacier length in southern South America. Global and Planetary Change 71(1), 85–108.
1264

1265 Magnússon, E., Gudmundsson, M.T., Roberts, M.J., Sigurðsson, G., Höskuldsson, F., Oddsson, B.,
1266 2012. Ice-volcano interactions during the 2010 Eyjafjallajökull eruption, as revealed by airborne
1267 imaging radar. Journal of Geophysical Research: Solid Earth 117(B7).
1268
1269 Major, J.J., Newhall, C.G., 1989. Snow and ice perturbation during historical volcanic eruptions and
1270 the formation of lahars and floods. Bulletin of volcanology 52 (1), 1–27.
1271
1272 Marangunic, C., 1974. The lahar provoked by the eruption of the Villarrica Volcano on December of
1273 1971. In: Abstracts International Symposium on Volcanology. IAVCEI, Santiago de Chile, pp.49.
1274
1275 Martinis, S., Scharrer, K., Münzer, U., Mayer, C., Guðmundsson, Á., 2007. Influence of the 2004
1276 jökulhlaup on ice dynamics of Skeidarárjökull, Iceland, using Terra-ASTER imagery.
1277 Photogrammetrie, Fernerkundung, Geoinformation 5, 337–347.
1278
1279 Masiokas, M., Rivera, A., Espizúa, L., Villalba, R., Delgado, S., Aravena, J.C., 2009. Glacier
1280 fluctuations in extratropical South America during the past 1000 years Palaeogeography,
1281 Palaeoclimatology, Palaeoecology 281, 242–268.
1282
1283 Mazzocchi, M., Hansstein, F., Ragona, M., 2010. The 2010 volcanic ash cloud and its financial impact
1284 on the European airline industry. CESifo Forum 11 (2). Ifo Institute for Economic Research at the
1285 University of Munich, 92–100.
1286
1287 McGimsey, R.G., Neal, C.A. and Girina, O.A., 2004. 1999 Volcanic activity in Alaska and Kamchatka:
1288 Summary of events and response of the Alaska Volcano Observatory. U.S. Geological Survey Scientific
1289 Investigations Open-File Report 2004-1033, pp.49.
1290

McGimsey, R.G., Neal, C.A., Girina, O.A., Chibisova, M., Rybin, A., 2014. 2009 Volcanic activity in Alaska, Kamchatka, and the Kurile Islands—Summary of events and response of the Alaska Volcano Observatory. U.S. Geological Survey Scientific Investigations Report 2013–5213.

McNutt, S.R., Miller, T.P., Taber, J.J., 1991. Geological and seismological evidence of increased explosivity during the 1986 eruptions of Pavlof volcano, Alaska. Bulletin of volcanology 53 (2), 86–98.

Melnik, O., Sparks, R.S.J., 1999. Nonlinear dynamics of lava dome extrusion. Nature 402 (6757), 37–41.

McConnell, J.R., Burke, A., Dunbar, N.W., Köhler, P., Thomas, J.L., Arienzo, M.M., Chellman, N.J., Maselli, O.J., Sigl, M., Adkins, J.F., Baggenstos, D., 2017. Synchronous volcanic eruptions and abrupt climate change~ 17.7 ka plausibly linked by stratospheric ozone depletion. Proceedings of the National Academy of Sciences 114 (38), 10035–10040.

Moreno, H., 1993. Volcán Villarrica: Geología y evaluación del riesgo, regiones IX-X, 39º25'S. Informe Final Proyecto Fondecyt, 1247.

Moreno, H., Fuentealba, G., 1994. The May 17-19 1994 Llaima volcano eruption, southern Andes 38° 42'8-71° 44'W. Andean Geology 21 (1), 167–171.

Morueta-Holme, N., Engemann, K., Sandoval-Acuña, P., Jonas, J.D., Segnitz, R.M., Svenning, J.C., 2015. Strong upslope shifts in Chimborazo's vegetation over two centuries since Humboldt. Proceedings of the National Academy of Sciences 112 (41), 12741–12745.

Muller, E.H., Coulter, H.W., 1957. Incipient glacier development within Katmai caldera, Alaska. Journal of Glaciology 3 (21), 13–17.

Muraviev, A.Ya., Muraviev, Ya.D., 2016. Fluctuations of glaciers of the Klyuchevskaya group of volcanoes in the 20th –21st centuries. Ice and Snow 56 (4), 480–492.

Muraviev, Ya.D., Muraviev, A.Ya., Osipova, G.B., 2010. Glacial surges in the areas of active volcanism. Tezisy XV glyatsilogicheskogo simpoziuma. Abstracts of the XV Glaciological Symposium. Kazan, 2010: pp.23. [In Russian].

Muraviev Ya.D., Muraviev A.Ya., Osipova G.B., 2011. Features of dynamics of ice files on active volcanoes, Kamchatka. Abstract, pp.92–93.

Muraviev, Ya.D., Tsvetkov, D.G., Muraviev, A.Ya. and Osipova, G.B. Dynamics of the Bilchenok surging glacier in the Klyuchevskaya volcano group. Led i Sneg. Ice and Snow. 2012, 2 (118): 31–39. [In Russian].

Neal, C.A., McGimsey, R.G., Dixon, J.P., Manevich, A., Rybin, A., 2009. 2006 Volcanic activity in Alaska, Kamchatka, and the Kurile Islands: Summary of events and response of the Alaska Volcano Observatory: U.S. Geological Survey Scientific Investigations Report 2008.

Nield, J.M., Chiverrell, R.C., Darby, S.E., Leyland, J., Vircavs, L.H., Jacobs, B., 2013. Complex spatial feedbacks of tephra redistribution, ice melt and surface roughness modulate ablation on tephra covered glaciers. Earth Surface Processes and Landforms 38 (1), 95–102.

Nielsen, N., 1937. A Volcano Under an Ice-Cap. Vatnajökull, Iceland, 1934-36. Geographical Journal, 6–20.

Orheim, O., Govorukha, L.S., 1982. Present-day glaciation in the South Shetland Islands. Annals of Glaciology 3, 233–238.

Patrick, M.R., Kauahikaua, J., Orr, T., Davies, A. and Ramsey, M., 2016. Operational thermal remote sensing and lava flow monitoring at the Hawaiian Volcano Observatory. In: Harris, A.J.L., De Groeve, T., Garel, F., Carn, S.A., 2016. (Eds.) Detecting, modelling and responding to effusive eruptions. Geological Society of London, Special Publications, 426, Geological Society of London, UK, pp.489–503.

Patrick, M.R., Smellie, J.L., 2013. Synthesis A spaceborne inventory of volcanic activity in Antarctica and southern oceans, 2000–10. Antarctic Science 25 (4), 475–500.

Pfeffer, W.T., Arendt, A.A., Bliss, A., Bolch, T., Cogley, J.G., Gardner, A.S., Hagen, J.O., Hock, R., Kaser, G., Kienholz, C., Miles, E.S., 2014. The Randolph Glacier Inventory: a globally complete inventory of glaciers. Journal of Glaciology 60 (221), 537–552.

Pierson, T.C., Janda, R.J., Thouret, J.C., Borrero, C.A., 1990. Perturbation and melting of snow and ice by the 13 November 1985 eruption of Nevado del Ruiz, Colombia, and consequent mobilization, flow and deposition of lahars. Journal of Volcanology and Geothermal Research 41(1–4), 17–66.

Praetorius, S., Mix, A., Jensen, B., Froese, D., Milne, G., Wolhowe, M., Addison, J., Prahl, F., 2016. Interaction between climate, volcanism, and isostatic rebound in Southeast Alaska during the last deglaciation. Earth and Planetary Science Letters 452, 79–89.

Radić, V., Bliss, A., Beedlow, A.C., Hock, R., Miles, E., Cogley, J.G., 2014. Regional and global projections of twenty-first century glacier mass changes in response to climate scenarios from global climate models. Climate Dynamics 42 (1–2), 37–58.

Rampino, M.R., Self, S., 1993. Climate-volcanism feedback and the Toba eruption of ~ 74,000 years ago. Quaternary Research 40 (3), 269–280.

1375

1376 Richardson, J.M., Brook, M.S., 2010. Ablation of debris-covered ice: some effects of the 25 September
1377 2007 Mt Ruapehu eruption. Journal of the Royal Society of New Zealand 40 (2), 45–55.

1378

1379 Rivera, A., Bown, F., 2013. Recent glacier variations on active ice capped volcanoes in the Southern
1380 Volcanic Zone (37°–46° S), Chilean Andes. Journal of South American Earth Sciences 45, 345–356.

1381

1382 Rivera, A., Bown, F., Carrión, D., Zenteno, P., 2012. Glacier responses to recent volcanic activity in
1383 Southern Chile. Environmental Research Letters 7 (1), 014036.

1384

1385 Russell, A.J., Duller, R., Mountney, N.P., 2010. Volcanogenic Jökulhlaups (Glacier Outburst Floods)
1386 from Mýrdalsjökull: Impacts on Proglacial Environments. Developments in Quaternary Sciences 13,
1387 181–207.

1388

1389 Salamatin, A.N., Murav'yev, Y.D., Shiraiwa, T., Matsuoka, K., 2000. Modelling dynamics of glaciers
1390 in volcanic craters. Journal of Glaciology 46 (153), 177–187.

1391

1392 Scanlon, K.E., Head, J.W., Wilson, L., Marchant, D.R., 2014. Volcano–ice interactions in the Arsia
1393 Mons tropical mountain glacier deposits. Icarus 237, 315–339.

1394

1395 Schilling, S.P., Carrara, P.E., Thompson, R.A., Iwatsubo, E.Y., 2004. Posteruption glacier development
1396 within the crater of Mount St. Helens, Washington, USA. Quaternary Research 61 (3), 325–329.

1397

1398 Sigmundsson, F., Hreinsdóttir, S., Hooper, A., Árnadóttir, T., Pedersen, R., Roberts, M.J., Óskarsson,
1399 N., Auriac, A., Decriem, J., Einarsson, P., Geirsson, H., Hensch, M., Ófeigsson, B.G., Sturkell, E.,
1400 Sveinbjörnsson, H., Feigl, K.L., 2010. Intrusion triggering of the 2010 Eyjafjallajökull explosive
1401 eruption. Nature 468 (7322), 426–430.

1402

1403 Sigurðsson, O., Williams, R.S., Martinis, S., Münzer, U., 2014. Remote sensing of mountain glaciers
1404 and ice caps in Iceland. In: Kargel, J.S., Leonard, G.J., Bishop, M.P., Kääb, A., Raup, B.H.
1405 (Eds.) Global land ice measurements from space. Springer Berlin Heidelberg, pp.409–425.
1406
1407 Simons, F.S., Mathewson, D.E., 1955. Geology of Great Sitkin Island, Alaska. US Government Printing
1408 Office.
1409
1410 Smellie, J.L., 2006. The relative importance of supraglacial versus subglacial meltwater escape in
1411 basaltic subglacial tuya eruptions: an important unresolved conundrum. Earth-Science Reviews 74 (3),
1412 241–268.
1413
1414 Smellie, J.L., 2009. Terrestrial subice volcanism: Landform morphology, sequence characteristics,
1415 environmental influences, and implications for candidate Mars examples. Geological Society of
1416 America Special Papers 453, 55–76.
1417
1418 Smellie, J.L., Edwards, B.R., 2016. Glaciovolcanism on Earth and Mars. Cambridge University Press,
1419 Cambridge.
1420
1421 Smellie, J.L., Rocchi, S., Wilch, T.I., Gemelli, M., Di Vincenzo, G., McIntosh, W., Dunbar, N., Panter,
1422 K., Fargo, A., 2014. Glaciovolcanic evidence for a polythermal Neogene East Antarctic Ice
1423 Sheet. Geology 42 (1), 39–41.
1424
1425 Seroussi, H., Ivins, E.R., Wiens, D.A., Bondzio, J., 2017. Influence of a West Antarctic mantle plume
1426 on ice sheet basal conditions. Journal of Geophysical Research: Solid Earth 122 (9), 7127–7155.
1427
1428 Stewart, S.F., Pinkerton, H., Blackburn, G.A., Gudmundsson, M.T., 2008. Monitoring active subglacial
1429 volcanoes: A case study using airborne remotely sensed imagery of Grímsvötn, Iceland. International
1430 journal of remote sensing 29 (22), 6501–6514.

Sturm, M., Benson, C., MacKeith, P., 1986. Effects of the 1966-68 Eruptions of Mount Redoubt on the Flow of Drift Glacier, Alaska, USA. Journal of Glaciology 32 (112), 355–362.

Sturm, M., Hall, D.K., Benson, C.S., Field, W.O., 1991. Non-climatic control of glacier-terminus fluctuations in the Wrangell and Ghugach Mountains, Alaska, USA. Journal of Glaciology 37 (127), 348–356.

Thouret, J.C., 1990. Effects of the November 13, 1985 eruption on the snow pack and ice cap of Nevado del Ruiz volcano, Colombia. Journal of Volcanology and Geothermal Research 41(1–4), 177–201.

Trabant, D.C., Meyer, D.F., 1992. Flood generation and destruction of "Drift" Glacier by the 1989–90 eruption of Redoubt Volcano, Alaska. Annals of Glaciology 16, 33–38.

Trabant, D.C., Waitt, R.B., Major, J.J., 1994. Disruption of Drift glacier and origin of floods during the 1989–1990 eruptions of Redoubt Volcano, Alaska. Journal of volcanology and geothermal research 62(1-4), 369–385.

Tuffen, H., 2010. How will melting of ice affect volcanic hazards in the twenty-first century?. Philosophical Transactions of the Royal Society of London A: Mathematical, Physical and Engineering Sciences 368 (1919), 2535–2558.

Vinogradov V.N., Muraviev YA.D., 1982. Izmenchivost' sovremennykh blednikov vulkanicheskikh rayonov Kamchatki. Variability of modern glaciers in volcanic areas of Kamchatka. Materialy Glyatsiologicheskikh Issledovaniy. Data of Glaciological Studies 42, 164–170. [In Russian].

1457 Vinogradov V.N., Muraviev YA.D., 1985. Vzaimodeystvie lavy i l'da na Klyuchevskom vulkane pri
1458 izverzhenii 1983 g. Lava and ice interaction at the Klyuchevskoy volcano during the 1983 eruption.
1459 Vulkanologiya i seysmologiya. Journ. of Volcanology and Seismology 1, 29–46. [In Russian].
1460
1461 Vogel, S.W., Tulaczyk, S., Carter, S., Renne, P., Turrin, B., Grunow, A., 2006. Geologic constraints on
1462 the existence and distribution of West Antarctic subglacial volcanism. Geophysical research letters 33
1463 (23), L23501.
1464
1465 Walder, J.S., LaHusen, R.G., Vallance, J.W., Schilling, S.P., 2007. Emplacement of a silicic lava dome
1466 through a crater glacier: Mount St Helens, 2004–06. Annals of Glaciology 45 (1), 14–20.
1467
1468 Walder, J.S., Schilling, S.P., Vallance, J.W., LaHusen, R.G., 2008. Effects of lava-dome growth on the
1469 Crater Glacier of Mount St. Helens, Washington. In: Sherrod, D.R., Scott, W.E., Stauffer, P.H. (Eds.)
1470 A Volcano Rekindled: The Renewed Eruption of Mount St. Helens, 2004–2006. U.S. Geological
1471 Survey Professional Paper 1750, pp.257–276.
1472
1473 Walder, J.S, Schilling, S.P., Sherrod, D.R., Vallance, J.W., 2010, Photographic Documentation of the
1474 Evolution of Crater Glacier, Mount St. Helens, Washington, September 2006—November 2009: U.S.
1475 Geological Survey Open-File Report 2010-1141.
1476
1477 Waitt, R.B., Gardner, C.A., Pierson, T.C., Major, J.J., Neal, C.A., 1994. Unusual ice diamicts emplaced
1478 during the December 15, 1989 eruption of Redoubt Volcano, Alaska. Journal of volcanology and
1479 geothermal research 62 (1–4), 409–428.
1480
1481 Watt, S.F., Pyle, D.M., Mather, T.A., 2013. The volcanic response to deglaciation: Evidence from
1482 glaciated arcs and a reassessment of global eruption records. Earth-Science Reviews 122, 77–102.
1483

Waythomas, C.F., Pierson, T.C., Major, J.J. Scott, W.E., 2013. Voluminous ice-rich and water-rich lahars generated during the 2009 eruption of Redoubt Volcano, Alaska. Journal of Volcanology and Geothermal Research 259, 389–413.

Westoby, M.J., Brasington, J., Glasser, N.F., Hambrey, M.J., Reynolds, J.M., 2012. 'Structure-from-Motion' photogrammetry: A low-cost, effective tool for geoscience applications. Geomorphology 179, 300–314.

Wilson, L., Smellie, J.L. and Head, J.W., 2013. Volcano-ice interaction. In: Fagents, S.A., Gregg, T.K.P. and Lopes, R.M.C. (Eds.) Modelling of volcanic processes: the physics and mathematics of volcanism. Cambridge, Cambridge University Press, pp. 275–299.

Worni, R., Huggel, C., Stoffel, M., Pulgarín, B., 2012. Challenges of modeling current very large lahars at Nevado del Huila Volcano, Colombia. Bulletin of volcanology 74 (2), 309–324.

Wright, R., Flynn, L.P., Garbeil, H., Harris, A.J., Pilger, E., 2004. MODVOLC: near-real-time thermal monitoring of global volcanism. Journal of Volcanology and Geothermal Research 135 (1), 29–49.

Wright, R., Blackett, M. and Hill-Butler, C., 2015. Some observations regarding the thermal flux from Earth's erupting volcanoes for the period of 2000 to 2014. Geophysical Research Letters 42 (2), 282–289.

1511 Supplementary Table 1. Instances where volcanic activity has affected the behaviour of modern (post AD 1800) glaciers. Volcano locations are shown in Fig.
1512 1. This table builds on Major and Newhall (1989) and Smellie and Edwards (2016). These data are also available as a kmz. file for viewing and editing in Goole
1513 Earth™ (Supplementary data 1).

Volcano number	Volcano name and location	Time period	Activity/event type	Activity/event details	Observed glaciological impacts	Citations
1	Great Sitkin (USA); 52.08°N, 176.13°W	1945	Subglacial dome growth and extrusion	Dome growth occurred beneath the caldera glacier.	A hole formed in the caldera glacier. Ice bulging (around the hole), with associated crevassing (this inference is based on a single photograph).	Simons and Mathewson (1955); Waythomas et al. (2003)
2	Makushin (USA); 53.89°N, 166.92°W	1983	Subglacial eruption	Subglacial fumarolic activity resulted in subglacial melt on the south flank of the volcano (at 870 m a.s.l.).	A ~ 100 m diameter hole was melted in the overriding glacier ice.	Motyka et al. (1983)
3	Mount Westdahl (USA); 54.52°N, 164.65°W	1978	Subglacial eruption	An explosive eruption resulted in subglacial melt.	Subglacial melt produced a 1.5 km diameter, 500 m deep, circular cauldron/crater through ~ 200 m of glacier ice.	Krafft et al. (1980); Lu et al. (2000, 2003)
			Flood/lahar	Water overflowed from the ice cauldron/crater (mentioned above).	A meltwater channel was incised into the surface of the glacier to the east of the cauldron/crater.	Dean et al. (2002); Lu et al. (2003); Smellie (2006)
		1991–92	Subglacial eruption	A subglacial fissure eruption resulted in ice melt.	A ~ 8km long fissure cut through the glacial cap. Several large craters and cracks ran parallel to this fissure.	Rowland et al. (1994); Dean et al. (2002); Smellie (2006)
			Supraglacial flooding	Meltwater emerged supraglacially through the eruptive ice fissure (mentioned above).	Meandering water flowed across and incised into the glacier surface.	Dean et al. (2002); Smellie (2006)

			Supraglacial lava flow	The fissure eruption, and associated lava fountains, resulted in supraglacial lava flow.	Supraglacial lava flow caused melt and associated debris flows.	Doukas et al. (1995); Dean et al. (2002)
4	Mount Shishaldin (USA); 54.76°N, 163.97°W	1999	Supraglacial lava flow	An eruption resulted in a large supraglacial lava flow on the north flank of the volcano.	Lava incised a 5–10 m deep channel into the glacier surface (at 500–1,000 m a.s.l). This channel is considered the product of melting and hydrological erosion (see below).	Stelling et al. (2002)
			Supraglacial flooding	Melting of ice/snow resulted in supraglacial flooding. This flow developed into a hyper-concentrated debris flow.	Floodwaters incised/enhanced channels in the glacier surface.	
5	Mount Pavlof (USA); 55.42°N, 161.89°W	2013 (these processes are also thought to have operated during eruptions in 1986, 1996, 2007)	Supraglacial pyroclastic flows (avalanches)	During the first days of the eruption, 'spatter' accumulated near the active vent. These accumulations of material periodically collapsed, and generated small pyroclastic flows (avalanches).	Pyroclastic flows (avalanches) eroded and melted ice and snow, leading to lahars on the north flank of the volcano.	McNutt et al. (1991); Waythomas et al. (2014)
			Supraglacial lahars (debris flows)	Hot lahars (debris flows) extended from the vent, and advanced over ice and snow.	Lahars (debris flows) cut 2–3 km long ice ravines (extending from the volcanic vent) into snow and ice on the NE flank of the volcano.	
			Supraglacial lava flows	Lava fountaining at the volcano summit resulted in supraglacial lava flows on the north flank of the volcano.	Lava melted snow and ice, forming minor lahars. However, pyroclastic flows (avalanches) were more efficient at melting ice and snow (see above).	
6	Mount Veniaminof (USA); 56.17°N, 159.38°W	1983–84, 1993–95, 2013	Supraglacial lava flows	Eruptions from pyroclastic cones that protruded through the ice-filled summit calderaproduced supraglacial lava flows.	Supraglacial lava flows melted an oval pit in the surface of the caldera-occupying glacier. In 1983–84, for example, this pit was ~ 1000 x 800 m across, and 30–50 m	Miller and Yount (1983); Yount et al. (1985); Rowland et al. (1994); Doukas et al. (1995); Neal

					deep. Fractures/crevasses surrounding this pit suggest subglacial melting, and/or ice flow towards the pit. In total, ~ 0.15 km^3 of the summit ice cap melted during this period. The 1983 event is thought to have produced a large volume of lava, the flow of which was focused down the south side of the cone.	et al. (1995, 2002); Smellie (2006); Welch et al. (2007)
			Subglacial melt	Melt formed subglacial caverns that later collapsed.	In combination with supraglacial lava flows (outlined above), subglacial eruptions directly caused melting and the formation of melt pits on the south side of the cone. The resulting meltwater was stored within the glacier (perhaps trapped within the caldera). Meltwater was only observed during the 1983 eruption, as a lake (formed within the surface pit) drained subglacially, along the caldera floor, but only resulted in a modest increase in fluvial discharge. No lahars or floods resulted. Most of the meltwater from the 1983 eruption likely drained into crevasses on the NW side of the melt pit, and joined the Cone Glacier drainage network.	
7	Mount Chiginagak (USA); 57.14°N, 156.99°W	2004–05	Enhanced subglacial heat flow	Geothermal heating in the summit crater resulted in subglacial melt.	A 105 m thick mass of snow and glacial ice was melted from the summit crater. This resulted in the formation of a ~ 400 m wide lake-filled ice cauldron. The lake later	Schaefer et al. (2008)

					partially drained in a subglacial and supraglacial flood/lahar (see below).	
			Flood/lahar	The summit lake (referred to above) partially drained, as a 3.8 x 10^6 m^3 flood of water and debris, beneath, within, and across a glacier that breaches the southern rim of the crater.	Lahar deposits were emplaced upon the glacier surface. Following the flood, the glacier surface was notably crevassed, suggesting ice acceleration.	
8	Novarupta (USA); 58.27°N, 155.16°W	1912	Supraglacial deposition of tephra and pyroclastic debris	Knife Creek Glaciers (part of the Trident volcanic group) 1–5 were (and remain) heavily mantled with tephra and other volcanic debris. This fallout was up to 12 m thick near glacier termini (but, in some cases, is now absent in accumulation areas). In addition, pyroclastic density currents ran up Knife Creek Glaciers 1–3, and feathered out in the saddles between summits. This left the glaciers covered with thin pyroclastic deposits.	Knife Creek Glaciers 1, 2 and 3 advanced ~ 250 m, ~ 300 m, and ~ 225 m respectively, between 1951 and 1987. Knife Creek Glacier 3 had initially experienced wasting in response to the Katmai Caldera collapse (see below). A ~ 670 m x 915 m section of the terminus of Knife Creek Glacier 4 was dislodged by a pyroclastic flow. The glacier later advanced ~ 500 m between 1919 and 1951, and ~ 150 m between 1951 and 1987. Knife Creek Glacier 5 advanced ~ 1,300 m between 1919 and 1951, but since 1951, the lower ~ 700 m of the glacier has thinned and stagnated (but not retreated noticeably). Between, 1987 and c.2003 the Knife Creek Glaciers did not retreat significantly, though small changes may have escaped detection.	Curtis (1968); Hildreth (1983) Fierstein and Hildreth, (1992); Hildreth et al. (2000, 2002, 2003a,b); Hildreth and Fierstein (2003, 2012); Giffen et al. (2014)
				Mount Griggs Glaciers 1–6 were covered with thick tephra. At present, only the	Between 1951 and 1987, three of the Mount Griggs Glaciers retreated, one advanced, and two remained largely unchanged. This	

				lower third of each glacier remains tephra covered.	variability is thought to reflect the combined impacts of supraglacial tephra, local variability in the steepness and roughness of glacier beds and variations in avalanche derived snow and debris.	
				Snowy Mountain Glaciers 1–12 were covered with 1–2 m of tephra. The thickness of this tephra reduced towards the north and east, and thickened to > 3 m in the SW. Much of this tephra was removed (through erosion and ice motion) from glaciers within a few decades, but thick deposits remain on glaciers in the SW (particularly in their ablation zones).	Between 1951 and 1984, nine of the Snowy Mountain Glaciers retreated, two were stationary, and one (the furthest SW) advanced ~ 150 m. The ash free glaciers (to the east of Snowy Mountain) have all retreated, whilst the ash-covered glaciers (to the west and SW of Snowy Mountain) have advanced or stagnated.	
				Almost the entire surface of Wishbone Glacier (on the south side of Trident) was (and remains) covered with fallout from the 1912 eruption.	The western terminus of Wishbone Glacier retreated by ≤ 30 m between 1951 and 1987, while the lowest 2 km thinned by ~ 10 m. Part of the western lobe of the glacier (~ 3 km above the terminus) advanced ~ 110 m between 1951 and 1987.	
				A glacier (GLIMS glacier ID: G204949E58236N): occupying the valley between Trident I and the south ridge of East Trident was mantled by thick tephra.	The glacier wasted drastically between 1951 and 1987, having already been largely stagnant by 1951.	
				Debris covered the East Katmai Icefield, and remains on the lower sectors of the glaciers.	The terminus of Ikagluik Glacier, the northernmost outlet of the icefield has moved little since 1951, whilst Noisy	

					Mountain Glacier, the southernmost outlet advanced ~ 150 m between 1951 and 1984, and has remained largely stationary since.	
9	Trident Volcanic group (USA); 58.24°N, 155.10°W	1953–60	Supraglacial debris deposition	At southwest Trident, a fragmental cone (consisting of multiple lava flows) accumulated.	The southeast side of the cone, and 1957 lava flow, completely buried a 1 km^2, ~ 700 m long, cirque glacier.	Hildreth et al. (2003a,b)
10	Mount Katmai (USA); 58.26°N, 154.98°W	1912	Summit collapse and caldera formation	Due to the 1912 eruption of Novarupta, the glacier-clad summit of Mount Katmai (~ 9 km to the east) collapsed, resulting in the formation of a 5.5 km^3 caldera.	A number of the glaciers occupying Mount Katmai were partly beheaded. However, because these glaciers were insulated by supraglacial tephra deposits from Novarupta (see above), the impact of beheading on terminus positions was limited. For example, Knife Creek Glacier 3 lost > 50% of its accumulation area, and has since thinned, but its lower sector has stagnated (under debris cover), and its terminus advanced between 1951 and 1987 (see above). Knife Creek Glacier 4 was partly beheaded, but has advanced ~ 650 m since 1919. Metrokin Glacier (directly south of the Katmai Crater) was partly beheaded, and subsequently retreated ~ 600 m between 1951 and 1989, and ~ 400 m between 1989 and 2001. However, rather than reflecting the impact of 'beheading' this retreat is thought to reflect enhanced melt beneath thin supraglacial debris. Three	Hildreth and Fierstein (2000, 2003, 2012)

					glaciers occupying the SE slope of Mount Katmai were beheaded during the collapse. The terminus of each of these glaciers has retreated > 1km since 1951. This may reflect the impact of beheading, or a regional warming trend. Glacier beheading left ice cliffs surrounding the crater rim at Mount Katmai (these cliffs effectively formed at the highest points of each glacier). Over subsequent decades, these ice cliffs gradually wasted, as the ice thinned and receded 50–800 m from the caldera edge.	
			New glacier formation	Following the collapse of Mount Katmai's summit, the caldera generated was initially ice-free. However, intra-caldera snow and ice then began to accumulate on inward sloping benches (300–400 m above the caldera floor). Snow patches had accumulated by 1917, modest snowfields by 1923, and the earliest confirmed report of active glacial ice comes from 1951. According to Muller and Coulter (1957a), these intra-caldera glaciers had effectively formed within 20 years of the caldera's formation.	Two entirely new intra-caldera glaciers formed: one at the caldera's north margin and one at its south. In addition, at the calderas SW margin, an ice tongue began to extend into the caldera from an icefield outside (the upper section of this glacier effectively experienced a local reversal in flow direction which resulted in an icefall which extends into the caldera). By 1953/54, the North glacier reached halfway down to the lake, the South glacier terminated in cliffs 50–80 m above the caldera lake, and the ice tongue on the SW wall reached half way to the lake. By 1987 all glaciers terminated just above lake level.	Griggs (1922); Fenner (1930); Muller and Coulter (1957a,b); Motyka (1977); Hildreth (1983); Hildreth and Fierstein (2000, 2012)

					By 1999 both the North and South glaciers reached the lake, while the ice tongue 'surged' in both 1976 and 2001 (temporarily reaching the lake) but then retreated back upslope. All three glaciers have reached lake level, then typically melted rapidly (since the water is heated). Thus, the volcanic lake has acted as a deterrent to glacier growth/advance. Since the 1930s, the lake level has increased (e.g., in 1953 the lake was 150 m deep, and by 2000 was > 250 m deep).	
11	Fourpeaked Mountain (USA); 58.77°N, 153.67°W	2006	Subglacial eruption	A phreatic eruption occurred at a ~ 1250 m long subglacial fissure.	A series of nine craters or pits were melted through the summit ice above the fissure. As a result, the adjacent glacial ice became heavily crevassed and disrupted.	Neal et al. (2009)
			Supraglacial lahar/flood	A lobate, dark, debris flow emerged from cracks in the ice and spread onto the surface of an unnamed north-trending glacier (~ 900 m below the summit). This flow included outburst flood material (i.e., it was a mixture of water and debris).	A steep-walled canyon > 100 m deep was scoured into the glacier surface. Blocks of glacial ice, 5–10 m across, were transported > 6 km down slope by this flow of water and debris.	
12	Mount Redoubt (USA); 60.49°N, 152.74°W	1966–68	Subglacial eruptions	Eruptions caused subglacial melt and/or the mechanical removal of ice.	Generated a crater and melt pits in the summit glacier.	Post and Mayo (1971); Sturm et al. (1983, 1986); Trabant et al. (1994).

			Supraglacial pyroclastic density currents	Explosions (and dome collapses) produced pyroclastic density currents that melted and entrained glacial ice.	~60 × 10^6 m^3 of ice was lost from the upper/gorge section of Drift Glacier (i.e., from the lava dome down to the top of the glacier's piedmont lobe, between 1500 and 2500 m a.s.l.). This effectively beheaded the glacier, and reduced ice flux to the lower (piedmont) section by more than 50%. Perturbations to the flow of Drift glacier lasted more than 20 years.	
			Floods	Rapid melting resulted in several jökulhlaups which travelled supraglacially, and subglacially.	The jökulhlaups (heavily laden with sand and debris) formed deeply incised supraglacial gullies, moulin-like holes, and cauldron-shaped collapse features. Flood sediments (locally > 5 m thick, and typically > 1 m thick) were deposited on the piedmont lobe of Drift Glacier (~10^6 m^2 of the piedmont lobe was covered with flood deposits). These supraglacial deposits acted to insulate the piedmont lobe, thereby limiting ablation.	
			Post-eruption impacts	During the 1966–68 eruptive period, Drift Glacier was beheaded, separating the crater glacier from the piedmont lobe below. By 1976 (8 years after the eruptive period), the upper section of Drift Glacier had re-formed (reforming ~ 15 x 10^7 m^3 of ice), and re-connected with the lower piedmont portion section.	When the regenerated part of the glacier re-connected with the lower ('abandoned') section, a kinematic wave of thickening (> 70 m) and surface acceleration (by an order of magnitude) was triggered in the lower section, whilst thinning (by ~ 70 m) was experienced in the upper section. This was accompanied by surface crevassing, and is	

					considered to reflect the glacier's return to its pre-eruption equilibrium condition.	
			Overall	A combination of the events and processes mentioned above.	During the 1966–68 eruptive period, ~6 x 10^7 m^3 of ice was removed from the volcano.	
		1989–90	Enhanced subglacial heat flow	Pre-eruption period of enhanced subglacial heat flow	Prior to the eruptions, due to subglacial mely, a new circular opening developed in the crater glacier (representing a loss of ~13–14 x 10^6 m^3 of perennial snow and ice).	Brantley (1990); Trabant and Meyer (1992); Gardner et al. (1994); Scott and McGimsey (1994); Trabant et al. (1994); Waitt et al. (1994); Trabant and Hawkins (1997); McGimsey et al. (2014); Waythomas (2015)
			Subglacial eruptions	Eruptions caused subglacial melt and the mechanical removal of ice.	Explosions blasted through ~ 50–100 m of crater-filling glacier ice and snow (at the head of Drift Glacier). During the eruption, ice flow reversal (toward the active vent) ensured continued melt of the crater glacier.	
			Supraglacial lahars, avalanches, and pyroclastic density currents	Explosions destroyed lava domes (which had formed in the summit crater). The collapsing domes resulted in debris flows, avalanches and pyroclastic-density currents, which travelled down Drift Glacier and, to a much lesser degree, Crescent Glacier. Pyroclastic currents typically transitioned from hot, dry *surges* to cold, wet *flows* (lahars), as they melted and entrained ice.	Pyroclastic density currents were funneled through the gorge section of Drift Glacier (between 750 m and 2500 m a.s.l.), and locally scoured (ice mechanically entrained) the glacier to bedrock (ice here was formerly ~ 100 m thick). This process effectively beheaded the glacier, isolating the piedmont lobe. The heavily crevassed icefall in the gorge section of Drift Glacier facilitated the mechanical entrainment of ice (on the shallower, less crevassed piedmont lobe, this was not the case). In the piedmont section, the pyroclastic density	

					currents (and associated lahars) incised supraglacial channels (often exploiting longitudinal crevasses). These channels were 10–100 m wide and deep (i.e., reaching the full ice thickness), resulting in a deeply incised ice-canyon system. In total, ~ 0.1 km^3 of Drift Glacier was removed by erosion and melting. An avalanche of snow and volcanic debris descended across the surface of Crescent glacier (flowing SW from the summit), and formed a surface deposit, locally up to 20 m thick, in the glacier's lower reaches. The resulting melt-out deposits (30–40 cm thick) insulated the glacier from further melting.	
			Lahars	Multiple lahars (at least 18) were generated by explosions and/or pyroclastic density currents.	Lahars melted and entrained glacier ice. This resulted in the supraglacial deposition of an 'ice diamict', composed of gravel-sized clasts of glacier ice, rock, and pumice in a matrix of sand, ash and ice (frozen pore water). On the piedmont lobe of Drift glacier, these deposits were 1–10 m thick (these areas were comparatively resistant to erosion by later pyroclastic density currents and lahars).	
			Overall	A combination of the events and processes mentioned above.	By the end of the 1989–90 eruptive period, ~2.9 x 10^8 m^3 ± 5% of ice was lost from the volcano (~ 30% of the total ice volume).	

		2008–09	Enhanced subglacial heat flow	Pre-eruption period (~ 8 months) of increased heat flow and fumarolic activity.	Heating caused subglacial melt, removing (~3–7 x 10^6 m^3) of snow and ice from the crater glacier and upper Drift Glacier. This generated collapse features and exposed bare ground on the formerly ice-covered 1990 lava dome. In September 2008 (i.e., prior to the March 2009 eruption), a summit fumarole and melt holes, including a 'skylight' above a 100 m high subglacial waterfall, were observed (both in the summit crater and in the gorge area of Drift Glacier). These melt holes were enlarged over subsequent months, and a ~150 m diameter subsidence structure (ice cauldron) developed within the crevassed ice plateau above the 1990 dome (at the margin of the summit caldera). This structure would eventually reach 225 m in diameter, and 100 m in depth. By January 2009, the enlargement of melt holes and opening and deformation of crevasses suggested sufficient heat flux to cause melting at a rate of 0.3 m^3 s^{-1}. By February 2009, the rate of melt had increased to 2.2 m^3 s^{-1}.	Schaefer (2012); Bleick et al. (2013); Bull and Buurman (2013); Waythomas et al. (2013); McGimsey et al. (2014); Waythomas (2015)
			Subglacial eruptions	Subglacial eruptions and lava dome collapses.	Initial vent-clearing explosions in March 2009 blasted through ~ 50–100 m of crater-filling glacier ice and snow (at the head of	

					Drift Glacier). This produced a crater (excavating 0.5–1.5×10^8 m^3 of ice and snow). Unlike during the eruption in 1989–90 (and in 1966–68), a substantial amount of ice in the gorge section of Drift Glacier remained intact, hence the piedmont section was not beheaded. Subsequent lava dome collapses enlarged the crater around the summit vent.	
			Supraglacial avalanches and pyroclastic density currents	Lava domes collapsed, resulting in hot supraglacial debris avalanches and pyroclastic density currents.	Pyroclastic density currents entrained and melted large volumes of snow and ice from Drift Glacier, scouring the glacier surface, and resulting in supraglacial lahars (see below). Pyroclastic currents were funneled through the gorge section of Drift Glacier (above ~ 700 m a.sl.), and locally scoured the glacier to bedrock. Upon emerging from the gorge section, these pyroclastic flows extended across the piedmont lobe of Drift Glacier, where they began to incise surface channels.	
			Lahars	During the ~ 3-week period of explosive activity, multiple lahars (at least 20) were generated by explosions, subglacial heating, and/or pyroclastic density currents.	Lahars melted and entrained glacier ice. Much of the piedmont lobe of Drift Glacier became covered by associated debris, which restricted thermal and mechanical erosion by later pyroclastic flows. Lahars were also channelled through, and contributed to the enlargement of, channels	

					in the surface of Drift Glacier's piedmont lobe.	
			Overall	A combination of the events and processes mentioned above.	By the end of the 2009 eruptive period, ~ 1–2.5 x 10^8 m^3 of ice was lost from the volcano (10–25% of the total ice volume). Though more crater ice was lost during this period, overall more ice was lost during the 1989/90 eruption, when the gorge section of Drift Glacier was destroyed.	
13	Mount Spurr (Crater Peak) (USA); 61.30°N, 152.25°W	1953	Subglacial eruption	The eruption resulted in melt and the mechanical removal of ice.	The glacial ice in the centre of the summit crater was completely destroyed (forming a cauldron melt pit) in the summit crater, and the southern part of the continuous ice rim was partly breached. In this breached section, the ice was eroded into pinnacles.	Juhle and Coulter (1955); Major and Newhall (1989); Meyer and Trabant (1995).
			Supraglacial floods/lahars	Melting of ice, combined with heavy rainfall resulted in flash floods.	Large block of ice, ~ 3 m in diameter were carried from the glacier, and into the Chakachatna River valley.	
			Supraglacial tephra deposition	Because of wind direction during the eruption, glaciers to the east of the volcano were covered by black tephra, while glaciers to the south, north and west were entirely tephra free. Considerable tephra was deposited on Kidazgeni and Straight Glaciers, but little was deposited on Crater or Barrier Glaciers.	Supraglacial tephra is thought to have reduced ablation on Kidazgeni and Straight Glaciers.	

		1992	Supraglacial pyroclastic density currents	During an eruptive period, hot pyroclastic density currents travelled across Kidzageni Glacier.	Pyroclastic density currents melted and eroded snow and glacial ice, generating lahars (see below). As pyroclastic flows descended the icefall on Kidzageni Glacier, ice blocks (up to 1 m in diameter) were entrained (erosion and entrainment was focused in this steep and crevassed icefall sector of the glacier). Pyroclastic debris was deposited on the shallower section of the glacier (e.g., below the icefall).	Eichelberger et al. (1995); Meyer and Trabant (1995); McGimsey (2001); Coombs et al. (2005)
			Floods and lahars	Supraglacial floods and lahars resulted from melting and erosion by pyroclastic density currents.	Meltwater eroded a series of canyons and plunge pools several metres wide and deep into the surface of Kidazgeni Glacier.	
		2004–06	Enhanced subglacial heat flow	Increased geothermal activity at the volcano's summit resulted.	Ice overlying the geothermally active summit basin melted to form a lake-filled cavity (ice-cauldron/collapse-pit) in the summit ice cap. The ice surrounding the cavity became encircled by arcuate crevasses (suggesting a larger area of subsidence). The cavity had vertical to overhanging walls, which exposed large englacial tunnels, and was gradually enlarged as ice fell from the surrounding steep ice walls, and melted in the lake. Sagging and holes in the ice outside the cavity, may reflect the pathway of warm (englacial) water draining from the summit lake (or reflect buried fumaroles).	McGimsey et al. (2004); Coombs et al. (2005); Neal et al. (2007); Mercier and Lowell (2016)

			Supraglacial lahars (debris flows)	Ice falling into the summit meltwater lake likely caused a water-debris mixture to be displaced, and emerge supraglacially (through crevasses) as dark, fluid debris flows.	Dark debris was deposited supraglacially. Some flows were associated with rills (metres deep), likely indicating erosion/melt of the glacier surface (either during the flow of warm debris, or post deposition, as dark debris was heated because of its lower albedo, and sank into the colder, higher albedo ice). The overall effect of this debris on the glacier/icefield is presumed to have been minimal.	
14	Mount Wrangell (USA); 62.00°N, 144.02°W	1899	Enhanced subglacial heat flow	An increase in subglacial volcanic heat flux followed a major regional earthquake.	Increased heat flux resulted in subglacial melt and glacier mass loss.	McGimsey et al. (2004)
		1964–ongoing	Enhanced subglacial heat flow	An increase in subglacial heat flux was centered under the North Crater. This was probably a result of the great Alaskan earthquake (March 1964).	Increased melting of ice (> 500 m thick) in the North crater resulted in ice-cauldron formation. For example, between 1908 and 1965, the glacial ice filling this crater is assumed to have been in equilibrium (with accumulation balanced by glacier flow and geothermally-induced basal melting), but since 1965 ice melt has increased. During periods when melting exceeded water removal, a lake formed in the crater (e.g., in 1974, 1979, 1981 and 1983). Since 1965, the 3 glaciers which emanate from the North Crater (i.e., Ahtna, and South and Centre MacKeith Glaciers) have advanced, unlike other glaciers on the volcano, and	Mendenhall (1905); Dunn (1909); Benson et al. (1975); Benson and Motyka (1978); Motyka et al. (1983); Benson and Follett (1986); Clarke et al. (1989); Sturm et al. (1991); Sturm (1995)

					elsewhere in the Wrangell Mountains. The rate of advance has been 5–18 m a^{-1} since 1965. This advance is assumed to be the result of volcanic meltwater which changed subglacial conditions. These glaciers also show little seasonal variation in their surface velocity, supporting the idea that volcanically-produced meltwater is driving flow (since volcanically-produced meltwater is not subject to seasonal change).	
		1999	Possible subglacial eruptions	Steam and ash were observed emanating from the volcano's north summit crater. Supraglacial debris also surrounded the crater.	On the upper section of Chestnina Glacier, chaotically jumbled blocks of ice were produced. The glacier surface became more crevassed than usual. This crevassing likely reflects glacier advance (though this was not directly observed). Holes in the glacier surface, surrounding fumaroles, were also enlarged.	McGimsey et al. (2004)
15	Mount Baker (USA); 48.78°N, 121.81°W	1958–76	Supraglacial avalanches and debris flows (possible lahars)	Due to enhanced subglacial geothermal activity (and meltwater produced by summer ablation), avalanches of snow, rock and mud flowed from Sherman Peak, and extended 2–2.6 km down Boulder Glacier (these avalanches occurred numerous times between 1958 and 1976). This debris was deposited as blocks of ice and snow on the upper half of Boulder	Avalanches and flows stripped snow and ice from the steep slopes of Sherman Peak (Part of Mount Baker). Along their flow paths, avalanches appear to have scoured into the glacier surface.	Frank et al. (1975); Weaver and Malone (1979)

				Glacier, and as a thin layer of supraglacial mud near the glacier's terminus.		
		1975–76	Enhanced subglacial heat flow	Long-term geothermal and fumarolic activity has progressed within the ice-filled Sherman Crater, near the summit of Mount Baker. This activity increased in 1975–76.	Long-term activity resulted in a large ice pit in the crater-occupying glacier, but prior to 1975, much of the ice was comparatively smooth, with few surface crevasses. During 1975–76, melting of the summit glacier increased, forming (and enlarging) a series of depressions, a ~ 50 m x 70 m collapse pit (which enlarged largely through calving) containing a small lake, and resulting in other disruptions to the ice, including forming a number of large crevasses, as the crater ice began to accelerate downslope (towards its east branch). Small surface ice pits also developed in the upper part of Boulder Glacier. During this period, almost half of the crater ice melted. Much of the increased meltwater readily drained though a well-developed spillway beneath Boulder Glacier.	Frank et al. (1975, 1977); Malone and Frank (1975); Weaver and Malone (1979); Coombs et al. (2005); Crider et al. (2011)
16	Mount St Helens (USA); 46.20°N, 122.18°W	1980	Subglacial dome growth	Prior to the major eruption in 1980, bulging (and minor eruptions) occurred.	Bulging resulted in deformation and crevassing of overlying glaciers.	Brugmand and Post (1981); Christiansen and Peterson (1981); Waitt et al. (1983); Schilling et al. (2004)
			Subglacial eruption	The volcano experienced a large horizontal blast. Before the eruption, the volcano hosted 13 small glaciers (11 named), covering ~ 5 km^2.	During the eruption, ~ 70% (0.13 km^3) of the 0.18 km^3 of glacial ice was removed (within minutes). Loowit and Leschi Glaciers were totally destroyed. Wishbone Glacier was almost totally destroyed.	

					Shoestring, Forsyth, Ape, and Nelson Glaciers were beheaded (due to crater formation). Others (e.g., Swift and Dryer Glaciers) were largely unaffected. Where glaciers were beheaded, ice avalanches frequently fell into the crater (where the ice soon melted). Ice cliffs (from beheaded glaciers) slowly retreated from the crater rim (due to ice flow and melting). Glacier beheading appears to have caused limited glacier retreat, because supraglacial tephra and pyroclastic deposits insulated glaciers (see below). Despite this, by September 2001, Shoestring, Nelson, Forsyth, and Dryer Glaciers had disappeared, while Ape Glacier had shrunk considerably.	
			Supraglacial tephra deposition	Tephra was deposited on numerous local glaciers. For example, a deposit ~ 1.3 m thick accumulated on Swift Glacier.	Glaciers on the south flank of the volcano experienced unusually high mass balance in 1980 due to insulation beneath supraglacial tephra.	
			Supraglacial pyroclastic density currents	Supraglacial pyroclastic density currents swept down many drainage basins (even during subsequent smaller eruptions).	Hot pyroclastic density currents melted or eroded minor amounts of ice from the surface of remaining glaciers (e.g., Nelson, Ape, Toutle and Talus Glaciers). Some of the snow/ice melt generated further mudflows (though smaller than those produced by the initial large eruption).	

			Floods/Lahars	Melting snow and ice triggered numerous supraglacial floods and mudflows (e.g., on Shoestring, Toutle, Talus, and Swift Glaciers). Blocks of snow and ice incorporated into deposits subsequently melted, leading to lahars. Following the eruption, the interaction between lava and glaciers continued to produce lahars until 1982.	Supraglacial rills and channels were eroded into remaining glaciers (e.g., Toutle and Talus Glaciers). These channels resulted from small supraglacial streams, formed either by rainfall, or from surface melt beneath hot pyroclastic deposits.	
		2004–06	New glacier formation and subsequent subglacial dome growth and extrusion	Following the 1980 eruption, a small glacier (~ 1 km^2, up to 200 m thick) formed in the summit crater of Mount St Helens. In 2004–06 a (solid state) lava dome developed beneath this glacier.	The dome growth produced a hole in, and then extruded through, the new crater glacier. This slit the glacier into two parts (East and West Crater Glaciers), which were then squeezed between the growing lava dome and the crater wall. As a result of this squeeze, the surfaces of East Crater Glacier (ECG) and West Crater Glacier (WCG) buckled, forming multiple crevasses. During this period, both glaciers locally doubled in thickness (at a rate of 0.6 md^{-1}). Since dome growth stopped, the glaciers have thinned in their upper reaches, and thickened in their lower (as 'normal' flow has resumed, and ice has been redistributed downslope). During this period, the terminus of ECG has also advanced.	Schilling et al. (2004); Walder et al. (2005, 2007, 2008, 2010); Price and Walder (2007)

17	Mount Hood (USA); 45.37°N, 121.70°W	1853–1869, 1907	Minor eruptions and enhanced subglacial heat flow	A series of minor eruptions and geothermal heating resulted in subglacial melt.	Melting bisected White River Glacier (sometime between 1894 and 1912). This partly beheaded the glacier by reducing its accumulation area. Between 1901 and the mid-1930s, a minor eruption and geothermal activity are assumed to have enhanced climatically-driven mass loss at the glacier (now known as Coalman Glacier).	Sylvester (1908a,b); Cameron (1988); Harris (1988); Lillquist and Walker (2006)
			Supraglacial debris deposition	Supraglacial volcaniclastic material accumulated on Eliot Glacier (which occupies Mount Hood).	Based on observations from 1984–89, this supraglacial debris limited surface ablation (i.e., resulting in mass balance that was less negative).	Lundstrom et al. (1993)
18	Iztaccíhuatl (Mexico); 19.18°N, 98.64°W	Late 20th century	Enhanced subglacial heat flow	Both geo- and hydro-thermal heat flow were enhanced.	Enhanced subglacial heat flow resulted in accelerated melt. Ayoloco Glacier experienced a four-fold increase in the rate of area loss between the 1958–1982 and 1982–1998 periods. Centro Oriental Glacier almost entirely disappeared due to this increased melt. A crevasse-like opening (~ 50 m long) developed in El Pecho Glacier, presumed to lie above a subglacial vent.	Delgado Granados et al. (2005); Schneider et al. (2008)
19		1994–2001	Subglacial eruptions	Active fumaroles developed beneath glaciers.	Fumaroles resulted in continuous, year-round, subglacial melt.	Delgado Granados (1997); Palacios and Marcos

	Popocatépetl (Mexico); 19.02°N, 98.63°W		Supraglacial pyroclastic density currents	Numerous eruptions resulted in supraglacial pyroclastic density currents.	Pyroclastic density currents incised the glacier surface (by up to 10 m), and triggered lahars, which entrained and transported ice blocks with diameters > 2 m.	(1998); Palacios et al. (1998, 2001); Huggel and Delgado (2000); Capra et al. (2004, 2015); Julio-Miranda et al. (2005, 2008); Tanarro et al (2005); Andrés et al. (2007); Delgado Granados (2007)
			Supraglacial deposition of tephra and other volcanic ejecta	Tephra covered the summit glacier. Due to deposition and remobilisation, the tephra was distributed heterogeneously. Hot incandescent material (repeatedly ejected during the eruptions) also landed supraglacially.	Heterogeneous tephra distribution (with spatial differences in thickness) resulted in differential ablation (i.e., some parts experienced high mass loss, while others were insulated). The upper part of the glacier (where tephra was thickest) was well insulated, and formed an almost flat area, separated from the irregular glacier surface below by a crevasse, which developed into a scarp. Further down-glacier, the glacier surface developed a 'stair-like' morphology (because of differential ablation). The insulation of the upper part of the glacier led to ice thickening, while the lower part of the glacier thinned. This increased the glacier's surface slope, resulting in ice being transmitted towards the terminus in a kinematic wave of ice thickening. This caused the glacier's terminus to uplift, but not advance. Because this kinematic wave transmitted ice towards the glacier's terminus, it resulted in increased melt (at this lower altitude). As melt continued, the	

					irregular stair-like glacier surface continued to develop. As tephra was remobilised, the tephra-meltwater mix repeatedly incised the glacier surface. Supraglacially deposited incandescent material also resulted in melting of the glacier surface, and the formation of holes and impact craters (formed by physical impact and subsequent melting). The net result of the above processes was that the glacier lost mass and recession accelerated. In 2000, the glacier front disappeared, and much of the remainder of the glacier began to fragment (by a combination of differential ablation and tephra remobilisation). Ultimately, tephra deposition notably enhanced climate related glacier recession. Between 1996 and 2001, 53% of the glacier surface area was lost. Between 2000 and 2001 (when melting was most intense), 19% of the glacier area was lost. In 2004, the glacier disappeared completely (or at least the remaining ice was no longer flowing), through a combination of climate warming, and this tephra impact.	
20	Nevado del Ruiz (Columbia); 4.90°N, 75.32°W	1985	Subglacial eruptions	Subglacial explosive activity.	Some crevasses appeared in the surface ice cap. Around the northern part of the main summit crater (Arenas Crater). These	Naranjo et al. (1986); Thouret et al. (1987, 2007);

					crevasses were concentric, with associated fumaroles. As ice collapse occurred along theses fractures, the Arenas Crater was enlarged into an ice-free caldera, 750–850 m wide and ~ 250 m deep.	Pierson et al. (1990); Thouret (1990); Ceballos et al. (2006); Huggel et al. (2007)
			Supraglacial deposition of tephra and other volcanic ejecta	Tephra and large ballistic blocks, accretionary lapilli, and bombs landed on the summit glaciers. Tephra (400-500°C) covered ~ 2/3 of the ice cap.	Large bombs produced melt pockets up to 2 m in diameter, and 0.5 m deep in the supraglacial snow. Where tephra was thinnest, some melting of the glacier surface also occurred.	
			Supraglacial pyroclastic density currents	Both dilute (surges) and concentrated (flows) pyroclastic density currents were produced.	Dilute, fast moving pyroclastic surges were unable to produce much melting (i.e., they did not have enough thermal mass), and had little impact on the snow-covered glaciers. However, higher density pyroclastic flows eroded into and melted (i.e., there were mechanical and thermal effects) the underlying glaciers. For example, on Nereidas, Azufrado and Lagunillas Glaciers, flows created flat-floored, graben-like, channels up to 100 m wide, and 2–4 m deep, with associated flow levees. In places, these channels were eroded through the ice, and into the underlying sediment. Furrows (typically < 2 m deep) were eroded into the steeply sloping parts of the summit ice cap (though these furrows were likely largely eroded into snow). Some of these furrows	

					were deepened by subsequent meltwater erosion. The extent of scouring diminished down slope, and was minimal at the glacier termini. The denser pyroclastic flows also caused mechanical abrasion of crevasses that they overran, and were particularly efficient at eroding fractured ice (i.e., in areas of steep and heavily crevassed glaciers). In these regions, seracs were planed smooth. Pyroclastic material was deposited supraglacially (inter-layered with tephra), and was deepest (4–6 m) on the east side of Arenas Crater.	
			Supraglacial avalanches	Seismic and volcanic activity fractured glaciers and resulted in various ice and rock avalanches. These avalanches were likely promoted by overriding pyroclastic flows.	Avalanches eroded supraglacial rills and gullies, and redistributed ice and snow. Ice avalanches (along with pyroclastic flows) also led to major ice losses from glaciers in the Azufrado, Lagunillas and Farallon-Guali basins. In particular, the 10–15 m thick, crevassed snout of the Lagunillas glacier and the hanging glaciers on the headwall of the Azufrado valley were removed (mechanically and through melting) by ice avalanches. The melt caused by these avalanches also contributed to lahars.	

			Overall impact	A combination of the events and processes mentioned above.	Following the 1985 eruption, ~ 25–30% of the summit ice cap at Nevado del Ruiz was destabilised (fractured, eroded and rendered unstable), ~16% (4.2 km^2) of the surface area and ~9% (0.06 km^3) of the total volume of snow and ice was lost. The destabilisation of the outlet glaciers was likely promoted by the formation of numerous englacial and subglacial tunnels (which likely promoted melt and detached glacier ice from the bedrock). Since the eruption, outlet glaciers have remained in fractured and unstable states (particularly Lagunillas and Azufrado Glaciers). These destabilised glaciers have been particularly susceptible to post-eruption retreat.	
21	Nevado del Huila (Columbia); 2.93°N, 76.03°W	2007–12	Subglacial eruptions	Numerous sub-glacial phreatic and phreatomagmatic eruptions occurred, with hot water released from fissures.	A crater (~ 500 m in diameter) formed in the summit ice. Fumaroles broke through the glacier surface. Large fissures, up to 2 km long and 50–80 m wide, formed in the summit ice. Hot water (from fissures) melted part of the summit ice and snow, leading to lahars. The glacier on the west flank of the volcano became heavily fractured. Prior to the eruptions, glaciers occupying the volcano covered ~ 10.7 km^2. By 2009, the glacier area had reduced to ~ 9.8 km^2.	Pulgarín et al. (2008, 2009, 2010, 2011); Cardona et al. (2009); Worni (2012); Worni et al., (2012); Rabatel et al. (2013); Delgado Granados et al. (2015)

			Subglacial dome growth	Domes formed between the Central and South peaks.	Domes caused deformation of the glacier surface.	
			Lahars	Water was produced through melting and from hydrothermal sources (see above).	Lahars eroded channels in the glacier surfaces, and a portion (~ 400,000 m^3) of El Oso Glacier tongue was lost.	
22	Cotopaxi (Ecuador); 0.68°S, 78.44°W	1877	Supraglacial pyroclastic surges and flows	Supraglacial pyroclastic surges and flows (scoria flows, rather than density currents) descended from the volcano's summit.	Melt occurred where pyroclastic flows made direct contact with ice, but not where the glacier (ice cap) surface was already covered by tephra (deposited during an earlier eruption). In addition to melt, flows entrained large chunks of glacial ice. These processes (thermal and mechanical) resulted in the formation of gullies (40–50 m deep) in the summit snow and ice. Melting due to pyroclastic flows also resulted in lahars. However, since flows and lahars were focused in supraglacial gullies, comparatively small parts of the glacier were affected by melt or scouring. The geometry of the volcano's crater rim focused flows down the west and east flanks, meaning that glaciers in these regions experienced most destruction.	Wolf (1878); Barberi et al. (1992); Aguilera et al. (2004); Pistolesi et al. (2013, 2014)
			Lahars	Large sectors of snow and ice melt produced lahars (see above).	Lahars entrained large chunks of glacial ice.	
23	Tungurahua (Ecuador); 1.47°S, 78.44°W	1999–2001	Supraglacial tephra deposition	Multiple eruptions led to tephra deposition on Tungurahua Volcano and fine/thin	Supraglacial tephra caused increased melt and accelerated glacier retreat at Chimborazo, though these effects are	Schotterer et al. (2003); Le Pennec et al. (2012); Morueta-Holme et al.

				tephra deposition on Chimborazo Volcano, ~ 40 km to the west.	thought to be comparatively small. The small glacier occupying the summit of Tungurahua Volcano was covered with dark tephra (~ 10–20 m). Though the impact of this tephra cover is unknown, its thickness suggests it insulated the ice.	(2015); La Frenierre and Mark (2017)
24	Nevado Sabancaya (Peru); 17.78°S, 71.85°W	1986–88	Enhanced subglacial heat flow and fumarolic activity	Heating resulted in increased subglacial melt.	Caused supraglacial fracturing and a decrease in the surface area of the summit ice cap.	Gerbe and Thouret (2004)
		1990–98	Subglacial eruptions	Period of alternating vulcanian and phreato-magmatic/phreatic eruptions.	The surface crater was enlarged (up to 400 m in diameter by 1995), and its surroundings became snow and ice-free. The area of the summit ice cap also decreased. As a result of this, and more recent activity, the volcano is now almost entirely glacier free.	Gerbe and Thouret (2004); Alcalá-Reygosa et al. (2016)
25	Volcán Guallatiri (Chile); 18.42°S, 69.09°W	Late 20^{th} Century	Enhanced subglacial heat flow	Enhanced subglacial heat occurred as a result of geothermal and fumarolic activity.	Glacier melt was most intense in two regions of fumarolic activity.	Rivera et al. (2005)
26	Tinguiririca (Chile); 34.81°S, 70.35°W	1994, 2006/07	Supraglacial ice avalanches	Ice avalanches occurred on the south flank of the volcano a few months after the eruption. However, it is not clear whether these avalanches were actually triggered by the eruption.	In 2006/07, a 0.46 km^2 section of glacier detached, and generated an ice avalanche with 10–14 × $10^6 m^3$ of ice and debris.	Iribarren Anacona and Boden (2010); Iribarren Anacona et al. (2015)

27	Volcán Peteroa (Planchón-Peteroa) (Chile); 35.27°S, 70.58°W	1963–91	Enhanced subglacial heat flow	Subglacial geothermal heating occurred prior to phreatomagmatic explosions in 1991.	Glacier advance between 1963 and 1990 is attributed to subglacial melt and increased basal sliding, in response to geothermal heating.	Liaudat et al. (2014)
		1991	Subglacial eruptions	Subglacial eruptions were characterised by phreatic explosions.	Phreatic explosions melted ice and resulted in a lahar down the western flank of the volcano.	
		2004–07	Enhanced subglacial heat flow	Subglacial geothermal heating occurred prior to phreatomagmatic explosions in 2010.	Slight glacier advance between 2004 and 2007 is attributed to subglacial melt and increased basal sliding, in response to this geothermal heating.	
		2010–11	Supraglacial tephra deposition	An eruptive phase characterised by phreatomagmatic activity deposited supraglacial tephra with a maximum thickness of ~ 4 m.	Tephra deposits likely contributed to rapid glacier recession since the eruption.	Liaudat et al. (2014); Aguilera et al. (2016)
28	Nevados de Chillán (Chile); 36.86°S, 71.38°W	1973–86	Supraglacial tephra deposition	The formation of a new cone (Volcán Arrau) at the Las Termas sub-complex resulted in frequent phreatomagmatic eruptions, lava flows, pyroclastic ejections and tephra deposition.	Due to supraglacial tephra deposition, the glacier surface area at the Nevados de Chillán volcanic complex reduced notably. For example, from an area of ~ 15.8 km^2, the annual rate of reduction between 1975 and 2011 was 0.36 km^2 a^{-1}.	Casertano (1963); González-Ferrán (1995); Dixon et al. (1999); Rivera and Bown (2013)
29	Volcán Llaima (Chile); 38.69°S, 71.73°W	1979	Supraglacial and subglacial lava flows	Lava extruded from central crater, followed by explosive activity.	Lava flows melted summit ice, and resulted in mixed flows/avalanches of snow, ice, and pyroclastic material.	Naranjo and Moreno (1991)

		1994	Subglacial lava flow	A ~ 500 m long fissure opened in the main crater. From this fissure, at least 4 fountains ejected lava up to ~ 200 m high. This lava flowed from the southern end of the fissure, beneath the western summit glacier for ~ 2 km, and emerged from the lower end of the glacier.	Subglacial lava flow resulted in violent ice melt and vapourisation (~ 3–4 x 10^6 m^3 of ice was melted). From a small notch on the SSW rim of the main summit crater, a ~ 50 m wide, ~ 500 m long supraglacial ice channel formed, where the subglacial lava had melted through the glacier. Further down-glacier, this channel increased to ~ 150 m wide, for a distance of ~ 1.5 km. Due to subglacial melt induced by lava flow, a number of crevasses formed on the glacier surface. This melting also resulted in a lahar, which entrained blocks of glacial ice, and carried them down the WSW flanks of the volcano.	Moreno and Fuentealba (1994); Naranjo and Moreno (2004)
		2008	Supraglacial lava flow	An eruption resulted in lava fountaining which caused the lava lake in the main summit crater to overflow at its western rim. The resulting supraglacial lava flow descended ~ 2 km down the western flank of the volcano.	Supraglacial lava flows melted part of the summit glacier, forming channels (10s of metres deep) in the ice surface. This melt resulted in lahars.	Venzke et al. (2009); Ruth et al. (2016)
30	Volcán Villarrica (Chile); 39.42°S, 71.93°W	1971	Supraglacial lava flow	The volcano often has an active lava lake within its summit crater (which is surrounded by ice). During the eruption, this lake overflowed, and supraglacial lava flows were produced on the SW flank of the Volcano.	Lava flows melted supraglacial vertical-walled channels up to 40 m deep (this melt occurred at a relatively slow rate, and did not result in floods or lahars). Volcanic activity continued, and a fissure (with lava fountains up to 400 m high) opened across the summit crater. This phase of the	González-Ferrán, (1973); Riffo et al. (1987); Moreno and Fuentealba (1994); Naranjo and Moreno (2004)

					eruption resulted in sufficient ice melt (over a period of ~ 1 month) to generate lahars (which bulked from watery flows into hyperconcentrated debris flows as they extended downslope).	
		1984–85	Supraglacial and subglacial lava flows	Multiple lava flows were produced during a Strombolian/Hawaiian eruption. Lava traveled subglacially (for ~ 150 m), before emerging supraglacially.	Lava melted channels in the ice and snow on the north and NE slopes of the volcano. Three separate channels were melted into the ice: one ~ 1 km long, 50 m wide and 30–40 m deep; one ~ 200 m long and 50 m wide; and one ~ 1 km long, 80 m wide and 40 m deep. Lava flows are also thought to have produced crevasses in surrounding ice, and triggered mixed snow and rock avalanches. During these events, small floods were triggered down the volcano's north lower flank, but effusion rates were likely too low to produce lahars (unlike during the 1971 eruption), though limited sediment availability may also partly explain this.	Moreno (1993); González-Ferran, (1984, 1985); Clavero and Moreno (2004); Naranjo and Moreno (2004)
			Supraglacial tephra and debris deposition	Supraglacial tephra and debris was deposited on Pichillancahue-Turbio Glacier (which occupies Volcán Villarrica).	For Pichillancahue-Turbio Glacier, tephra cover in the ablation area acted to insulate the surface, and reduce surface ablation. As a result, over recent decades, glacier retreat has been slower than for other glaciers in the area. At Volcán Villarrica, Brock et al (2007) showed that a tephra layer even < 1	Brock et al. (2007); Rivera et al. (2006, 2008, 2012); Masiokas et al. (2009)

					cm thick could lead to insulation. This is typically lower than the critical thickness documented in other areas, and likely reflects the tephra's low thermal conductivity (see Rivera et al. 2012).	
		Various	Enhanced subglacial heat flow	Geothermal heating resulted in melt beneath Pichillancahue-Turbio Glacier.	Recently, the glacier has retreated at a faster rate than other glaciers in the region. This is thought to be partly due to enhanced basal melt in response to geothermal heating.	
31	Puyehue-Cordón Caulle (Chile); 40.59°S, 72.12°W	2011	Supraglacial tephra deposition	A discontinuous tephra layer was deposited on Sollipulli Glacier (to the north of Puyehue-Cordón Caulle). Tephra deposition was discontinuous, resulting in both thin layers and thick debris cones.	Melt was enhanced under discontinuous tephra, and hindered under continuous tephra (e.g., under debris cones). Because much of the tephra was discontinuous, the overall impact was to increase ablation.	Hobbs et al. (2011)
32	Volcán Calbuco (Chile); 41.33°S, 72.61°W	1961	Enhanced subglacial heat flow	Subglacial heating occurred hours prior to the onset of eruptive activity.	Heating caused subglacial melt, which triggered a lahar.	Casertano (1961); Klohn (1963); Tazieff (1963)
			Subglacial eruption	A Subglacial eruption caused subglacial melt.	The eruption melted through the crater-occupying glacier.	Klohn (1963); Hickey-Vargas et al. (1995); Castruccio et al. (2010)
			Subglacial lava flow	Subglacial lava extruded from the south vent.	Events resulted in a doming of the overlying ice and produced a supraglacial system of concentric and radial cracks/fissures ~ 200 long.	
			Supraglacial pyroclastic density currents	Supraglacial pyroclastic density currents were triggered by active dome collapse.	Pyroclastic density currents resulted in supraglacial melt, which triggered a lahar.	

33	Volcán Michinmahuida (Chile); 42.79°S, 72.44°W	2007–08	Enhanced subglacial heat flow	Subglacial geothermal heating occurred several months prior to an eruption at Volcán Chaitén (~ 15 km to the west and connected by faults to Michinmahuida).	Subglacial melt resulted in a period of glacier advance and acceleration (despite reduced albedo because of tephra cover—see below). For example, Glaciar Amarillo retreated at a rate of ~ 76 m yr^{-1} between 1961 and 2007, but advanced 243 ± 49 m between November 2007 and September 2009 (after which, glacier retreat resumed).	Rivera et al. (2012); Rivera and Bown (2013)
34	Volcán Chaitén (Chile); 42.84°S, 72.65°W	2008	Supraglacial tephra deposition	An eruption deposited a 10–20 cm tephra layer on glaciers covering nearby (15 km to the east) Volcán Michinmahuida (see above).	Supraglacial tephra caused a notable reduction in the surface albedo of these glaciers—particularly those in the direct path of tephra (i.e., those on the western slopes of the volcano). This likely had some impact on ice conditions, however glacier dynamics appear to have been dominated by geothermal heating (see above), though increased surface melt (due to reduced albedo) may have allowed meltwater to form, drain to the bed, and increase basal sliding.	Alfano et al. (2011); Rivera et al. (2012); Rivera and Bown (2013)
35	Volcán Hudson (Chile); 45.90°S, 72.97°W	1971	Subglacial eruption	Explosive subglacial eruption.	Resulted in the destruction or melt of 50–80% (60 km^2) of the intra caldera ice (i.e., the glacier draining to the NW was partly beheaded). This volume of ice reformed by 1979.	Fuenzalida (1976); Guzmán (1981); Best (1992); Branney and Gilbert (1995); González-Ferrán (1995); Naranjo and Stern (1998); Rivera et al. (2012); Rivera and Bown (2013)
			Subglacial lava flow	A lava flow extended beneath ice cover near the volcano's summit.	Subglacial lava likely caused melting at the head of Huemules Glacier.	

			Lahars	Lahars were produced because of ice melt.	Lahars entrained blocks of glacial ice, and lahar deposits were emplaced on Huemules Glacier.	
		1991	Subglacial eruptions	A fissure eruption was followed by a massive magma explosion from the SW part of the ice-filled summit caldera.	Eruptions melted caldera ice, and triggered lahars down Huemules Glacier (see below). A cauldron (~ 1 km diameter) bounded by crevasses, formed in the summit ice. Ultimately, the eruption destroyed or melted much (~20 km^2) of the intra caldera ice.	Banks and Iven (1991); Naranjo et al. (1993); Branney and Gilbert (1995); González-Ferrán, (1995); Naranjo and Stern (1998); Rivera et al. (2012); Amigo (2013); River and Bown (2013)
			Supraglacial and subglacial lava flows	Lava flowed from a ~ 5 km long fissure on the western margin of the caldera, then on, and beneath, Huemules Glacier. The supraglacial lava flow was 50–300 m wide and 3.5 km long.	Lava flow rapidly melted the ice, and associated meltwater likely contributed to lahars.	
			Lahars	Small lahars were triggered by initial melt. A larger lahar was likely triggered when meltwater accumulated in the caldera, before being released down Huemules Glacier.	The largest lahars entrained blocks of glacial ice (> 5 m in diameter). Lahar deposits were also emplaced on Huemules Glacier. In all, the lahars are a possible cause of ~ 150 m recession at the snout of Huemules Glacier.	
			Supraglacial tephra deposition	Tephra was deposited across much of the local area (particularly within the caldera), with thicknesses ranging from 15 to 100 cm.	Meltwater produced by hot tephra likely contributed to lahars.	
			Overall	A combination of the events and processes mentioned above.	Due to the 1991 eruption, glaciers occupying Volcán Hudson experienced more mass loss than any other glaciers	

					occupying volcanoes in the Southern Andes.	
		2011	Enhanced subglacial heat flow	Months prior to an eruption, hotspots were evident in thermal imagery (possibly indicating a pre eruptive phase of increased geothermal activity).	Subglacial heating caused ice melt, triggering lahars.	Delgado et al. (2014)
			Subglacial eruption	An eruption caused subglacial melt.	Melt generated three craters (each < 500 m in diameter) and concentric crevasses in the intra-caldera ice surface.	Amigo et al. (2012)
			Lahars	Ice melt triggered lahars, which descended from the caldera down numerous valleys.	Lahars entrained blocks of ice from Huemules Glacier, and appear to have caused changes in the glacier surface elevation.	
36	Volcán Lautaro (Chile); 49.02°S, 73.55°W	Various 20th Century	Supraglacial tephra deposition	Eruptions deposited tephra on a number of adjacent glaciers (many of them outlets of the South Patagonian Ice Field).	O'Higgins Glacier experienced rapid retreat (~ 14.6 km) between 1945 and 1986. However, whether this was a result of increased calving or the impact of supraglacial tephra (and perhaps geothermal heating) is unclear.	Lliboutry (1956); Kilian (1990); Warren and Rivera (1994); Motoki et al. (2003, 2006); Lopez et al. (2010)
37	Deception Island (Sub-Antarctic Islands); 62.97°S, 60.65°W	1969	Subglacial eruption from a volcanic fissure	Magma and superheated steam likely initiated rapid subglacial melting.	Produced fissures (500–1000 m long, 100–150 m wide) in the overlying ice cap. In total, 76 x 10^6 m^3 of ice melted.	Baker et al. (1969, 1975); Orheim and Govorukha (1982); Smellie (2002); Smellie and Edwards (2016)
			Supraglacial tephra and debris deposition	From surface fissures, pyroclastic cones formed, and spread onto the surrounding	Surface deposits lowered albedo, and resulted in particularly negative mass	

				ice. The eruption also resulted in notable tephra deposition.	balance for the three subsequent years (up to 1973).	
			Flooding	Fissures were the source of a large jökulhlaup, which flowed across (and presumably under) the ice cap surface.	Downslope from the fissures, the ice experienced a short 'surge'-like advance. Floods also eroded supraglacial channels.	
38	Bristol Island (Sub-Antarctic Islands); 59.04°S, 26.53°W	1935–1962	Subglacial eruption	A subglacial eruption led to melt.	A crater and fissure formed in the overlying ice cap. The 1962 crater was ~ 220 m wide, and 60 m deep.	Holdgate and Baker (1979); Patrick and Smellie (2013)
39	Mt Belinda (Sub-Antarctic Islands); 58.42°S, 26.33°W	2001–07	Eruption from a pyroclastic cone within an ice-filled caldera	Eruptions (several effusive events and low-intensity explosive activity) triggered subglacial melt.	An adjacent valley glacier advanced a few hundred metres into the sea.	Patrick et al. (2005); Patrick and Smellie (2013); Smellie and Edwards (2016)
			Supraglacial lava flow	Effusive events resulted in lava flow.	Lava melted deep gullies in the surrounding ice.	
			Supraglacial ejection of bobs and other material	Material scattered the snow-covered Mt Belinda	Numerous pits were melted into snow, though impacts on underlying glaciers are less clear.	
40	Mawson Peak (Sub-Antarctic Islands); 53.11°S, 73.51°E	2006-08	Supraglacial lava flow	During an eruptive period, short (typically < 300 m long) supraglacial lava flows extended from the summit.	A supraglacial channel formed, leading from the summit to a crevasse-bounded depression (melt pit). This may have resulted from supraglacial lava flow and subsequent ponding.	Patrick and Smellie (2013)
41	Mount Ruapehu (New Zealand); 39.28°S, 175.57°E	1995–96	Lahars	Lahars were triggered by eruptions through the near-permanent Crater Lake, which resulted in the ejection of water and lithic material onto surrounding glaciers.	Waves on Crater Lake undercut Crater Basin Glacier, resulting in an ice cliff, and an adjacent heavily crevassed zone. On the eastern side of the summit ice cap, the ice	Cronin et al. (1996); Manville et al. (2000); Kilgour et al. (2010); Conway et al. (2015)

					on the crater rim was thinned by cascading water and other debris from Crater Lake. This material also led Whangaehu Glacier to become gullied and pot-holed. Avalanches and icefalls were triggered by lahars undercutting stable slopes. Lahars re-opened a former channel through Whangaehu Glacier, and caused the retreat of the adjacent Tuwharetoa Glacier.	
			Supraglacial tephra deposition	Tephra and other ejected material was deposited on glaciers occupying the volcano.	Tephra layers < 5 mm thick caused the fastest melting. Layers > 20 mm thick inhibited melting. As a whole, the thin tephra cover on the snow/ice covered areas enhanced melting of the seasonal snowpack, and reduced the size of all six glaciers that occupy the volcano.	Manville et al. (2000); Chinn et al. (2014)
		2007	Lahars	As in 1995–96, lahars were initiated by eruptions through the near-permanent Crater Lake, which resulted in the ejection of water and lithic material onto surrounding glaciers.	Lahars entrained snow and ice from the head of the Whangaehu Glacier, and eroded shallow gullies and potholes into the glacier surface.	Kilgour et al. (2010)
			Supraglacial tephra deposition	An explosion (from the Crater Lake) deposited ash, mud and rocks over the snow-covered plateau icefield (occupying the summit).	Ablation was maximised under 70 mm thick tephra, minimised under 400 mm of tephra, and the critical thickness was 120 mm.	Richardson and Brook (2010)
42	Mutnovsky (Russia);	2000	Subglacial eruption	The volcano experienced a powerful phreatic explosion.	Activity partially melted the overlying summit ice, reopening a formerly subglacial crater.	Kiryukhin et al. (2008)

	52.45°N, 158.20°E	Ongoing	Enhanced subglacial heat flow and fumarolic activity	A number of fumaroles in the glacier occupied crater resulted in subglacial heating.	Subglacial melt was enhanced.	Waltham (2001); Kiryukhin et al. (2005): Eichelberger et al. (2009)
43	Avachinsky (Russia); 53.26°N, 158.83°E	1945	Supraglacial tephra and debris deposition	The surface of Kozelsky Glacier was covered by 1.5–2 m thick tephra/debris layer.	Kozelsky Glacier advanced ~ 250 m between 1977 and 2004 (though positive mass balance during the 1960s and 1970s is presumed to reflect climatic forcing). Over much of the 20th century, the glacier is presumed to have largely stagnated (rather than advanced), due to accumulated volcanic debris.	Vinogradov and Muraviev (1982); Solomina et al. (1995, 2007); Muraviev et al. (2011); Manevich et al. (2015)
		1991	Supraglacial lava flows, debris avalanches and lahars	Lava overflows from the crater were accompanied by hot debris avalanches that triggered two lahars.	Halaktyrsky Glacier (which occupies the volcano's southern slope) began an advance that continues to this day, though the exact cause of this advance is unclear.	Muraviev et al. (2011); Viccaro et al. (2012)
44	Tolbachik (Russia); 55.82°N, 160.38°E	1975–76	Subglacial eruption	A fissure eruption of Plosky Tolbachik caused caldera collapse and subglacial melt.	Tolbachinsky Glacier, which occupies the caldera, lost two-thirds (1 km^2) of its surface area (decreasing from 1.54 to 0.5 km^2). Cheremoshny Glacier began to advance.	Fedotov et al. (1980); Vinogradov and Muraviev (1982); Muraviev et al. (2011); Muraviev and Muraviev (2016)
		2012–13	Supraglacial lava flow	Lava from the eruption travelled over snow and ice.	Lava caused limited melt of ice or snow	Edwards et al. (2014)
45	Bezymianny (Russia);	1955–57	Subglacial eruption	A subglacial eruption resulted in ice loss.	A glacier occupying the volcano's NW slope was completely destroyed.	

	55.98°N, 160.59°E		Pyroclastic density current	Pyroclastic debris was deposited supraglacially.	Shelty Glacier retreated slightly, but the front was reasonably stationary during subsequent years.	Vinogradov (1975); Muraviev and Muraviev (2016)
46	Klyuchevskoy (Russia); 56.06°N, 160.64°E	1944–45	Supraglacial debris deposition	An eruption led to a landslide of ice and erupted material (250–300 million m^3) onto the accumulation area of Erman and Vlodavtsa Glaciers.	Supraglacial debris caused the advance of Erman and Vlodavtsa Glaciers. Erman advanced by ~ 4 km, and this is ongoing.	Muraviev and Salamatin (1993); Muraviev et al. (2011); Muraviev and Muraviev (2016); Dokukin et al. (2017)
		1953	Subglacial eruption	The eruption led to increased subglacial melt.	Sopochny Glacier increased from 3.6 to 4.6 km^2, and advanced 1-2 km.	Muraviev and Muraviev (2016); Dokukin et al. (2017)
		1966–68	Subglacial eruption	The eruption led to increased subglacial melt.	Vlodavtsa Glacier increased from 2.6 to 3.1 km^2, and advanced 2.2 km. Sopochny Glacier also advanced.	Vinogradov (1975, 1985); Muraviev and Muraviev (2016); Dokukin et al. (2017)
		1977–80	Subglacial eruption	The eruption led to increased subglacial melt.	Shmidta Glacier advanced until 1987, when part of the glacier tongue was destroyed by an eruption.	Muraviev et al. (2010, 2011); Muraviev and Muraviev (2016)
		1982–83	Subglacial eruption	The volcano experienced a lateral eruption of its east flank.	A sizeable part of Kellya Glacier's accumulation area was destroyed.	Vinogradov and Muraviev (1982, 1985); Muraviev and Muraviev (2016)
		1984–85	Supraglacial lava flow	The volcano experienced an eruption, with an associated supraglacial lava flow.	Lava melted ice and triggered a lahar.	Ivanov (1984); Dvigalo and Melekestsev (2000)
		1985–86	Supraglacial lava flow	An explosion occurred on the volcano's NW flank.	Lava melted a supraglacial channel, and triggered a lahar that travelled 35 km.	Fedotov and Ivanov (1985); Dvigalo and Melekestsev (2000)
		1986–90	Supraglacial lava flow	A 5–6 m wide supraglacial lava flow extended ~ 600 m.	Lava caused ice melt, and triggered a 10–12 km long mud flow.	Zharinov et al. (1993)

			Lahars	An eruption triggered lahars.	Part of a glacier's terminus was destroyed (the glacier had been advancing). The eruption also destroyed part of the accumulation area.	Muraviev et al. (2011); Dokukin et al (2017)
		2005–10	Subglacial eruption	The eruption led to increased subglacial melt.	Shmidta Glacier advanced.	Muraviev et al. (2010, 2011)
			Lahar	Melting in 2007 triggered a lahar.	Part of the terminus of Sopochny Glacier was broken off.	Muraviev et al. (2010); Dokukin et al. (2017)
47	Ushkovsky (Russia); 56.07°N, 160.47°E	1959–60, 1982–84	Enhanced subglacial heat flow	The region is presumed to have experienced a strengthening of seismic (and perhaps volcanic) activity.	Bilchenok Glacier, which emanates from the ice-filled caldera and occupies the NW slope of the volcano, advanced ('surged') 1050–1150 m in 1959–1960 and 700–800 m in 1982–84.	Muraviev et al. (2011, 2012), Muraviev and Muraviev (2016)
48	Shiveluch (Russia); 56.65°N, 161.36°E	1964	Subglacial eruption	The volcano experienced a large directed blast.	Blocks of glacial ice (10–15 m^3) were found > 10 km from the volcano.	Gorshkov and Dubik (1970)
49	Mount Kazbek (Russia/Georgia)	Various 20th and 21st Century	Enhanced subglacial heat flow (possible)	The region is presumed to have experienced periods of increased volcanic/geothermal activity.	Catastrophic debris flows (water, debris, and glacial ice) emanated from three of the region's glaciers (Devdorak, Kolka, and Abano). Parts of the glacier termini were destabilised/dislocated, triggering floods, ice-rock avalanches/debris flows and mudslides. These glaciers may also have undergone acceleration and/or advance. The exact cause of these events remains unclear, and they may have been triggered	Muravyev (2004); Zaporozhchenko and Chernomorets (2004); Tutubalina et al. (2005); Chernomorets et al (2005, 2006, 2007)

					by seismic activity, high rainfall events, and/or volcanic/geothermal activity.	
50	Beerenberg (Jan Mayen Island); 71.08°N, 8.16°W	1970–72	Supraglacial lava flow	Lava fountains up to 200 m high emanated from fissures. This lava flowed supraglacially (mainly across Dufferinbreen and Sigurdbreen).	Lava caused rapid supraglacial melt, which triggered floods/lahars.	Siggerud (1973); Sylvester (1975); Birkenmajer (1972)
			Supraglacial tephra deposition	Tephra and other volcanic debris was deposited supraglacially.	Supraglacial material (e.g., at Sørbreen, but also other glaciers) reduced surface ablation and thus slowed the rate of glacier retreat. This persisted until 1978.	Anda et al. (1985)
51	Grímsvötn (Iceland); 64.42°N, 17.33°W	1934	Subglacial eruption	An eruption occurred under Vatnajökull ice cap.	Subglacial melt increased, and supraglacial cauldrons were formed.	Nielsen (1937)
			Flooding	Subglacial melt triggered a large jökulhlaup.	Blocks of ice were torn from the terminus of Skeidarárjökull, resulting in 40 m high fracture faces.	
		2004	Subglacial eruption	An eruption caused subglacial melt.	~ 0.1 km^3 (150–200 m thick) of ice was melted, forming a 750 m long, 550 m wide ice cauldron.	Vogfjörd et al. (2005); Jude-Eton et al. (2012)
			Supraglacial tephra deposition	Tephra covered ~ 1280 km^2 of the NW part of Vatnajökull, and a ~ 200 m diameter tephra ring formed within the ice cauldron.	The glacier albedo was affected for several years after the eruption (albedo decreased by up to 0.35 when compared to modelled, undisturbed conditions). These impacts showed considerable spatial variability.	Möller et al. (2014)
			Flooding	The onset of a jökulhlaup preceded the eruption by four days.	The subglacial jökulhlaup caused an increase in the flow velocity of Skeidarárjökull (an outlet of Vatnajökull), by up to 0.4 m d^{-1}, compared to annual	Sigurðsson et al. (2014)

					values. This acceleration occurred over the entire width of the glacier, and is presumed to have been caused by increased glacier sliding due to widespread basal lubrication.	
		2011	Supraglacial tephra deposition	An eruption led to tephra deposition on Svínafellsjökull.	Supraglacial tephra reduced ablation rates at Svínafellsjökull by up to 59%.	Nield et al. (2013)
52	Gjálp (Iceland); 64.52°N, 17.39°W	1996	Subglacial eruption	An eruption under a 600–750 m thick NW section of the Vatnajökull ice cap resulted in the accumulation of meltwater.	Two 2 km wide and 100 m deep ice cauldrons formed above the main vents. This resulted in rapid ice flow towards the cauldrons, and the formation of a system of concentric crevasses. In one location, the eruption melted through 500 m of ice. Within 13 days (when the eruption ended), 3 km^3 of ice had melted, with a further 1.2 km^3 melting over the following three months.	Gudmundsson et al. (1997, 2002, 2004); Stefánsdóttir and Gislason (2005)
			Subglacial lava flow	The opening of a volcanic fissure possibly caused the formation of a feeder dyke that overshot the bedrock–ice interface and penetrated up into the ~500–600 m thick overlying ice cap.	A long, straight crevasse formed over the southernmost part of the volcanic fissure. This crevasse was 500–600 m deep and ~ 1 m wide.	
			Supraglacial flooding	Some meltwater flowed supraglacially, before draining to the bed (through moulins).	Supraglacial meltwater formed a 3.5 km long ice canyon, with near vertical ice walls (formed by warm water melting as it flowed through the canyon). Moulins developed (and/or were enlarged) as water drained to the bed.	

			Subglacial flooding	Meltwater (15–20°C) travelled subglacially (along a narrow channel) 15 km to the south and into Grímsvötn subglacial lake. Grímsvötn then drained, causing a jökulhlaup.	Melting occurred above the meltwater flow into Grímsvötn, in the lake, and on the jökulhlaup path out of the lake. This melting resulted in surface subsidence, and the formation of a shallow linear depression in the ice surface (along the meltwater flow path towards Grímsvötn lake). Gudmundsson et al. (1997) suggests that other than in these areas, the ice surface remained intact.	
53	Bárðarbunga (Iceland); 64.64°N, 17.53°W	2014	Subglacial eruption	A dyke erupted under the NW sector of Vatnajökull, and caused direct subglacial melt.	This subglacial melt caused glacier surface subsidence.	Gudmundsson et al. (2014)
54	Katla (Iceland); 63.63°N, 19.05°W	1918	Flooding	An eruption beneath a ~ 400 m thick section of the Mýrdalsjökull ice cap triggered a major jökulhlaup, with water flowing supraglacially (in prominent rivers) and subglacially.	The force of subglacial meltwater tore icebergs (50–60 m diameter) from the glacier terminus. During the jökulhlaup, the glacier terminus floated and may have moved forward. A gorge (1,460–1,830 m long, 366–550 m wide, and 145 m deep) was also blasted into the terminus.	Jónsson (1982); Tómasson (1996); Russell et al. (2010)
55	Eyjafjallajökull/ Fimmvörðuháls (Iceland); 63.63°N, 19.62°W	2010	Subglacial eruption	Effusive, then explosive activity caused direct subglacial melt.	Supraglacial cauldrons, with vertical walls, formed over vents (this involved melting through ~ 200 m thick caldera ice in 3–4 hours). Because of comparatively thin ice, surface deformation outside this cauldron was minimal (i.e., there was no evidence of concentric crevasses). Between the 14th and	Edwards et al. (2012); Gudmundsson et al. (2012); Magnússon et al. (2012)

					20th of April, 2010, ~10% (~0.08 km^3) of the pre-eruption caldera ice melted.	
			Supraglacial lava flow	Lava flowed ~ 3 km down the surface of Gígjökull.	Lava is thought to have largely advanced on top of the snow, without appreciable melting of the underlying ice.	
			Subglacial lava flow	On the eighth day following the eruption, lava flowed beneath Gígjökull, advancing ~ 2 km in a few days.	Subglacial lava gradually melted through Gígjökull, with ice melt (subglacial) occurring above the advancing lava front.	
			Supraglacial tephra deposition	Tephra was deposited on the summit ice cap (ice cap = 80 km^2, typically 50–200 m thick, but locally up to 30 m thick).	Snow and ice melt was limited, and tephra largely insulated the glacier surface.	
			Flooding	Beneath Gígjökull, constricted water flow likely produced high water pressures, which destroyed the subglacial channel roof. Thus, drainage was subglacial for the first 1–1.5 km, but then emerged supraglacially and flowed down both sides of the glacier. During the first days following the main explosive eruption, meltwater drained supraglacially down Gígjökull in several jökulhlaups.	Ice melt occurred along the subglacial flood path (due to the thermal and frictional energy of floodwaters). Ice was also mechanically eroded from the flood path, and surface openings formed above flood channels.	
56	Hekla (Iceland); 63.98°N, 19.70°W	1947	Flooding	During an eruption, snowmelt (likely caused by a blast of hot steam) triggered a (heated) Jökulhlaup.	The jökulhlaup eroded underlying glacier remnants.	Kjartansson (1951); Smellie and Edwards (2016)
			Supraglacial lava flow	Lava from the eruption travelled over snow and ice.	Lava did not melt much ice (not enough to cause lahars or floods).	
			Supraglacial tephra deposition	Tephra was deposited on comparatively distal glaciers.	Caused the advance of Gígjökull.	Kirkbride and Dugmore (2003)

Table references

Aguilera, E., Pareschi, M.T., Rosi, M. Zanchetta, G., 2004. Risk from lahars in the northern valleys of Cotopaxi Volcano (Ecuador). Natural Hazards 33 (2), 161–189.

Aguilera, F., Benavente, Ó., Gutiérrez, F., Romero, J., Saltori, O., González, R., Agusto, M., Caselli, A., Pizarro, M., 2016. Eruptive activity of Planchón-Peteroa volcano for period 2010-2011, Southern Andean Volcanic Zone, Chile. Andean Geology 43 (1), 20–46.

Alcalá-Reygosa, J., Palacios, D., Zamorano Orozco, J.J., 2016. Geomorphology of the Ampato volcanic complex (Southern Peru). Journal of Maps 12 (5), 1160–1169.

Alfano, F., Bonadonna, C., Volentik, A.C., Connor, C.B., Watt, S.F., Pyle, D.M., Connor, L.J., 2011. Tephra stratigraphy and eruptive volume of the May, 2008, Chaitén eruption, Chile. Bulletin of Volcanology 73 (5), 613–630.

Amigo, A., 2013. Estimation of tephra-fall and lahar hazards at Hudson Volcano, southern Chile: Insights from numerical models. Geological Society of America Special Papers 498, 177–199.

Amigo, A., Silva, C., Orozco, G., Bertin, D., Lara, L., 2012. La crisis eruptiva del volcán Hudson durante Octubre-Noviembre 2011. XIII Congreso Geológico Chileno, Antofagasta, pp.457–459.

Anda, E., Orheim, O., Mangerud, J., 1985. Late Holocene glacier variations and climate at Jan Mayen. Polar Research 3 (2), 129–140.

Andrés, N., Zamorano, J.J., Sanjosé, J.J., Atkinson, A., Palacios, D., 2007. Glacier retreat during the recent eruptive period of Popocatépetl volcano, Mexico. Annals of Glaciology 45 (1), 73–82.

Baker, P.E., Davies, T.G., Roobol, M.J., 1969. Volcanic activity at Deception Island in 1967 and 1969. Nature 224 (5219), 553–560.

Baker, P.E., McReath, I., Harvey, M.R., Roobol, M.J., Davies , T.G., 1975. The geology of the South Shetland Islands: V. Volcanic evolution of Deception Island. British Antarctic Survey Scientific Reports, 78.

Banks, N.G., Iven, M., 1991. Report of the United Nations Mission to Volcán Hudson, Chile, 20 August-15 September 1991. Unpublished Report, US Geological Survery, Cascades Volcano Observatory.

Barberi, F., Caruso, P., Macedonio, G., Pareschi, M.T., Rosi, M., 1992. Reconstruction and numerical simulation of the lahar of the 1877 eruption of Cotopaxi volcano (Ecuador). Acta Vulcanol 2, 35–44.

Benson, C.S., Follett, A.B., 1986. Application of photogrammetry to the study of volcano-glacier interactions on Mount Wrangell, Alaska. Photogram Eng Rein Sens 52, 813–827.

Benson, C.S., Motyka, R.J., 1978. Glacier-volcano interactions on Mt Wrangell, Alaska. Geophys Inst Univ Alaska Biennial Report 1977-78.

Benson, C.S., Bingham, D.K., Wharton, G.B., 1975. Glaciological and volcanological studies at the summit of Mt. Wrangell, Alaska. Proceedings XV General Assembly, IUGG, Moscow. IASH-AISH Publication No. 104, pp.95–98.

Best, J.L., 1992. Sedimentology and event timing of a catastrophic volcaniclastic mass flow, Volcán Hudson, Southern Chile. Bull Volcanol 54, 299–318.

Birkenmajer, K., 1972. Geotectonic aspects of the Beerenberg Volcano eruption 1970, Jan Mayen island. Acta Geologica Polonica 22 (1), 1–16.

Bleick, H.A., Coombs, M.L., Cervelli, P.F., Bull, K.F., Wessels, R.L., 2013. Volcano–ice interactions precursory to the 2009 eruption of Redoubt Volcano, Alaska. Journal of Volcanology and Geothermal Research 259, 373–388.

Branney, M.J., Gilbert, J.S., 1995. Ice-melt collapse pits and associated features in the 1991 lahar deposits of Volcán Hudson, Chile: criteria to distinguish eruption-induced glacier melt. Bulletin of Volcanology 57 (5), 293–302.

Brantley, S.R., (Ed.) 1990. The eruption of Redoubt volcano, Alaska, December 14, 1989–August 31, 1990. U.S. Geological Survey Circular C 1061.

Brock, B., Rivera, A., Casassa, G., Bown, F., Acuñn, C., 2007. The surface energy balance of an active ice-covered volcano: Villarrica Volcano, southern Chile. Annals of Glaciology 45 (1), 104–114.

Brugman, M.M., Post, A., 1981. Effects of volcanism on the glaciers of Mount St. Helens. Geological Survey Circular 850—D, 1–11.

Bull, K.F., Buurman, H., 2013. An overview of the 2009 eruption of Redoubt Volcano, Alaska. Journal of Volcanology and Geothermal Research 259, pp.2–15.

Cameron, K.A., 1988. Fumarole fields and thermal features at Mount Hood, Oregon. Northwest Science 62, 82.

Capra, L., Poblete, M.A., Alvarado, R., 2004. The 1997 and 2001 lahars of Popocatépetl volcano (Central Mexico): Textural and sedimentological constraints on their origin and hazards. J. Volcan. Geotherm. Res. 131 (3–4), 351–369.

Capra, L., Roverato, M., Groppelli, G., Caballero, L., Sulpizio, R., Norini, G., 2015. Glacier melting during lava dome growth at Nevado de Toluca volcano (Mexico): Evidences of a major threat before main eruptive phases at ice-caped volcanoes. Journal of Volcanology and Geothermal Research 294, 1–10.

Cardona, C., Santacoloma, C., White, R., McCausland, W., Trujillo, N., Narváez, A., Bolaños, R., Manzo, O., 2009. Sismicidad tipo “drumbeat” asociada a la erupción y emplazamiento de un domo en el volcán Nevado del Huila, noviembre de 2008. In: Memorias XII Congreso Colombiano de Geologı´a. Paipa, Colombia, 7-11 September 2009.

Casertano, L., 1961. Descriptions of volcanic eruptions -Chile: Bull Volcanol Erupt 1, 6.

Casertano, L., 1963. Catalogue of the active volcanoes of the world including solfatara fields, Part XV-Chilean volcanoes. IAVCEI, Rome: pp 1-55

Castruccio, A., Clavero, J., Rivera, A., 2010. Comparative study of lahars generated by the 1961 and 1971 eruptions of Calbuco and Villarrica volcanoes, Southern Andes of Chile. Journal of Volcanology and Geothermal Research 190 (3), 297–311.

Ceballos, J.L., Euscátegui, C., Ramírez, J., Cañon, M., Huggel, C., Haeberli, W., Machguth, H., 2006. Fast shrinkage of tropical glaciers in Colombia. Annals of Glaciology 43 (1), 194–201.

Chernomorets, S.S., Tutubalina, O.V., Petrakov, D.A. 2006. Glaciers of Mt. Kazbek as a source of natural hazard: risk assessment. Otsenka i Upravlenie Prirodnymi Riskami; Materialy Vserossiyskoy Konferentsii “Risk-2006”. Moscow: Izdatelstvo RUDN: 226–228. [In Russian].

1603 Chernomorets, S.S., Tutubalina, O.V., Seinova, I.B., Petrakov, D.A., Nosov, K.N., Zaporozhchenko, 2007. Glacier and debris flow disasters around Mt. Kazbek,
1604 Russia/Georgia. In: Chen, C.L., Major, J.J. (eds.) Debris-Flow Hazards Mitigation: Mechanics, Prediction, and Assessment. Millpress, Netherlands pp.691–
1605 702.

1606

1607 Chinn, T.J., Kargel, J.S., Leonard, G.J., Haritashya, U.K., Pleasants, M., 2014. New Zealand's glaciers. In: Kargel, J.S., Leonard, G.J., Bishop, M.P., Kääb, A.,
1608 Raup, B.H. (Eds.) Global land ice measurements from space. Springer Berlin Heidelberg, pp.675–715.

1609

1610 Christiansen, R.L., Peterson, D.W., 1981. Chronology of the 1980 eruptive activity. US Geol. Surv. Prof. Pap 1250, 17–30.

1611

1612 Clarke, G.K.C., Cross, G.M., Benson, C.S., 1989. Radar imaging of glaciovolcanic stratigraphy, Mount Wrangell caldera, Alaska: interpretation model and
1613 results. Journal of Geophysical Research 94 (B6), 7237–7249.

1614

1615 Clavero, J., Moreno, H., 2004. Evolution of Villarrica volcano. In Lara, L.E., Clavero, J., (Eds). Villarrica Volcano (39.5°S), Southern Andes, Chile: Servicio
1616 Nacional de Geología y Minería, pp.17–27.

1617

1618 Conway, C.E., Townsend, D.B., Leonard, G.S., Wilson, C.J.N., Calvert, A.T., Gamble, J.A., 2015. Lava-ice interaction on a large composite volcano: a case
1619 study from Ruapehu, New Zealand. Bulletin of Volcanology 77 (3), 21.

1620

1621 Coombs, M.L., Neal, C.A., Wessels, R.L., McGimsey, R.G., 2005. Geothermal disruption of summit glaciers at Mount Spurr Volcano, 2004–6: an unusual
1622 manifestation of volcanic unrest. US Geol Surv Professional Paper.
1623
1624 Crider, J.G., Frank, D., Malone, S.D., Poland, M.P., Werner, C., Caplan-Auerbach, J., 2011. Magma at depth: a retrospective analysis of the 1975 unrest at
1625 Mount Baker, Washington, USA. Bulletin of Volcanology 73 (2), 175–189.
1626
1627 Cronin, S.J., Neall, V.E., Lecointre, J.A., Palmer, A.S., 1996. Unusual "snow slurry" lahars from Ruapehu volcano, New Zealand, September 1995. Geology 24
1628 (12), 1107–1110.
1629
1630 Curtis, G.H., 1968. The stratigraphy of the ejecta from the 1912 eruption of Mount Katmai and Novarupta, Alaska. Geological Society of America Memoirs 116,
1631 153–210.
1632
1633 Dean, K.G., Engle, K., Groves, J., Dehn, J., Partington, K., 2002. Analysis of surface processes using SAR data: Westdahl Volcano, Alaska. International
1634 Journal of Remote Sensing 23 (21), 4529–4550.
1635
1636 Delgado, F., Pritchard, M., Lohman, R., Naranjo, J.A., 2014. The 2011 Hudson volcano eruption (Southern Andes, Chile): Pre-eruptive inflation and hotspots
1637 observed with InSAR and thermal imagery. Bulletin of Volcanology 76 (5), 815.
1638

1639 Delgado Granados, H., 1997. The glaciers of Popocatépetl volcano (Mexico): changes and causes. Quaternary International 43, 53–60.
1640
1641 Delgado Granados, H., Miranda, P.J., Álvarez, R., Cabral-Cano, E., González, L.C., Mora, F.C., Alonso, M.L., Huggel, C., 2005. Study of Ayoloco Glacier at
1642 Iztaccíhuatl volcano (Mexico): hazards related to volcanic activity — ice cover interactions. Zeitschrift für Geomorphologie, Special Issue on Volcanic
1643 Geomorphology and Hazards 140, 181–193.
1644
1645 Delgado Granados, H.., Miranda, P.J., Huggel, C., Del Valle, S.O., Ibargüengoitia, M.A., 2007. Chronicle of a death foretold: Extinction of the small-size
1646 tropical glaciers of Popocatépetl volcano (Mexico). Global and Planetary Change 56 (1), 13–22.
1647
1648 Delgado Granados, H., Miranda, P.J., Núñez, G.C., Alzate, P., Mothes, P., Roa, H.M., Correa, B.E.C. and Ramos, J.C., 2015.Hazards at Ice-Clad Volcanoes:
1649 Phenomena, Processes, and Examples From Mexico, Colombia, Ecuador, and Chile. In: Haeberli, W., Whiteman, C. (Eds.) Hazards at Ice-clad volcanoes. Snow
1650 and Ice-Related Hazards, Risks, and Disasters. Elsevier, Amsterdam, pp.607–636.
1651
1652 Dixon, H.J., Murphy, M.D., Sparks, S.J., Chavez, R., Naranjo, J.A., Dunkley, P.N., Young, S.R., Gilbert, J.S., Pringle, M.R., 1999. The geology of Nevados de
1653 Chillán volcano, Chile. Revista geológica de Chile 26(2), 227–253.
1654
1655 Dokukin, M.D., Seynova, I.B., Savernyuk, E.A., Chernomorets, S.S., 2017. On advancing of glaciers due to activity of the Klyuchevskaya Sopka volcano
1656 (Kamchatka). Ice and Snow 57 (1), 10–24.

Doukas, M.P., McGimsey, R.G., Dorava, J.M., 1995. 10 Years of Volcanic Activity in Alaska 1983-1992: A Video. US Geological Survey.

Dunn, R., 1909. Conquering our gratest volcano. Harper's Monthly Magazine 118 (706), 497–509.

Dvigalo, V.N., Melekestsev, I.V., 2000. Recent large-scale downfalls on the cone of Klychevskoy volcano: a revision of the consequences of the events of 1944–1945, 1984–1985 and 1999. Volcanol. Seismol. 22, 1–23.

Edwards, B., Magnússon, E., Thordarson, T., Guðmundsson, M.T., Höskuldsson, A., Oddsson, B., Haklar, J., 2012. Interactions between lava and snow/ice during the 2010 Fimmvörðuháls eruption, south-central Iceland. Journal of Geophysical Research: Solid Earth 117(B4).

Eichelberger, J.C., Keith, T.E., Miller, T.P., Nye, C.J., 1995. The 1992 eruptions of Crater Peak vent, Mount Spurr volcano, Alaska: chronology and summary. In: Keith, T.E.C., (Ed.) The 1992 eruptions of Crater Peak vent, Mount Spurr volcano, Alaska, U.S. Geological Survey Bulleting 2139, pp.1–18.

Eichelberger, J., Kiryukhin, A., Simon, A., 2009. The Magma-Hydrothermal System at Mutnovsky Volcano, Kamchatka Peninsula, Russia. Scientific Drilling 7, 54–59.

Fedotov SA. and Ivanov BV (1985) Descriptions of volcanic events—USSR. SEAN Bulletin 10–12, 4.

Fedotov, S.A., Chirkov, A.M., Gusev, N.A., Kovalev, G.N., Slezin, Y.B., 1980. The large fissure eruption in the region of Plosky Tolbachik volcano in Kamchatka, 1975–1976. Bulletin of Volcanology 43 (1), 47–60.

Fenner, C.N., 1930. Mount Katmai and Mount Mageik. Zeitschrift für Vulkanologie 13, 1–24.

Fierstein, J., Hildreth, W., 1992, The plinian eruptions of 1912 at Novarupta, Katmai National Park, Alaska. Bulletin of Volcanology 54, 646–684.

Frank, D., Meier, M.F., Swanson, D.A., 1977. Assessment of increased thermal activity at Mount Baker, Washington, March 1975—March 1976. U.S. Geological Survey Professional Paper 1022.

Frank, D., Post, A. and Friedman, J.D., 1975. Recurrent geothermally induced debris avalanches on Boulder Glacier, Mount Baker, Washington. U.S. Geological Survey J Res, 3, 77–87.

Fuenzalida, R., 1976. The Hudson Volcano. In: González, O. (Ed.), Proceedings of the Symposium on Andean and Antarctic Volcanology Problems. Napoli, Italy, 78–87.

Gardner, C.A., Neal, C.A., Waitt, R.B., Janda, R.J., 1994. Proximal pyroclastic deposits from the 1989–1990 eruption of Redoubt Volcano, Alaska—stratigraphy, distribution, and physical characteristics. Journal of Volcanology and Geothermal Research 62 (1–4), 213–250.

Gerbe, M.C., Thouret, J.C., 2004. Role of magma mixing in the petrogenesis of tephra erupted during the 1990–98 explosive activity of Nevado Sabancaya, southern Peru. Bulletin of Volcanology 66 (6), 541–561.

Giffen, B.A., Hall, D.K., Chien, J.Y., 2014. Alaska: Glaciers of Kenai Fjords National Park and Katmai National Park and Preserve. In: Kargel, J.S., Leonard, G.J., Bishop, M.P., Kääb, A., Raup, B.H. (Eds.) Global land ice measurements from space. Springer Berlin Heidelberg, pp. 241–261.

González-Ferrán, O., 1973. Description of volcanic eruptions - Chile. Bull Volcanol Erupt 11, 41.

González-Ferrán, O., 1984. Descriptions of volcanic events - Chile. SEAN Bull 9-11, 2.

González-Ferrán, O., 1985. Descriptions of volcanic events - Chile. SEAN Bull 10-1, 3.

Gonzalez-Ferran O, 1995. Volcanes de Chile. Santiago: Instituto Geografico Militar.

Gorshkov, G.S., Dubik, Y.M., 1970. Gigantic directed blast at Shiveluch volcano (Kamchatka). Bulletin of Volcanology 34 (1), 261–288.

Griggs, R.F., 1922. The Valley of Ten Thousand Smokes: Washington, D.C., National Geographic Society, Washington.

Gudmundsson, M.T., Sigmundsson, F., Bjornsson, H., 1997. Ice-volcano interaction of the 1996 Gjalp subglacial eruption, Vatnajokull, Iceland. Nature 389 (6654), 954–957.

Gudmundsson, M.T., Pálsson, F., Björnsson, H., Högnadóttir, H., 2002. The hyaloclastite ridge formed in the subglacial 1996 eruption in Gjálp, Vatnajökull, Iceland: present day shape and future preservation. Geological Society, London, Special Publications 202(1), 319–335.

Gudmundsson, M.T., Sigmundsson, F., Björnsson, H., Högnadóttir, T., 2004. The 1996 eruption at Gjálp, Vatnajökull ice cap, Iceland: efficiency of heat transfer, ice deformation and subglacial water pressure. Bulletin of Volcanology 66 (1), 46–65.

Gudmundsson, M.T., Thordarson, T., Höskuldsson, Á., Larsen, G., Björnsson, H., Prata, F.J., Oddsson, B., Magnússon, E., Högnadóttir, T., Petersen, G.N., Hayward, C.L., Stevenson, J.A. Jónsdóttir, I., 2012. Ash generation and distribution from the April-May 2010 eruption of Eyjafjallajökull, Iceland. Scientific reports 2 (572), 1–12.

Gudmundsson, A., Lecoeur, N., Mohajeri, N., Thordarson, T., 2014. Dike emplacement at Bardarbunga, Iceland, induces unusual stress changes, caldera deformation, and earthquakes. Bulletin of Volcanology 76 (10), 869.

Guzmán, J.C. 1981. Informe preliminar sobre erupción del volcán Hudson norte o Volcán Huemules. Trapananda 1, 35–42.

Harris, S. L., 1988. Fire mountains of the West: The Cascade and Mono Lake volcanoes. Mountain Press, Missoula.

Hickey-Vargas, R., Abdollahi, M.J., Parada, M.A., López-Escobar, L., Frey, F.A., 1995. Crustal xenoliths from Calbuco Volcano, Andean Southern Volcanic Zone: implications for crustal composition and magma-crust interaction. Contributions to Mineralogy and Petrology 119 (4), 331–344.

Hildreth, W., 1983. The compositionally zoned eruption of 1912 in the valley of ten thousand smokes, Katmai National Park, Alaska. Journal of Volcanology and Geothermal Research 18(1–4), 1–56.

Hildreth, W., Fierstein, J., 2000. Katmai volcanic cluster and the great eruption of 1912. Geological Society of America Bulletin 112 (10), 1594–1620.

Hildreth, W., Fierstein, J., 2003, Geologic map of the Katmai Volcanic Cluster, Katmai National Park, Alaska: U.S. Geological Survey Map I-2778, scale 1:63,360.

Hildreth, W., Fierstein, J., 2012. The Novarupta-Katmai Eruption of 1912—Largest Eruption of the Twentieth Century: Centennial Perspectives. U.S. Geological Survey Professional Paper, 1791.

Hildreth, W., Fierstein, J., Lanphere, M.A., Siems, D.F., 2000. Mount Mageik: A compound stratovolcano in Katmai National Park. In: Kelly, K.D., Gough, L.P., (Eds.) Geologic Studies in Alaska by the U.S. Geological Survey, 1998. US Geol Surv Prof Paper 1615, 23–41.

Hildreth, W., Fierstein, J., Lanphere, M., 2003a. Eruptive history and geochronology of the Mount Baker volcanic field, Washington. Geological Society of America Bulletin 115 (6), 7293–764.

Hildreth, W., Fierstein, J., Lanphere, M.A., Siems, D.F., 2002 Mount Griggs: A compositionally distinctive Quaternary stratovolcano behind the main volcanic line in Katmai National Park. In: Wilson, F.H., Galloway, J.P., (Eds.) Studies by the U.S. Geological Survey in Alaska, 2000. US Geol Surv Prof Paper 1662, 87–112.

Hildreth, W., Fierstein, J., Lanphere, M.A., Siems, D.F., 2003b. Trident Volcano: Four contiguous stratocones adjacent to Katmai pass, Alaska Peninsula. In: Galloway, J.P., (Ed.) Studies by the U.S. Geological Survey in Alaska, 2001. US Geol Surv Prof Paper 1678, 153–180.

Hobbs, L., Gilbert, J., Lane, S., 2011. The role of cold volcanic debris in glacier ablation. AGU Fall Meeting EP51B-0846.

Holdgate, M.W., Baker, P.E., 1979. The South Sandwich Islands: I. General description, 91. British Antarctic Survey.

1765 Huggel, C., Delgado, H., 2000. Glacier monitoring at Popocatépetl Volcano, México: glacier shrinkage and possible causes. Beiträge zur Geomorphologie,
1766 Proc. der Frachtagun der Schweizerieschen Geomorphologischen vom, Branois, Switzerland 97–106.
1767
1768 Huggel, C., Ceballos, J.L., Pulgarín, B., Ramírez, J., Thouret, J.C., 2007. Review and reassessment of hazards owing to volcano–glacier interactions in
1769 Colombia. Annals of Glaciology 45 (1), 128–136.
1770
1771 Iribarren Anacona, P., Bodin X., 2010. Geomorphic consequences of two large glacier and rock glacier destabilizations in the Central and Northern Chilean
1772 Andes. Geophysical Research Abstracts 12, 7162–7165.
1773
1774 Iribarren Anacona, P., Mackintosh, A., Norton, K.P., 2015. Hazardous processes and events from glacier and permafrost areas: lessons from the Chilean and
1775 Argentinean Andes. Earth Surface Processes and Landforms 40 (1), 2–21.
1776
1777 Ivanov, B.V., 1984. Descriptions of volcanic events - USSR. SEAN Bull 9-8, 2
1778
1779 Jónsson, J., 1982. Notes on Katla volcanoglacial debris flows. Jökull 32, 61–68.
1780
1781 Jude-Eton, T.C., Thordarson, T., Gudmundsson, M.T., Oddsson, B., 2012. Dynamics, stratigraphy and proximal dispersal of supraglacial tephra during the ice-
1782 confined 2004 eruption at Grímsvötn Volcano, Iceland. Bulletin of volcanology 74 (5), 1057–1082.

1783

1784 Juhle, W., Coulter, H., 1955. The Mt. Spurr eruption, July 9, 1953. Eos, Transactions American Geophysical Union 36 (2), 199–202.

1785

1786 Julio-Miranda, P., González Huesca, A.E., Delgado-Granados, H., Kääb, A., 2005. Glacier melting and lahar formation during January 22, 2001 eruption,
1787 Popocatépetl Volcano (Mexico). Z. fur Geomorphol. 140, 93–102.

1788

1789 Julio-Miranda, P., Delgado-Granados, H., Huggel, C., Kääb, A., 2008. Impact of the eruptive activity on glacier evolution at Popocatépetl Volcano (México)
1790 during 1994–2004. Journal of Volcanology and Geothermal Research 170(1), 86–98.

1791

1792 Kilgour, G., Manville, V., Della Pasqua, F., Graettinger, A., Hodgson, K.A., Jolly, G.E., 2010. The 25 September 2007 eruption of Mount Ruapehu, New
1793 Zealand: directed ballistics, surtseyan jets, and ice-slurry lahars. Journal of Volcanology and Geothermal Research 191 (1), 1–14.

1794

1795 Kilian, R., 1990. The Austral Andean Volcanic Zone (South Patagonia). In Intemational Symposium on Andean Geology (ISAG) 1, 301–305.

1796

1797 Kirkbride, M.P., Dugmore, A.J., 2003. Glaciological response to distal tephra fallout from the 1947 eruption of Hekla, south Iceland. Journal of Glaciology 49
1798 (166), 420–428.

1799

Kiryukhin, A.V., Leonov, V.L., Slovtsov, I.B., Delemen, I.F., Puzankov, M.Yu., Polyakov, A.Yu., Ivanysko, G.O., Bataeva, O.P., Zelenskii, M.E., 2005. Modeling the utilization of area Dachnyi of the Mutnovskii geothermal field in connection with the supply of heat-transfer agent to the 50 MW Mutnovskii Geologic Power Station. Vulkanologiya i Seismologiya 5, 19–44. [In Russian].

Kiryukhin, A., Ramsey, M., Droznin, V., Carter, A., Rose, S., Dvigalo, V., Dubrovskaya, I., Heat discharge of Mutnovsky Volcano. Proceedings of the Thirty-Third Workshop on Geothermal Reservoir Engineering Stanford University, Stanford, California, January 28–30, SGP-TR-185.

Kjartansson, G., 1951. Water flood and mudflows. In: Einarsson, T., Kjartansson, G., Thorarinsson, S., (Eds.) The eruption of Hekla 1947–48. Visindafelag Islendinga (Soc Sci Islandica) Reykjavik II 4, 1–51.

Klohn, E., 1963. The February 1961 eruption of Calbuco volcano. Bulletin of the Seismological Society of America 53 (6), 1435–1436.

Krafft, M., Miller, T., Kienle, J. 1980. Descriptions of volcanic eruptions–Aleutian Islands. Bull Volcanol Erupt 18, 65.

La Frenierre, J., Mark, B.G., 2017. Detecting patterns of climate change at Volcán Chimborazo, Ecuador, by integrating instrumental data, public observations, and glacier change analysis. Annals of the American Association of Geographers 107 (4), 1–19.

1817 Le Pennec, J.L., Ruiz, G.A., Ramón, P., Palacios, E., Mothes, P., Yepes, H., 2012. Impact of tephra falls on Andean communities: The influences of eruption
1818 size and weather conditions during the 1999–2001 activity of Tungurahua volcano, Ecuador. Journal of Volcanology and Geothermal Research 217, 91–103.
1819
1820 Liaudat, D.T., Penas, P., Aloy, G., 2014. Impact of volcanic processes on the cryospheric system of the Peteroa Volcano, Andes of southern Mendoza,
1821 Argentina. Geomorphology 208, 74–87.
1822
1823 Lillquist, K., Walker, K., 2006. Historical glacier and climate fluctuations at Mount Hood, Oregon. Arctic, Antarctic, and Alpine Research 38 (3), 399–412.
1824
1825 Lliboutry, L., 1956. Nieves y glaciares de Chile. Fundamentos de glaciologia, Santiago.
1826
1827 Lopez, P., Chevallier, P., Favier, V., Pouyaud, B., Ordenes, F., Oerlemans, J., 2010. A regional view of fluctuations in glacier length in southern South
1828 America. Global and Planetary Change 71(1), 85–108.
1829
1830 Lu, Z., Wicks, C., Dzurisin, D., Thatcher, W., Freymueller, J.T., McNutt, S.R., Mann, D., 2000. Aseismic inflation of Westdahl volcano, Alaska, revealed by
1831 satellite radar interferometry. Geophysical Research Letters 27 (11), 1567–1570.
1832
1833 Lu, Z., Masterlark, T., Dzurisin, D., Rykhus, R., Wicks, C., 2003. Magma supply dynamics at Westdahl volcano, Alaska, modeled from satellite radar
1834 interferometry. Journal of Geophysical Research: Solid Earth 108(B7).

Lundstrom, S.C., McCafferty, A.E., Coe, J.A., 1993. Photogrammetric analysis of 1984-89 surface altitude change of the partially debris-covered Eliot Glacier, Mount Hood, Oregon, USA. Annals of Glaciology 17 (1), 167–170.

Magnússon, E., Gudmundsson, M.T., Roberts, M.J., Sigurðsson, G., Höskuldsson, F., Oddsson, B., 2012. Ice-volcano interactions during the 2010 Eyjafjallajökull eruption, as revealed by airborne imaging radar. Journal of Geophysical Research: Solid Earth 117(B7).

Major, J.J., Newhall, C.G., 1989. Snow and ice perturbation during historical volcanic eruptions and the formation of lahars and floods. Bulletin of volcanology 52 (1), 1–27.

Malone, S.D., Frank, D., 1975. Increased heat emission from Mount Baker, Washington. Eos, Transactions American Geophysical Union 56 (10), 679–685.

Manevich, T.M., Muraviev, YA.D., Samoilenko, S.B., 2015. Glaciers of the Avachinskaya volcano group: current condition (state). Ice and Snow 55 (3), 14–26.

Manville, V., Hodgson, K.A., Houghton, B.F., White, J.D.L., 2000. Tephra, snow and water: complex sedimentary responses at an active snow-capped stratovolcano, Ruapehu, New Zealand. Bulletin of Volcanology 62 (4–5), 278–293.

1853 Masiokas, M.H., Rivera, A., Espizua, L.E., Villalba, R., Delgado, S., Aravena, J.C., 2009. Glacier fluctuations in extratropical South America during the past
1854 1000years. Palaeogeography, Palaeoclimatology, Palaeoecology 281 (3), 242–268.
1855
1856 McGimsey, G., 2001. Redoubt Volcano and the Alaska Volcano Observatory, 10 years later. In: Gough, L.P., Wilson, F.H., (Eds) Geologic studies in Alaska
1857 by the US Geological Survey, 1999. U.S. Geological Survey Professional Paper 1633.
1858
1859 McGimsey, R.G., Neal, C.A., Girina, O.A., 2004. 1999 Volcanic activity in Alaska and Kamchatka: Summary of events and response of the Alaska Volcano
1860 Observatory. U.S. Geological Survey Open-File Report 2004-1033.
1861
1862 McGimsey, R.G., Neal, C.A., Girina, O.A., Chibisova, M.V., Rybin, A.V., 2014. 2009 Volcanic activity in Alaska, Kamchatka, and the Kurile Islands—
1863 Summary of events and response of the Alaska Volcano Observatory. U.S. Geological Survey Scientific Investigations Report 2013–5213.
1864
1865 McNutt, S.R., Miller, T.P., Taber, J.J., 1991. Geological and seismological evidence of increased explosivity during the 1986 eruptions of Pavlof volcano,
1866 Alaska. Bulletin of volcanology 53 (2), 86–98.
1867
1868 Mendenhall, W.C., 1905. Geology of the central Copper River region, Alaska. U.S. Geological Survey Professional Paper 41.
1869

Mercier, D., Lowell, R.P., 2016. A quantitative analysis of volcanic unrest: Mt. Spurr Alaska, 2002–2006. Journal of Volcanology and Geothermal Research 323, 97–109.

Meyer, D.F., Trabant, D.C., 1995, Lahars from the 1992 eruptions of Crater Peak, Mount Spurr Volcano, Alaska. In: Keith, T.E.C., (Ed) The 1992 eruptions of Crater Peak vent, Mount Spurr Volcano, Alaska: U.S. Geological Survey Bulletin 2139, pp.183–198.

Miller, T., Yount, E., 1983. Descriptions of volcanic events - Alaska. SEAN Bull 8-6, 6.

Möller, R., Möller, M., Björnsson, H., Guðmundsson, S., Pálsson, F., Oddsson, B., Kukla, P.A. and Schneider, C., 2014. MODIS-derived albedo changes of Vatnajökull (Iceland) due to tephra deposition from the 2004 Grímsvötn eruption. International Journal of Applied Earth Observation and Geoinformation 26, 256–269.

Moreno, H., 1993. Volcán Villarrica: Geología y evaluación del riesgo, regiones IX-X, 39º25'S. Informe Final Proyecto Fondecyt 1247, 112.

Moreno, H., Fuentealba, G., 1994. The May 17-19 1994 Llaima volcano eruption, southern Andes 38° 42'8-71° 44'W. Andean Geology 21 (1), 167–171.

Morueta-Holme, N., Engemann, K., Sandoval-Acuña, P., Jonas, J.D., Segnitz, R.M., Svenning, J.C., 2015. Strong upslope shifts in Chimborazo's vegetation over two centuries since Humboldt. Proceedings of the National Academy of Sciences 112 (41), 12741–12745.

Motoki, A., Orihashi, Y., Naranjo, J.A., Hirata, D., Hosono, T., Cario, F.D., Anma, R., 2003. Geologic occurrence and recent eruptive materials of the Lautaro Volcano, Chilean Patagonia. The Journal of the Geological Society of Japan 109 (5), IX-X.

Motoki, A., Orihashi, Y., Naranjo, J.A., Hirata, D., Skvarca, P., Anma, R., 2006. Geologic reconnaissance of Lautaro Volcano, Chilean Patagonia. Revista geológica de Chile 33 (1), 177–187.

Motyka, R.J., 1977, Katmai Caldera: Glacier growth, lake rise and geothermal activity, in Alaska. In: Division of Geological & Geophysical Surveys, Short Notes on Alaskan Geology – 1977. Alaska Division of Geological & Geophysical Surveys Geologic Report 55E, pp.17–21.

Motyka, R.J., Moorman, M.A. and Poreda, R., 1983. Progress Report, Thermal Fluid Investigations of the Makushin Geothermal Area. State of Alaska, Department of Natural Resources, Division of Geological & Geophysical Surveys, pp.1–57.

Muller, E.H., Coulter, H.W., 1957a. Incipient glacier development within Katmai caldera, Alaska. Journal of Glaciology 3 (21), 13–17.

Muller, E.H., Coulter, H.W., 1957b. The Knife Creek glaciers of Katmai National Monument, Alaska. Journal of Glaciology 3 (22), 116–122.

Muraviev, A.Ya., Muraviev, Ya.D., 2016. Fluctuations of glaciers of the Klyuchevskaya group of volcanoes in the 20th –21st centuries. Ice and Snow 56 (4), 480–492.

Muravyev, Ya.D., 2004. Subglacial geothermal eruption – the possible reason of the catastrophic surge of Kolka Glacier in the Kazbek volcanic massif. Vestnik KRAUNTs Earth Sciences 4, 6–20. [In Russian.

Muraviev, Ya.D., Muraviev, A.Ya., Osipova, G.B., 2010. Glacial surges in the areas of active volcanism. Tezisy XV glyatsilogicheskogo simpoziuma. Abstracts of the XV Glaciological Symposium. Kazan 23. [In Russian].

Muraviev Ya.D., Muraviev A.Ya., Osipova G.B., 2011. Features of dynamics of ice files on active volcanoes, Kamchatka. Abstract, 92–93.

Muraviev, Ya.D., Salamatin, A.N., 1993. Predictive estimate of ice mass dynamics in volcano-tectonic valleys of the Klyuchevskoy volcano. Vulkanologiya i seysmologiya. Volcanology and Seismology 4, 43–53. [In Russian].

Muraviev, Ya.D., Tsvetkov, D.G., Muraviev, A.Ya., Osipova, G.B., 2012. Dynamics of the Bilchenok surging glacier in the Klyuchevskaya volcano group. Led i Sneg. Ice and Snow 2 (118), 31–39. [In Russian].

1922 Naranjo, J.A., Moreno, H., 1991. Actividad explosiva postglacial en el Volcán Llaima, Andes del Sur (38 45'S). Andean Geology 18(1), 69–80.
1923
1924 Naranjo, J. A. and Moreno, H., 2004. Laharic debris-flows from Villarrica volcano. In: Lara, L.E., Clavero, J. (Eds.) Boletín Servicio Nacional de Geología y
1925 Minería, 61, Santiago, Chile, 28–38.
1926
1927 Naranjo, J.A., Stern, C., 1998. Holocene explosive activity of Hudson volcano, southern Andes. Bull Volcanology 59 (4), 291–306.
1928
1929 Naranjo, J.L., Sigurdsson, H., Carey, S.N., Fritz, W.J. 1986. Eruption of the Nevado del Ruiz Volcano, Colombia, on 13 November 1985: tephra fall and lahars.
1930 Science 233, 961–963
1931
1932 Naranjo, J.A., Moreno, H., Banks, N., 1993. La erupción del Volcán Hudson en 1991 (46° S), Región XI, Aisén. Chile. Serv Nac Geol Min Bol. 44, 1–50.
1933
1934 Neal, C.A., Coombs, M., Wessels, R., McGimsey, R.G., 2007. Volcanic Disruption of Summit Ice at Mount Spurr Volcano, Alaska, 2004–2007, GSA
1935 Cordilleran Section - 103rd Annual Meeting (4–6 May 2007). GSA, Bellingham, WA.
1936
1937 Neal, C.A., Doukas, M.P., McGimsey, R.G., 1995. Volcanic activity in Alaska: summary of events and response of the Alaska Volcano Observatory 1994. U.S.
1938 Geological Survey Open-File Report 95-271.
1939

1940 Neal, C.A., McGimsey, R.G., Diggles, M.F., 2002. Volcanoes of the Alaska Peninsula and Aleutian Islands: Selected Photographs. U.S. Geological Survey
1941 Digital Data Series DDS-40 Version 1.1.
1942
1943 Neal, C.A., McGimsey, R.G., Dixon, J.P., 2009. 2006 Volcanic Activity in Alaska, Kamchatka, and the Kurile Islands: Summary of Events and Response of
1944 the Alaska Volcano Observatory, U.S. Geological Survey Scientific Investigations Report 2008–5214.
1945
1946 Nield, J.M., Chiverrell, R.C., Darby, S.E., Leyland, J., Vircavs, L.H., Jacobs, B., 2013. Complex spatial feedbacks of tephra redistribution, ice melt and surface
1947 roughness modulate ablation on tephra covered glaciers. Earth Surface Processes and Landforms 38 (1), 95–102.
1948
1949 Nielsen, N., 1937. A Volcano Under an Ice-Cap. Vatnajökull, Iceland, 1934-36. Geographical Journal 90 (1), 6–20.
1950
1951 Orheim, O., Govorukha, L.S., 1982. Present-day glaciation in the South Shetland Islands. Annals of Glaciology 3, 233–238.
1952
1953 Palacios, D., Marcos, J., 1998. Glacial retreat and its geomorphologic effects on Mexico's active volcanoes, 1994– 95. J. Glaciol. 44 (146), 63–67.
1954
1955 Palacios, D., Zamorano, J.J., Parrilla, G., 1998. Proglacial debris flows in Popocate´petl North Face and their relation to 1995 eruption. Z. Geomorph. N. P. 42
1956 (3), 273–295.
1957

Palacios, D., Zamorano, J.J., Gómez, A., 2001. The impact of present lahars on the geomorphologic evolution of proglacial gorges: Popocatépetl, Mexico. Geomorphology 37 (1–2), 15–42.

Patrick, M.R., Smellie, J.L., 2013. Synthesis A spaceborne inventory of volcanic activity in Antarctica and southern oceans, 2000–10. Antarctic Science 25 (4), 475–500.

Patrick, M.R., Smellie, J.L., Harris, A.J., Wright, R., Dean, K., Izbekov, P., Garbeil, H., Pilger, E., 2005. First recorded eruption of Mount Belinda volcano (Montagu Island), South Sandwich Islands. Bulletin of Volcanology 67 (5), 415–422.

Pierson, T.C., Janda, R.J., Thouret, J.C., Borrero, C.A., 1990. Perturbation and melting of snow and ice by the 13 November 1985 eruption of Nevado del Ruiz, Colombia, and consequent mobilization, flow and deposition of lahars. Journal of Volcanology and Geothermal Research 41(1–4), 17–66.

Pistolesi, M., Cioni, R., Rosi, M., Cashman, K.V., Rossotti, A., Aguilera, E., 2013. Evidence for lahar-triggering mechanisms in complex stratigraphic sequences: the post-twelfth century eruptive activity of Cotopaxi Volcano, Ecuador. Bulletin of volcanology 75(3), 698.

Pistolesi, M., Cioni, R., Rosi, M., Aguilera, E., 2014. Lahar hazard assessment in the southern drainage system of Cotopaxi volcano, Ecuador: Results from multiscale lahar simulations. Geomorphology 207, 51–63.

Post, A., Mayo, L., 1971. Glacier dammed lakes and outburst floods in Alaska. V.S. Geological Survey. Hydrologic Atlas HA- 455.

Price, S.F., Walder, J.S., 2007, Modeling the dynamic response of a crater glacier to lava-dome emplacement: Mount St. Helens, Washington, U.S.A. Annals of Glaciology 45 (1), 21–28.

Pulgarín, B., Cardona, C., Santacoloma, C., Agudelo, A., Calvache, M., Monsalve, M.L., 2008. Erupciones del volca´n Nevado del Huila y cambios en su masa glaciar: 2007. Boletín Geológico INGEOMINAS 42, 113–132.

Pulgarín, B., Cardona, C., Agudelo, A., Santacoloma, C., Monsalve, M.L., Calvache, M., Murcia, H., Ibáñez, D., García, J., Murcia, C., Cuellar, M., Ordoñez, M., Medina, E., Balanta, R., Calderón, Y., Leiva, O., 2009. Erupciones Históricas Recientes del Volcán Nevado del Huila, cambios morfolágicos y lahares asociados. In: Memorias XII Congreso Colombiano de Geología, 7–11 September 2009 (Paipa, Colombia).

Pulgarín, B., Cardona, C., Santacoloma, C., Agudelo, A., Calvache, M., Monsalve, M.L., 2010. Erupciones del volcán Nevado del Huila (Colombia) en febrero y abril de 2007 y cambios en su masa glaciar. In: López, C.D., Ramírez, J. (Eds.), Glaciares, nieves y hielos de América Latina, cambio climático y amenazas glaciares, Coleccio´n Glaciares, Nevados y Medio
Ambiente. INGEOMINAS, 279–305.

1993 Pulgarín, B., Agudelo, A., Calvache, M., Cardona, C., Santacoloma, C., Monsalve, M.L., 2011. Nevado del Huila (Colombia): 2007-2008 eruptions, lahars and
1994 crisis management. In: Britkreuz, C., Gursky, H.J. (Eds.), Geo-risk management - a German Latin American approach, C538. Freiberger Forschungshefte,
1995 Geowissenchaften, 69–80.
1996
1997 Rabatel, A., Francou, B., Soruco, A., Gomez, J., Cáceres, B., Ceballos, J.L., Basantes, R., Vuille, M., Sicart, J.E., Huggel, C. and Scheel, M., 2013. Current
1998 state of glaciers in the tropical Andes: a multi-century perspective on glacier evolution and climate change. The Cryosphere 7 (1), 81–102.
1999
2000 Richardson, J.M., Brook, M.S., 2010. Ablation of debris-covered ice: some effects of the 25 September 2007 Mt Ruapehu eruption. Journal of the Royal Society
2001 of New Zealand 40 (2), 45–55.
2002
2003 Riffo, P., Fuentealba, G., Urra, L.H., 1987. Sintesis historica de las erupciones del volcan Villarrica (Chile). Boletin de Vulcanologia 18. Universidad Nacional,
2004 Observatorio Vulcano-logica y Sismologica de Costa Rica, 8–11.
2005
2006 Rivera, A., Bown, F., 2013. Recent glacier variations on active ice capped volcanoes in the Southern Volcanic Zone (37°–46°S), Chilean Andes. Journal of
2007 South American Earth Sciences 45, 345–356.
2008
2009 Rivera, A., Bown, F., Casassa, G., Acuña, C., Clavero, J., 2005. Glacier shrinkage and negative mass balance in the Chilean Lake District (40°S). Hydrological
2010 Sciences Journal 50 (6), 963–974.

Rivera, A., Bown, F., Mella, R., Wendt, J., Casassa, G., Acuña, C., Rignot, E., Clavero, J., Brock, B., 2006. Ice volumetric changes on active volcanoes in southern Chile. Annals of Glaciology 43 (1), 111–122.

Rivera, A., Corripio, J.G., Brock, B., Clavero, J., Wendt, J., 2008. Monitoring ice-capped active Volćan Villarrica, southern Chile, using terrestrial photography combined with automatic weather stations and global positioning systems. Journal of Glaciology 54 (188), 920–930.

Rivera, A., Bown, F., Carrión, D., Zenteno, P., 2012. Glacier responses to recent volcanic activity in Southern Chile. Environmental Research Letters 7 (1), 014036.

Rowland, S.K., Smith, G.A., Mouginis-Mark, P.J., 1994. Preliminary ERS-1 observations of Alaskan and Aleutian volcanoes. Remote Sensing of Environment 48 (3), 358–369.

Russell, A.J., Duller, R., Mountney, N.P., 2010. Volcanogenic Jökulhlaups (Glacier Outburst Floods) from Mýrdalsjökull: Impacts on Proglacial Environments. Developments in Quaternary Sciences 13, 181–207.

Ruth, D.C., Cottrell, E., Cortés, J.A., Kelley, K.A., Calder, E.S., 2016. From Passive Degassing to Violent Strombolian Eruption: the Case of the 2008 Eruption of Llaima Volcano, Chile. Journal of Petrology 57 (9), 1833–1864.

Schaefer, J.R. (Ed.), 2012. The 2009 eruption of Redoubt Volcano, Alaska, Alaska Division of Geological and Geophysical Surveys Report of Investigation 2011–5.

Schaefer, J.R., Scott, W.E., Evans, W.C., Jorgenson, J., McGimsey, R.G., Wang, B., 2008. The 2005 catastrophic acid crater lake drainage, lahar, and acidic aerosol formation at Mount Chiginagak volcano, Alaska, USA: field observations and preliminary water and vegetation chemistry results. Geochemistry, Geophysics, Geosystems 9 (7), 1–29.

Schilling, S.P., Carrara, P.E., Thompson, R.A. and Iwatsubo, E.Y., 2004. Posteruption glacier development within the crater of Mount St. Helens, Washington, USA. Quaternary Research, 61(3), pp.325-329.

Schneider, D., Granados, H.D., Huggel, C., Kääb, A., 2008. Assessing lahars from ice-capped volcanoes using ASTER satellite data, the SRTM DTM and two different flow models: case study on Iztaccíhuatl (Central Mexico). Natural Hazards and Earth System Science 8 (3), 559–571.

Schotterer, U., Grosjean, M., Stichler, W., Ginot, P., Kull, C., Bonnaveira, H., Francou, B., Gäggeler, H.W., Gallaire, R., Hoffmann, G., Pouyaud, B., 2003. Glaciers and climate in the Andes between the Equator and 30° S: What is recorded under extreme environmental conditions?. Climatic Change 59 (1), 157–175.

Scott, W.E., McGimsey, R.G., 1994. Character, mass, distribution, and origin of tephra-fall deposits of the 1989–1990 eruption of Redoubt volcano, south-central Alaska. J. Volcanol. Geotherm. Res. 62 (1), 251–272.

Siggerud, T., 1973. Descriptions of volcanic eruptions - Norway. Bull Volcanol Erupt 11, 45.

Sigurðsson, O., Williams, R.S., Martinis, S., Münzer, U., 2014. Remote sensing of mountain glaciers and ice caps in Iceland. In: Kargel, J.S., Leonard, G.J., Bishop, M.P., Kääb, A., Raup, B.H. (Eds.) Global land ice measurements from space. Springer Berlin Heidelberg, 409–425).

Simons, F.S., Mathewson, D.E., 1955. Geology of Great Sitkin Island, Alaska. US Government Printing Office.

Smellie, J.L., 2002. The 1969 subglacial eruption on Deception Island (Antarctica): events and processes during an eruption beneath a thin glacier and implications for volcanic hazards. Geological Society, London, Special Publications 202 (1), 59–79.

Smellie, J.L., 2006. The relative importance of supraglacial versus subglacial meltwater escape in basaltic subglacial tuya eruptions: an important unresolved conundrum. Earth-Science Reviews 74 (3), 241–268.

Smellie, J.L., Edwards, B.R., 2016. Glaciovolcanism on Earth and Mars. Cambridge University Press.

2065 Solomina, O.N., Muraviev, Y.D. Bazanova, L.I., 1995. “Little Ice Age” glaciers in Kamchatka, northeastern Russia. Annals of Glaciology 21 (1), 240–244.
2066
2067 Solomina, O., Wiles, G., Shiraiwa, T., d'Arrigo, R., 2007. Multiproxy records of climate variability for Kamchatka for the past 400 years. Climate of the Past 3
2068 (1), 119–128.
2069
2070 Stefánsdóttir, M.B., Gíslason, S.R., 2005. The erosion and suspended matter/seawater interaction during and after the 1996 outburst flood from the Vatnajökull
2071 Glacier, Iceland. Earth and Planetary Science Letters 237 (3), 433–452.
2072
2073 Stelling, P., Beget, J., Nye, C., Gardner, J., Devine, J., George, R., 2002. Geology and petrology of ejecta from the 1999 eruption of Shishaldin Volcano,
2074 Alaska. Bulletin of Volcanology 64 (8), 548–561.
2075
2076 Sturm, M., 1995. Short-period velocity fluctuations of two glaciers on Mt. Wrangell, Alaska. Physical Geography 16 (1), 42–58.
2077
2078 Sturm, M., Benson, C.S., MacKeith, P., Kienle, J., 1983. Glacier- volcano interactions on Mt. Redoubt, Alaska with related flooding hazards. Univ Alaska
2079 Geophys Inst Rept.
2080
2081 Sturm, M., Benson, C., MacKeith, P., 1986. Effects of the 1966-68 Eruptions of Mount Redoubt on the Flow of Drift Glacier, Alaska, USA. Journal of
2082 Glaciology 32 (112), 355–362.

Sturm, M., Hall, D.K., Benson, C.S., Field, W.O., 1991. Non-climatic control of glacier-terminus fluctuations in the Wrangell and Ghugach Mountains, Alaska, USA. Journal of Glaciology 37 (127), 348–356.

Sylvester, A. H., 1908a: Evidences of recent volcanic activity and the glaciers of Mt. Hood, Oregon. Science 27, 585.

Sylvester, A. H., 1908b: Is our noblest volcano awakening to new life: A description of the glaciers and evidences of volcanic activity of Mount Hood. National Geographic 19, 515–525.

Sylvester, A.G., 1975. History and surveillance of volcanic activity on Jan Mayen Island. Bulletin of Volcanology 39 (2), 313–335.

Tanarro, L.M., Zamorano, J.J., Palacios, D., 2005. Glacier degradation and lahar formation on the Popocatépetl volcano (Mexico) during the last eruptive period (1994–2003). Z. Geomorph. N. P. 140, 73–92.

Tazieff, H., 1963. Descriptions of volcanic eruptions - Chile. Bull Volcanol Erupt 3, 8.

Thouret, J.C., 1990. Effects of the November 13, 1985 eruption on the snow pack and ice cap of Nevado del Ruiz volcano, Colombia. Journal of Volcanology and Geothermal Research 41(1–4), 177–201.

Thouret, J.C., Janda, I.L.l., Pierson, T.C., Calvache, M.L., Cendrero, A., 1987. L'rruption du 13 novembre 1985 au Nevado E1 Ruiz (Cordillrre Centrale, Colombie): interactions entre le dy- namisme 6ruptif, la fusion glaciaire et la grnrse d'rcoule- ments volcano-glaciaires. C R Acad Sci 305, 505–509

Thouret, J.C., Ramirez, J.C., Gibert-Malengreau, B., Vargas, C.A., Naranjo, J.L., Vandemeulebrouck, J., Valla, F., Funk, M., 2007. Volcano–glacier interactions on composite cones and lahar generation: Nevado del Ruiz, Colombia, case study. Annals of Glaciology 45 (1), 115–127.

Tómasson, H., 1996. The jökulhlaup from Katla in 1918. Annals of Glaciology, 22 (1), 249–254.

Trabant, D.C., Hawkins, D.B., 1997. Glacier ice-volume modeling and glacier volumes on Redoubt Volcano, Alaska. U.S. Geological Survey Water-resources investigations report WRI 97-4187.

Trabant, D.C., Meyer, D.F., 1992. Flood generation and destruction of “Drift” Glacier by the 1989–90 eruption of Redoubt Volcano, Alaska. Annals of Glaciology 16, 33–38.

Trabant, D.C., Waitt, R.B., Major, J.J., 1994. Disruption of Drift glacier and origin of floods during the 1989–1990 eruptions of Redoubt Volcano, Alaska. Journal of volcanology and geothermal research 62 (1–4), 369–385.

2119 Tutubalina, O.V., Chernomorets, S.S., Petrakov, D.A. 2005. Kolka Glacier before the 2002 collapse: new data. Kriosfera Zemli 9 (4), 62–71. [In Russian].
2120
2121 Venzke, E., Sennert, S.K., Wunderman, R., 2009. Reports from the Smithsonian's Global Volcanism Network, June 2008. Bulletin of Volcanology 71 (2), 229–
2122 231.
2123
2124 Viccaro, M., Giuffrida, M., Nicotra, E., Ozerov, A.Y., 2012. Magma storage, ascent and recharge history prior to the 1991 eruption at Avachinsky Volcano,
2125 Kamchatka, Russia: Inferences on the plumbing system geometry. Lithos 140, 11–24.
2126
2127 Vinogradov V.N., 1975. Sovremennoe oledenenie rayonov aktivnogo vulkanizma Kamchatki. Modern glaciation of active volcanism areas in Kamchatka.
2128 Moscow: Nauka. [In Russian].
2129
2130 Vinogradov V.N., 1985. Vulkanizm i oledenenie. Volcanism and glaciation. Glyaciologicheskie issledovaniya. Glaciological Studies 27, 7–25. [In Russian].
2131
2132 Vinogradov V.N., Muraviev YA.D., 1982. Izmenchivost' sovremennykh blednikov vulkanicheskikh rayonov Kamchatki. Variability of modern glaciers in
2133 volcanic areas of Kamchatka. Materialy Glyatsiologicheskikh Issledovaniy. Data of Glaciological Studies 42, 164–170. [In Russian].
2134
2135 Vinogradov V.N., Muraviev YA.D., 1985. Vzaimodeystvie lavy i l'da na Klyuchevskom vulkane pri izverzhenii 1983. Lava and ice interaction at the
2136 Klyuchevskoy volcano during the 1983 eruption. Vulkanologiya i seysmologiya. Journ. of Volcanology and Seismology 1, 29–46. [In Russian].

Vogfjörd, K.S., Jakobsdóttir, S.S., Gudmundsson, G.B., Roberts, M.J., Ágústsson, K., Arason, T., Geirsson, H., Karlsdóttir, S., Hjaltadóttir, S., Ólafsdóttir, U., Thorbjarnardóttir, B., 2005. Forecasting and monitoring a subglacial eruption in Iceland. Eos, Transactions American Geophysical Union 86 (26), 245–248.

Waitt, R.B., Pierson, T.C., MacLeod, N.S., Janda, R.J., Voight, B., Holcomb, R.T., 1983. Eruption-triggered avalanche, flood, and lahar at Mount St. Helens—effects of winter snowpack. Science 221 (4618), 1394–1397.

Waitt, R.B., Gardner, C.A., Pierson, T.C., Major, J.J., Neal, C.A., 1994. Unusual ice diamicts emplaced during the December 15, 1989 eruption of Redoubt Volcano, Alaska. Journal of volcanology and geothermal research 62 (1–4), 409–428.

Walder, J.S., LaHusen, R.G., Vallance, J.W., Schilling, S.P., 2005. Crater glaciers on active volcanoes: hydrological anomalies. Eos, Transactions American Geophysical Union 86 (50), 521–528.

Walder, J.S., LaHusen, R.G., Vallance, J.W., Schilling, S.P., 2007. Emplacement of a silicic lava dome through a crater glacier: Mount St Helens, 2004–06. Annals of Glaciology 45 (1), 14–20.

Walder, J.S., Schilling, S.P., Vallance, J.W., LaHusen, R.G., 2008. Effects of lava-dome growth on the Crater Glacier of Mount St. Helens, Washington. In: Sherrod, D.R., Scott, W.E., Stauffer, P.H., (Eds.) A Volcano Rekindled: The Renewed Eruption of Mount St. Helens, 2004–2006. U.S. Geological Survey Professional Paper 1750, pp.257–276.

Walder, J.S, Schilling, S.P., Sherrod, D.R., Vallance, J.W., 2010, Evolution of Crater Glacier, Mount St. Helens, Washington, September 2006—November 2009: U.S. Geological Survey Open-File Report 2010-1141,

Waltham, T., 2001. A guide to the volcanoes of southern Kamchatka, Russia. Proceedings of the Geologists' Association 112 (1), 67–78.

Warren, C.R., Rivera, A., 1994. Non-linear climatic response of Calving Glaciers: A case study of Pio XI Glacier, Chilean Patagonia. Revista Chilena de Historia Natural 67, 385–394.

Waythomas, C.F., 2015. Geomorphic consequences of volcanic eruptions in Alaska: A review. Geomorphology 246, 123–145.

Waythomas, C.F., Miller, T.P., Nye, C.J., 2003. Preliminary volcano-hazard assessment for Great Sitkin Volcano, Alaska. U.S. Geological Survey Open-File Report 03–112.

2170 Waythomas, C.F., Haney, M.M., Fee, D., Schneider, D.J., Wech, A., 2014. The 2013 eruption of Pavlof Volcano, Alaska: a spatter eruption at an ice-and snow-
2171 clad volcano. Bulletin of Volcanology 76 (10), 862.
2172
2173 Waythomas, C.F., Pierson, T.C., Major, J.J., Scott, W.E., 2013. Voluminous ice-rich and water-rich lahars generated during the 2009 eruption of Redoubt
2174 Volcano, Alaska. Journal of Volcanology and Geothermal Research 259, 389–413.
2175
2176 Weaver, C.S., Malone, S.D., 1979. Seismic evidence for discrete glacier motion at the rock-ice interface. Journal of Glaciology 23 (89), 171–184.
2177
2178 Welch, B.C., Dwyer, K., Helgen, M., Waythomas, C.F., Jacobel, R.W., 2007. Geophysical survey of the intra-caldera icefield of Mt Veniaminof, Alaska. Annals
2179 of Glaciology 45 (1), 58–65.
2180
2181 Wolf, T., 1878. Geognostische Mitteilungen aus Ecuador; Der Cotopaxi und seine letzte Eruption am 26 Juni 1877. Neues Jahrb Mineral Geol Paleontol 113-
2182 167.
2183
2184 Worni, R.P., 2012. Characteristics of glacial lake hazards and extreme flow events: advanced approaches to model processes and process chains, Unpublished
2185 PhD Thesis, University of Geneva.
2186

2187 Worni, R., Huggel, C., Stoffel, M., Pulgarín, B., 2012. Challenges of modeling current very large lahars at Nevado del Huila Volcano, Colombia. Bulletin of
2188 volcanology 74 (2), 309–324.
2189
2190 Yount, E.M., Miller, T.P., Emanuel, R.P., Wilson, F.H., 1985. Eruption in and ice-filled caldera, Mount Veniaminof, Alaska Peninsula. In: Bartsch-Winkler,
2191 S., Reed, K.M., (Eds.). The United States Geological Survey in Alaska: Accomplishments During 1983. U.S. Geological Survey Circular 945, 59–60.
2192
2193 Zaporozhchenko, E.V., Chernomorets, S.S. 2004. History and studies of Kazbek blockages. Vestnik
2194 Kavkazskogo gornogo obshestva 5, 33–54. [In Russian].
2195
2196 Zharinov, N.A., Gorelchik, V.I., Zhdanova, E.Y., Andreev, V.N., Belousov, A.B., Belousova, M.G., Gavrilenko, V.A., Garbuzova, V.T., Demyanchuk, Y.V.,
2197 Khanzutin, V.P., 1993. The Eruptions of the Northern Group of Volcanoes on Kamchatka in 1988-1989: Seismological and Geodesic Data. Volcanology and
2198 Seismology 13, 649–681.

2199